NRC FORM 402
(3-81)

U.S. NUCLEAR REGULATORY COMMISSION

TRIP REPORT

TO:	FROM
Robert L. Johnson, Project Manager Repository Projects Branch Division of Waste Management	TRAVELER: John C. Voglewede BRANCH: Engineering Branch, WM

PLACE(S) VISITED	DATE(S) OF TRIP
A. Pacific Northwest Laboratory B. Office of Nuclear Waste Isolation	A. 8/12/86 - 8/13/86 B. 8/15/86

PERSON(S) CONTACTED

See attached list of attendees (A & B).

PURPOSE OF TRIP

A. Examination of Metal Barriers Testing Program and Waste Package Environmental Studies sponsored by the Salt Repository Project and conducted by Battelle Pacific Northwest Laboratory.
B. Examination of draft program documents and plans related to the salt repository waste package at the Office of Nuclear Waste Isolation (Battelle Memorial Institute).

ACCOMPLISHMENTS

A. NRC and contractor staff reviewed test data, test procedures, testing approaches and methodologies, experimental techniques and test apparatus used in the Metal Barriers Testing Program. The Staff also reviewed experimental conditions as indicated by the Waste Package Environmental Program.
B. NRC and contractor staff reviewed draft documents related to waste package program planning and strategy. The Staff also reviewed several draft technical positions related to the salt waste package.

PROBLEMS ENCOUNTERED

None

PENDING ACTIONS

One document (R.E. Westerman et al., Corrosion and Environmental-Mechanical Characterization of Iron-Base Nuclear Waste Package Structural Barrier Materials, PNL-5426, March 1986) was retained by the staff. In accordance with the Appendix 7 guidelines, a copy of that report is attached.

The NRC salt repository team was briefed upon completion of the visit.

RECOMMENDATIONS

A greater amount of time should be allocated to document review indicated in Part B of the trip above.

Tilak R. Verma
Tilak R. Verma 9/02/86

SIGNATURE – TRAVELER: John C. Voglewede
John C. Voglewede
DATE: 8/22/86

DOE/NRC/PNL MEETING
(Appendix 7 Meeting)

August 12-13, 1986

Name	Organization
Larry G. Morgan	PNL
V. J. Rutkauskas	BPMD/ONWI
K. K. (Roger) Wu	DOE/SRPO
John C. Voglewede	NRC/NMSS/DWM
Richard E. Westerman	PNL
Paul J. Turner	PNL
John A. Carr	Battelle/ONWI
Karl H. Pool	PNL
Tilak R. (Teek) Verma	NRC/Columbus
Stan G. Pitman	PNL
Monty R. Telander	PNL
John H. Haberman	PNL
Michael B. McNeil	NRC/RES
Anna C. Fraker	NBS (National Bureau of Standards)
Larry R. Pederson	PNL

SRPO/ONWI/NRC MEETING
(Appendix 7 Meeting)

August 15, 1986

John Carr	BMI/ONWI
Harold Cleary	(SRPO Contractor)
Matt Golis	BMI/ONWI
Chuck Interrante	NBS (NRC Contractor)
Jim Kilgore	BMI/ONWI
Chuck Peterson	NRC/NMSS/DWM
Teek Verma	NRC/NMSS/DWM
John Voglewede	NRC/NMSS/DWM
K. K. (Roger) Wu	DOE/SRPO

Distribution:
WM File 202.2
WMEG
NMSS
REBrowning
MJBell
JTGreeves
TCJohnson
MNataraja
MTokar
Materials Section
JOBunting
PJustus
JJLinehan
RLJohnson
TVerma
MBMcNeil
CInterrante, NBS (c/o EAWick)
AFraker, NBS (c/o EAWick)

OFC	NMSS/WMEG	NMSS/WMEG	NMSS/DWM				
NAME	JCVoglewede	TCJohnson	TRVerma				
DATE	09/ /86	09/ /86	09/ /86				

Encl. to 9/2/86 Memo to RJohnson from Vollewede Appendix 7 Site

PNL-5426
UC-70

106
P-13

Annual Report – FY 1984

Corrosion and Environmental-Mechanical Characterization of Iron-Base Nuclear Waste Package Structural Barrier Materials

R. E. Westerman
J. H. Haberman
S. G. Pitman
B. A. Pulsipher
L. A. Sigalla

March 1986

Prepared for
the Salt Repository Project
U.S. Department of Energy
under Contract DE-AC06-76RLO 1830

Pacific Northwest Laboratory
Operated for the U.S. Department of Energy
by Battelle Memorial Institute

Battelle

PNL-5426

PACIFIC NORTHWEST LABORATORY
operated by
BATTELLE
for the
UNITED STATES DEPARTMENT OF ENERGY
under Contract DE-AC06-76RLO 1830

Printed in the United States of America
Available from
National Technical Information Service
United States Department of Commerce
5285 Port Royal Road
Springfield, Virginia 22161

NTIS Price Codes
Microfiche A01

Printed Copy

Pages	Price Codes
001-025	A02
026-050	A03
051-075	A04
076-100	A05
101-125	A06
126-150	A07
151-175	A08
176-200	A09
201-225	A010
226-250	A011
251-275	A012
276-300	A013

PNL-5426
UC-70

ANNUAL REPORT--FY 1984

CORROSION AND ENVIRONMENTAL-MECHANICAL CHARACTERIZATION OF IRON-BASE NUCLEAR WASTE PACKAGE STRUCTURAL BARRIER MATERIALS

R. E. Westerman
J. H. Haberman
S. G. Pitman
B. A. Pulsipher
L. A. Sigalla

March 1986

Prepared for
the Salt Repository Project
U.S. Department of Energy
under Contract DE-AC06-76RLO 1830

Pacific Northwest Laboratory
Richland, Washington 99352

ACKNOWLEDGMENTS

The authors wish to acknowledge the technical assistance of H. E. Kissinger, L. R. Pederson, K. H. Pool, D. M. Squier, and M. R. Telander, PNL; the programmatic assistance offered by D. J. Bradley, PNL, and D. E. Clark and J. S. Perrin, ONWI; the editorial assistance of P. L. Whiting, PNL; and the programmatic support provided by the Office of Nuclear Waste Isolation under the U.S. Department of Energy Contract DE-AC06-76RLO 1830.

ABSTRACT

The disposal of high-level nuclear waste in deep underground repositories may require the development of waste packages that will keep the radioisotopes contained for time periods up to 1000 years. The primary geologic media currently being considered in the United States for repository siting are salt, basalt, tuff, and granite. A number of iron-base materials are being considered for the structrual barrier members of waste packages. Their uniform and nonuniform (pitting and intergranular) corrosion behavior and their resistance to stress-corrosion cracking in aqueous environments relevant to salt media are under study at Pacific Northwest Laboratory (PNL). The purpose of the work is to provide data for a materials degradation model that can ultimately be used to predict the effective lifetime of a waste package overpack in the actual repository environment. This report summarizes the results of the studies conducted at PNL during the FY 1983-FY 1984 time period in support of the Salt Repository Project of the Department of Energy.

The corrosion behavior of the candidate materials was investigated in simulated intrusion brine (essentially NaCl) in flowing autoclave tests at 150°C, and in combinations of intrusion/inclusion (high-Mg) brine environments in moist salt tests, also at 150°C. Studies utilizing a ^{60}Co irradiation facility were performed to determine the corrosion resistance of the candidate materials to products of brine radiolysis at dose rates of 2×10^3 and 1×10^5 rad/h and a temperature of 150°C. These irradiation-corrosion tests were "overtests," as the irradiation intensities employed were 10 to 1000 times as high as those expected at the surface of a thick-walled waste package.

Slow-strain-rate (SSR) tests and corrosion fatigue tests conducted in intrusion brine environments at 150°C and, in the case of some SSR tests, with a superimposed radiation field of 3×10^5 rad/h, were used to determine the resistance of the candidate alloys to environmentally enhanced crack propagation.

With the exception of the high general corrosion rates found in the tests using moist salt containing high-Mg brines, the ferrous materials exhibited a degree of corrosion resistance that indicates a potentially satisfactory application to waste package structural barrier members in a salt repository environment.

CONTENTS

FIGURES

TABLES

INTRODUCTION

The Geologic Repository Deployment (GRD) program of the U.S. Department of Energy (DOE) is responsible for developing technology and providing facilities for the safe, environmentally acceptable, permanent disposal of high-level nuclear waste. The current program focuses on waste disposal in repositories located in deep geologic formations of salt, tuff, basalt, and granite. In each repository, the waste form, currently considered to be spent fuel, would be enclosed in a waste package incorporating a primary corrosion barrier, or overpack.[a] The overpack is expected to perform the principal waste containment function of the waste package and, as such, it could be required to remain intact for time periods up to 1000 years.[b] The overpack must therefore be designed to resist a number of corrosion-associated failure modes that could compromise its effectiveness in its containment role. Some of the potentially important degradation phenomena are uniform corrosion; nonuniform corrosion (pitting, crevice corrosion); irradiation-enhanced corrosion; stress-corrosion cracking (SCC); hydrogen embrittlement; aging reactions; bacterial corrosion; and mechanical overload.

The Waste Package Program (WPP) sponsored by the Salt Repository Project (SRP) of the DOE at Pacific Northwest Laboratory (PNL)[c] has as one of its objectives the corrosion/environmental-mechanical characterization of candidate iron-base waste package overpack materials in salt-repository-relevant environments. This report summarizes the results of the work performed toward these objectives under the auspices of the WPP in the time period FY 1983 through FY 1984. The testing addressed the characterization and quantification of metal degradation that would occur under two conditions of brine formation and subsequent contact of the brine with the waste package: the intrusion brine scenario and the inclusion brine scenario. In the former, brine is assumed to

(a) The outer metallic engineered barrier of the waste package.
(b) "Containment of the high-level waste within the waste package must be substantially complete during the period when radiation and thermal conditions within the waste package are dominated by fission products decay. Such time period would be between 300 and 1000 years..." (Nuclear Regulatory Commission Regulation 10 CFR Part 60).
(c) Operated for the DOE by Battelle Memorial Institute.

form through dissolution of salt resulting from the intrusion of large amounts of water into the repository horizon from some outside source; for example, an aquifer lying just above the repository horizon. Intrusion brines reflect the gross salt composition of the repository horizon, and so are primarily halite-saturated sodium chloride brines.

If the waste package is to be contacted by brine at all, however, it is considered much more likely that the source of the brine will be brine-filled inclusions present in the salt that migrate to the waste package under the influence of the thermal gradient existing in the vicinity of the waste package. These "inclusion brines" can effectively concentrate certain more-soluble species present in the normal repository horizon, such as magnesium, and therefore exhibit compositions very different from those of intrusion brines.

Both the intrusion brine and inclusion brine scenarios were taken into account in developing the testing approach utilized in the present study. It is obviously impossible to simulate anticipated repository conditions in the laboratory when the repository conditions are not known exactly. For this reason, recourse is being made to testing over a wide range of each test variable, in order to develop a model to be used to predict material behavior when the repository conditions can be better defined.

The iron-base materials investigated consisted of two cast mild steels (a cast mild steel corresponding to ASTM Casting Specification A216 Grade WCA is currently considered to be the reference overpack material); a low-alloy Cr-Mo steel, nominally 2-1/2% Cr, 1% Mo; a wrought mild steel; a ductile (nodular) cast iron; and a high-purity iron. Testing was not extended to weldments of the ferrous materials. Statistical treatments of the data are included to provide insights into data trends, comparison of materials performance, and data variability; and a compilation of all of the relevant data obtained under the Structural Barrier Task of the WPP in the time period FY 1983 through FY 1984 can be found in the appendices to the report.

OBJECTIVE

The ultimate objective of the work presented here was to provide initial data for a material degradation model that can ultimately be used to predict, with the appropriate degree of confidence, the effective lifetime of a given waste package overpack in the actual repository environment. The reported work constitutes only a part of the data required for such a model, however, because the ranges of important test parameters (e.g., temperature, radiation intensity, flow rate, material processing parameters, and composition of the test environment) have been too narrow to permit specific, quantitative assessment of even individually operative causalities. (Tests planned for FY 1985 and beyond are directed toward providing data for development of the required predictive model.)

The specific experimental objectives of the reported work consisted of quantifying, to the degree possible, the susceptibilities of a number of iron-base alloys to uniform corrosion, nonuniform corrosion (e.g., pitting) and stress-corrosion cracking. These are the degradation modes judged potentially most deleterious to an iron-base alloy exposed to a salt repository environment.

APPROACH

The experimental approach used in the present study to determine the susceptibility of candidate iron-base alloys to uniform corrosion, nonuniform corrosion, and stress-corrosion cracking involved first estimating the environmental conditions that would exist in an actual repository constructed in a salt medium, then simulating these environmental conditions in laboratory test systems. In general, tests were done under what were considered to be conservative conditions, i.e., in an "overtest" mode, when anticipated repository conditions (for example, brine flow rates) were considered to be difficult to either predict or simulate. Overtests were also used when the intent was to enhance the effect of a test variable on corrosion, in order to demonstrate whether or not it was a significant corrosion-inducing factor (for example, irradiation intensity).

A possible exception to the generality of conservative testing is the temperature factor, which was held at 150°C throughout essentially all of the test program. This was done in order to explore the numerous other factors involved in materials degradation.

The uniform and nonuniform corrosion tests were performed in both refreshed autoclaves, where testing was intended to simulate intrusion-brine conditions, and sealed gas-tight cans, where testing was primarily to simulate inclusion-brine scenarios.

Stress-corrosion cracking was addressed by means of slow-strain-rate tests and corrosion fatigue tests. The slow-strain-rate tests were done in both static and refreshed autoclaves. The corrosion fatigue studies were done under refreshed autoclave conditions only.

The specific type of laboratory test used to investigate the susceptibility of the candidate barrier materials to the three principal corrosion modes addressed in the present study, with the test variable controlled in each test, is presented in the following table.

Degradation Mode	Controlled Test Variable	Range
Uniform and non-uniform corrosion[a]	Temperature	150°C
	Brine composition	Pure NaCl to simulated high-Mg "inclusion" brine
	Dissolved oxygen	0 to 1.5 wppm
	Radiation intensity	0, 2 x 10^3, and 1 x 10^5 rad/h
	Pressure[b]	12 MPa (1500 psig)
	Flow rate	0 and 35 mL/h
Stress-corrosion cracking		
• Slow-strain-rate tests	Temperature	150°C
	Environments	Simulated intrusion brine; air; deionized water
	Radiation intensity	0 and 3 x 10^5 rad/h
	Pressure	Ambient to 1.7 MPa gage (250 psig)
	Brine flow rate	0 to 35 mL/h
	Strain rate	2 x 10^{-7} to 1 x 10^{-4}/s
• Corrosion fatigue tests	Temperature	150°C
	Environment	Simulated intrusion brine; air; deionized water
	Radiation intensity	0
	Pressure	0 to 2.1 MPa gage (200 psig)

(a) All tests for uniform corrosion were considered to be tests for some aspect(s) (e.g., pitting) of nonuniform corrosion as well.
(b) Controlled only in autoclave tests. Pressure was not controlled in tests utilizing seal-welded, gas-tight cans ("moist salt" tests).

Degradation Mode	Controlled Test Variable	Range
• Corrosion fatigue tests (cont'd)	Brine flow rate	35 mL/h
	Cyclic frequency	0.1 to 10 Hz
	R value $\frac{\text{(min. load)}}{\text{(max. load)}}$	0.1
	ΔK (stress intensity)	20 to 57 MPa$\sqrt{m}$

MATERIALS

Prior investigations[1,2] using intrusion brine test environments, a controlled dissolved-oxygen ingress, and irradiation-intensity levels near those expected under actual repository conditions revealed the possibility of using relatively inexpensive and abundant iron-base alloys in salt brines. Accordingly, recent testing has continued to emphasize ferrous materials. The six materials investigated, and their chemical compositions, are listed in Table 1.

The ASTM A216 Grade WCA material is currently considered to be the reference waste package overpack material by the Salt Repository Project (SRP). The ASTM specification technically calls for this material to be supplied in the annealed, normalized, or normalized and tempered condition. However, in the present study, the as-cast material was emphasized, as it is not certain that the improvement in mechanical properties brought about by heat treatment would be required in the final overpack design.

As in the case of the ASTM A216 material, the other cast ferrous materials were generally tested in the as-cast condition. All cast-steel specimens were obtained from castings weighing ~160 kg (352 lb), with a minimum dimension of ~120 mm (4.7 in.). All of the test specimens used in the present study were obtained from one casting, hence one heat of steel.

Before corrosion testing, the cast steel specimens were ground with an aluminum oxide wheel to produce a surface finish of 32 to 63 μm rms. The same wheel produced a surface finish of 8 μm rms on the ductile cast iron specimens. The wrought steel sheet was surface ground with a 50-grit disc. The high-purity iron specimens were cut from a forging, and tested in the surface-ground condition. The surface pretreatments are of course arbitrary, without some knowledge of how the actual overpack will be treated. The main concern is to provide a surface on each specimen that is easy to duplicate, while not deviating too far from anticipated waste package surface treatments consistent with a casting operation followed by some form of surface cleanup. The most likely cleanup is considered to be some mechanical operation, such as grinding, machining, or grit-blasting.

TABLE 1. Compositions of Metallic Materials

Material	Element, wt%								
	C	Mn	Si	P	S	Mo	Cr	Ni	Fe
Cast mild steel,[a] ASTM A216 Grade WCA	0.225	0.71	0.45	0.018	0.018	0.05	0.41	0.23	bal.
Cast mild steel,[b] ASTM A27, Grade 60-30	0.245	0.69	0.59	0.016	0.018	0.04	0.43	0.20	bal.
Wrought steel sheet, AISI 1025	0.07[c]	0.40	0.03	0.015	0.021	---	---	---	bal.
2-1/2% Cr, 1% Mo cast steel	0.116	0.57	0.57	0.020	0.004	1.02	2.46	---	bal.
Ductile cast iron, ASTM A536-77, Grade 60-40-18	3.53	0.31	2.51	0.05	0.004	---	---	---	bal.
High-purity iron	0.018	0.05	0.01	0.002	0.003	0.01	0.01	0.01	99.87

(a) Used in the as-cast condition; in the normalized condition (930°C, 1 h, air cool); and in the "homogenized" condition (930°C, 24 h, air cool).
(b) Used in the as-cast condition and in the normalized condition (927°C, 5 h, air cool).
(c) Spectrographic analysis. Low apparent carbon due to surface decarburization.

Three brine compositions, designated Permian Basin Brine No. 1 (PBB1), No. 2 (PBB2), and No. 3 (PBB3), have been used throughout the studies. The recipe for PBB1, a simulated intrusion brine, was derived from dissolution of salt cores from a Permian Basin salt horizon considered to be representative of a bedded-salt-site repository.[a] The recipe for PBB2 was obtained by holding PBB1 at 150°C in an autoclave for several days, then performing an analysis of the supernatant fluid existing with the precipitated solids. PBB2 is expected

(a) Cores were selected from the Texas Bureau of Economic Geology Core Library on May 25, 1982. The cores were derived from the G. Friemel Hole No. 1 at depths in the range of 2440.2 to 2575.5 ft (Cycle 4). Six-in.-long cores were obtained at 15-ft intervals. One-eighth of each core was blended for experimental use, and the remainder was archived.

to be representative of the brine composition that results when water intrudes into the repository horizon, dissolves salt to saturation, then attains a temperature of 150°C as it approaches the surface of the overpack. Additionally, use of PBB2 mitigated precipitation of solids (primarily carbonates) due to inverse solubility effects in the inlet lines of the refreshed autoclave systems. As mentioned in the introduction of this report, the more likely overpack corrosion situation will be caused by migration of brine inclusions up the thermal gradient toward the waste package. Such brines are expected to contain higher levels of magnesium and calcium than the intrusion brines previously described. PBB3 is a simulated inclusion brine being used as an approximation to the inclusion brine expected to exist in a Permian Basin salt horizon. The compositions of the brines are detailed in Table 2. All salts and brines used in the studies were synthetic. The most significant difference among the three brine formulations, from the standpoint of corrosion of ferrous materials, is the high concentration of magnesium in PBB3.

In addition, a moist salt test was conducted that utilized an environment consisting of high-purity (reagent grade) NaCl and deionized water.

TABLE 2. Brine Compositions

Ion	Concentration, mg/L		
	PBB1	PBB2	PBB3
Na^+	123,000	123,000	23,200
Ca^{2+}	1,560	1,110	14,700
Mg^{2+}	134	122	53,200
K^+	39	39	10,500
Sr^{2+}	35	35	---
Zn^{2+}	7.8	7.9	8
Cl^-	191,000	191,000	210,000
SO_4^{2-}	3,200	1,910	160
HCO_3^-	30	23	---
Br^-	32	24	2,400
F^-	1.1	1.0	---
I^-	---	---	---
BO_3^{3-}	---	---	---

EXPERIMENTAL

The investigation of uniform and nonuniform corrosion of the candidate ferrous materials is addressed under the headings of General Corrosion Testing and Irradiation-Corrosion Testing in the remainder of the report, and the investigation of stress-corrosion cracking susceptibility is described in the section entitled Environmental-Mechanical Testing.

GENERAL CORROSION TESTING--INTRUSION BRINE

General corrosion tests performed under unirradiated conditions are used first as an initial material selection/rejection tool, and secondly, if radiation effects are not pronounced, as a preliminary basis for the prediction of longevity. In addition to providing data on uniform corrosion, the tests are expected to provide information on the susceptibility of materials to pitting and intergranular corrosion.

A schematic of a typical flowing autoclave corrosion test facility is shown in Figure 1. A reservoir contained simulated intrusion brine, made up to a specific composition. A positive displacement pump delivered brine to the autoclave at ~35 mL/h, the lowest flow rate easy to maintain with existing high-pressure pumps. The autoclaves were operated at a pressure higher than the vapor pressure of water at the given test temperature, e.g., a total pressure of 7 MPa (1000 psi) for a test temperature of 150°C.

The dissolved oxygen concentration in the feed water was controlled by an argon gas purge containing either 0% or 20% oxygen. The former yielded a feed water termed "anoxic," which typically contained ~50 ppb oxygen. The latter yielded a brine feed containing ~1.5 ppm oxygen.[a] This solution was termed "oxic" in the present study, though the amount of dissolved oxygen actually being delivered to the test system was small in terms of observed corrosion, and, in fact, was routinely found to be much less than the oxygen stoichiometrically present in the corrosion product films on the specimens in the

(a) Oxygen concentrations were determined colorimetrically by means of reagent-filled ampoules produced by CHEMetrics, Inc., Calverton, Virginia.

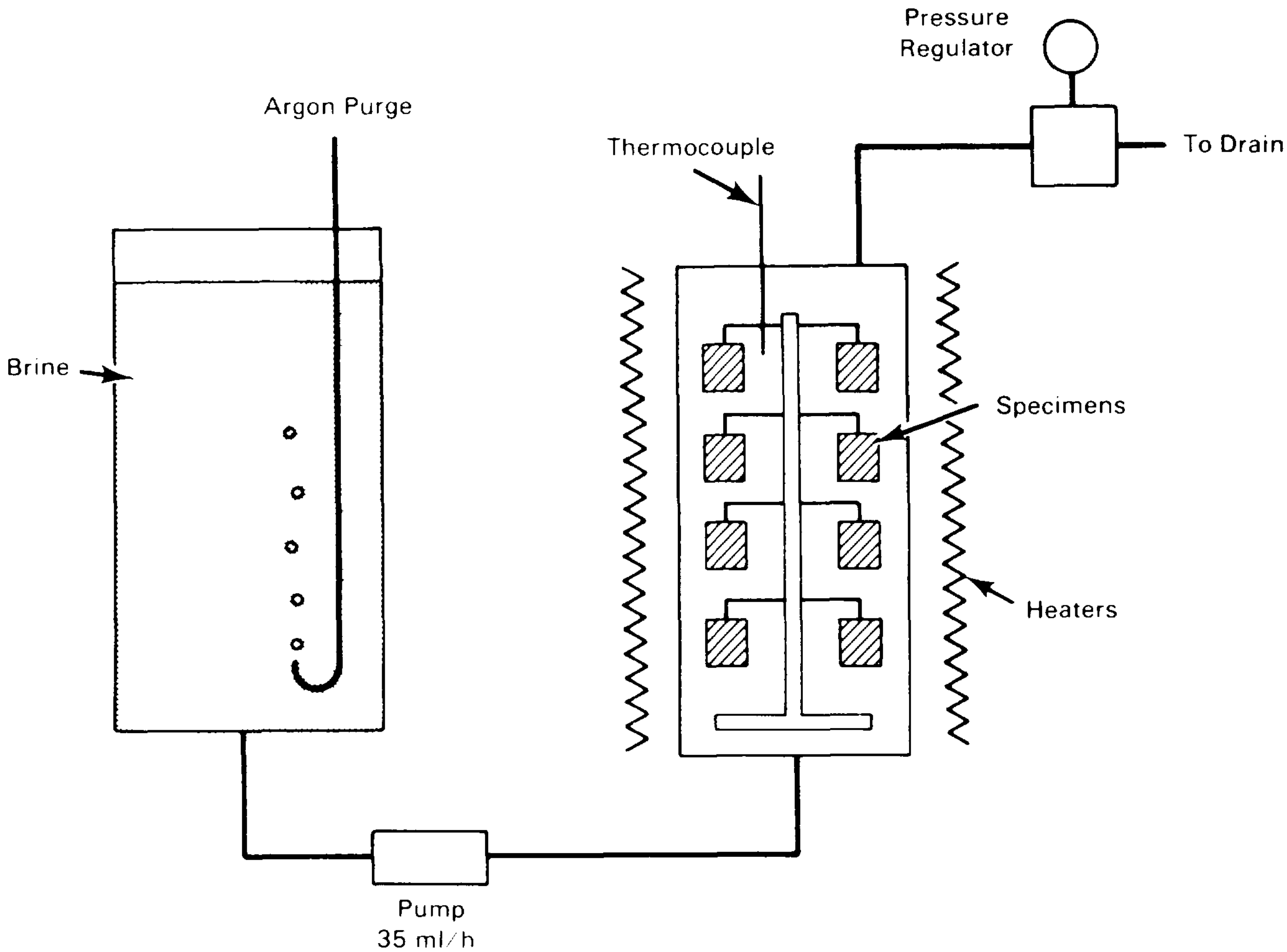

FIGURE 1. Schematic of Typical Flowing Autoclave System Used in General Corrosion Study

autoclave. This finding indicates that the major source of oxygen in the corrosion product films is the reaction of iron with water in the test environment.

Once the desired test duration had been achieved, the specimens were removed and visually examined. Selected specimens of the iron-base alloys, generally duplicates, were stripped of their corrosion product films by a combination of gentle abrasion and immersion in formaldehyde-inhibited HCl. The specimens were then weighed, and the weight loss exhibited was converted to a metal penetration.[b] The data in this report were generally derived from specimens that had been stripped only once, i.e., for one reported weight change (or metal penetration). On the few occasions where stripped specimens were reinserted in the test environment, the subsequent corrosion rates were found to be consistent with specimens used only once. This suggests that the method of surface preparation does not strongly influence the corrosion kinetics subsequently observed in these metal/environment systems.

GENERAL CORROSION TESTING--MOIST SALT

In the moist salt test, specimens of the ferrous materials were embedded in simulated, predried (90°C, 18 h) PBB1 or reagent-grade NaCl salt in welded Inconel 600 cans. Sufficient liquid, either in the form of PBB1, PBB3, or saturated NaCl brine, was added through the liquid inlet tube to bring the total moist salt environment to a predetermined level of H_2O. A total of 12 specimens, with 4 specimens in each of 3 tiers, was exposed in each can. Each specimen was square, 15.2 mm (0.60 in.) on a side. After the brine addition was made, the inlet tube was welded shut and the can leak-checked. The welding of the lid and inlet tube was done in an inert-atmosphere glove box. The atmosphere in each can before testing consisted of a mixture of Ar, He, and water vapor. The general test arrangement is shown in Figure 2.

The cans were held at 150°C in an oven during the exposure period. At the prescribed time, selected cans were removed from the oven, cooled, vented to relieve the pressure (and determine the volume) of corrosion-product H_2, and cut open on a lathe. The specimens were removed from the salt mass, examined, washed, stripped of any oxide film using formaldehyde-inhibited HCl, and re-examined for signs of nonuniform attack. Corrosion rates were then determined by weight loss determination.

IRRADIATION-CORROSION TESTING--INTRUSION BRINE

Irradiation-corrosion tests have the same objectives as the unirradiated general corrosion tests, i.e., to characterize candidate waste package materials

(b) A typical specimen of reference steel will lose only about 2% of its weight to corrosion during a six-month test under the test conditions described, necessitating a careful approach to all specimen measurement, preparation, and weighing.

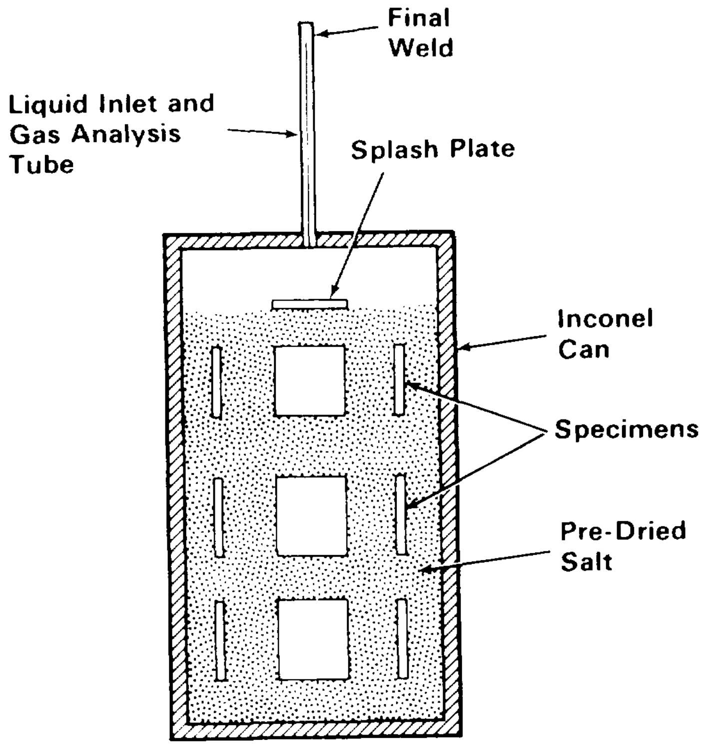

FIGURE 2. Moist Salt Test Configuration (not to scale)

for initial material selection/rejection and finally as a basis for longevity prediction. Irradiation-corrosion investigations are necessary because, unless special precautions are taken, the surface of the outermost structural barrier will be exposed at some time to brine modified by gamma irradiation emanating from the waste form. Predicting the effects of radiolysis on metal corrosion rates is difficult a priori. For example, in pure water, radiolysis produces strong oxidizing agents such as peroxides, which can increase the corrosion rate of metals by facilitating the cathodic process (i.e., by acting as cathodic depolarizers). This process could enhance the corrosion rates of iron-based alloys, for example. On the other hand, peroxides can, under other circumstances, lead to anodic passivation, which could decrease the corrosion rate relative to the unirradiated environment. Such uncertainties make experimental determination of irradiation-corrosion essential. As in the general corrosion tests, it was anticipated that a tendency of a material to exhibit nonuniform attack, such as pitting, might be evidenced in the course of a test of reasonable duration; and examining specimens for such phenomena constituted a routine part of the post-test specimen examination.

In order to study potential irradiation effects on the corrosion of candidate structural barrier materials in brine, an existing ^{60}Co irradiation facility (administered by Westinghouse Hanford Company) was modified to accept three high-pressure, high-temperature flowing autoclaves. Figure 3 is a schematic of the facility. The electrically heated autoclaves lie within dry access tubes in the water pool. Each autoclave has an independent water inlet, sampling, and effluent system. The system is capable of exposing specimens to flowing simulated ground-water environments at a maximum temperature of 250°C and a maximum ^{60}Co gamma radiation dose rate to the brine test environment of ~1 x 10^6 rad/h. In the tests described in this report, the temperature was maintained at 150°C, and the environment used was anoxic PBB2. Irradiation intensities of 1 x 10^5 rad/h and 2 x 10^3 rad/h were imposed on the tests. Both radiation levels are considered to be overtests, in that the expected irradiation intensity at the surface of a waste package is expected to be much less

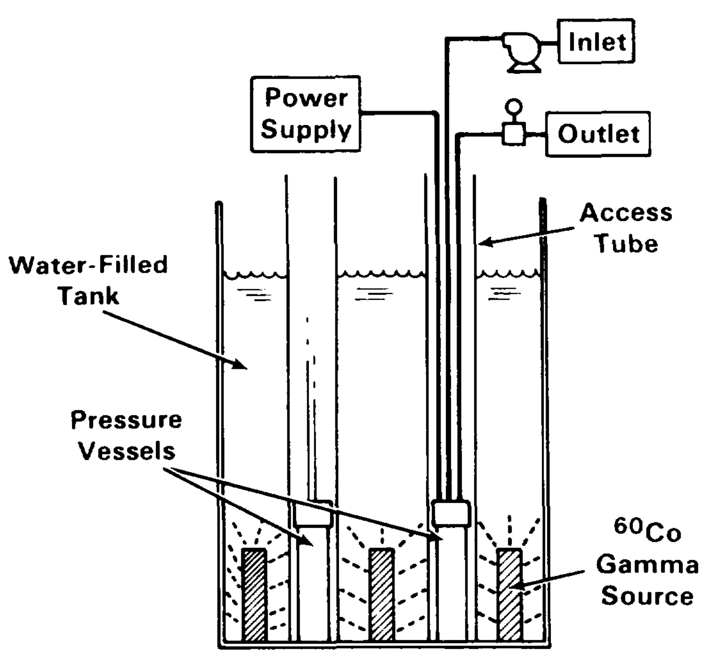

FIGURE 3. Schematic of Irradiation-Corrosion Test Facility

than 2 x 10^3 rad/h.[3] The primary reason for the tests was to determine whether a corrosion-enhancement effect existed, and what degree of importance should be ascribed to it if it did. As in the unirradiated test procedure described earlier, the usual autoclave flow rate (refreshment rate) was set at 35 mL/h, a flow rate easy to maintain with existing high-pressure pumps. In these tests, the system pressure was maintained at ~3 MPa (400 psi). Post-test specimen examination procedures were the same as those used in the nonirradiated general corrosion studies.

ENVIRONMENTAL-MECHANICAL TESTING--SLOW-STRAIN-RATE TESTS AND CORROSION FATIGUE TESTS

Stress-corrosion cracking is a form of degradation in which residual or applied tensile stresses, in conjunction with a corrosive environment, assist in the initiation of cracks and their propagation through the structure. It is an extremely important mode of failure, as cracking can occur in ordinarily corrosion-resistant materials in a very short time under the proper circumstances of tensile stress, temperature, environmental chemistry, and surface flaws, which provide the appropriate stress state and local chemical environment to promote cracking. Because all engineered structures have flaws (flaws associated with weldments are a good example), and because all nondestructive testing techniques have some limit on their abilities to detect flaws, it is essential to ensure that the candidate overpack material is not SCC-susceptible under the combination of material, mechanical stress, environment, temperature, and chemistry present in the repository system.

It is clear that any conservative testing program for SCC in overpack materials must eliminate the initiation time for SCC and measure the resistance of the materials to environmentally enhanced crack propagation alone. The approach taken to date has emphasized two test methods: the slow-strain-rate (SSR) test and the corrosion fatigue test. Both methods use active straining of the specimen surface to eliminate the initiation time for SCC, and are considered conservative methods for determining susceptibility to SCC.

The SSR test, in which a specimen is loaded in tension and strained to failure at low displacement rates, has been found to be a severe test for

SCC.[4] The straining of any material in tension increases the surface area so that unoxidized material is continuously exposed; at the same time, deformation mechanisms take place in the material. Slip planes emerging at the surface provide sites for environment-metal interaction. At high strain rates, the failure occurs so quickly that reactions between the environment and the metal are limited; at sufficiently low strain rates, the metal typically repassivates as the oxide film is broken and damage from the environment is again limited. At intermediate loading rates, interaction between the environment and the metal occurs as the film is broken and SCC occurs.[4] Susceptibility to SCC is usually expressed as loss of ductility at a particular strain rate. The SSR test is an accelerated test relative to statically loaded tests, but it is qualitative in nature. That is, data from these tests can show susceptibility to a certain environment, but the data may not be useful in a quantitative sense to a designer. One factor that is missing in tests using ordinary tension specimens is the presence of a crack. This factor may be allowed for by using precracked specimens of suitably thick material or by using corrosion fatigue tests.

The corrosion fatigue test is a powerful tool for evaluating the susceptibility of metals to SCC. It is primarily used to determine whether existing flaws will propagate under the stresses and environmental conditions that are present. The test provides a combination of three factors that cannot be duplicated in any other available test method: a quantified triaxial stress state, cyclic loading, and a localized crevice chemistry. The quantitative stress intensity factor determination that accompanies the test method is useful in determining flaw lengths when the design stresses are known and in determining the likely rates of crack propagation when allowable flaw lengths and design stresses are known. Another potential use of corrosion fatigue tests is to determine a "threshold" stress intensity for a metal/environment system, i.e., a stress intensity below which existing cracks will not propagate. Although there is some controversy concerning the use and existence of such thresholds, this approach could prove to be extremely useful in designing overpacks to preclude crack growth if it could be shown that such a threshold exists in the brine systems under study. Briefly, because the stress intensity is a function of stress and flow size and shape, it is possible to define the flow size/shape compatible with a given level of stress, e.g., yield, if the permissible "threshold" stress intensity is known. With this knowledge, a designer can apply nondestructive testing techniques that will locate all defects that could give rise to eventual cracking failure.

The cyclic loading causes the protective film on the specimen surface to rupture, exposing unprotected material to the environment. Cyclic loading is not anticipated in repositories; however, there are many possible mechanisms for removal of the protective film or destruction of its protective nature. For example, slowly increasing geologic or pressure stresses could rupture the corrosion product film the same way cyclic stresses break the film during corrosion fatigue tests. Similarly, long-term chemical effects may destroy the protective nature of the film, in effect exposing unprotected metal to the environment. Such long-term chemical effects could include migration of brine containing corrosive elements, such as magnesium, to the area around the waste package. These chemical changes may have profound effects, as has been demonstrated by the moist salt corrosion tests.

It is important that the cracking takes place under conditions of localized crevice chemistry, because the environmental conditions in a crevice can differ vastly from the general environment surrounding the crevice, or the general environment on the surface of a smooth specimen, such as a U-bend specimen. These environmental conditions can be expected to occur whenever oxygen is depleted locally--in flaws or fabrication defects that are exposed in the environment, in cracks that are present due to environmentally assisted cracking, and in areas where the overpack is in contact with salt or other structural components.

A diagram of an unirradiated SSR test facility is shown in Figure 4. An SSR test device specially designed for use in an irradiated environment is shown in Figure 5. The long motor drive/pull rod assembly permits placement of the test autoclave in the bottom of an access tube of the irradiation facility (Figure 3).

A corrosion fatigue facility is shown in Figure 6. Only tests in unirradiated environments have been performed in the corrosion fatigue systems.

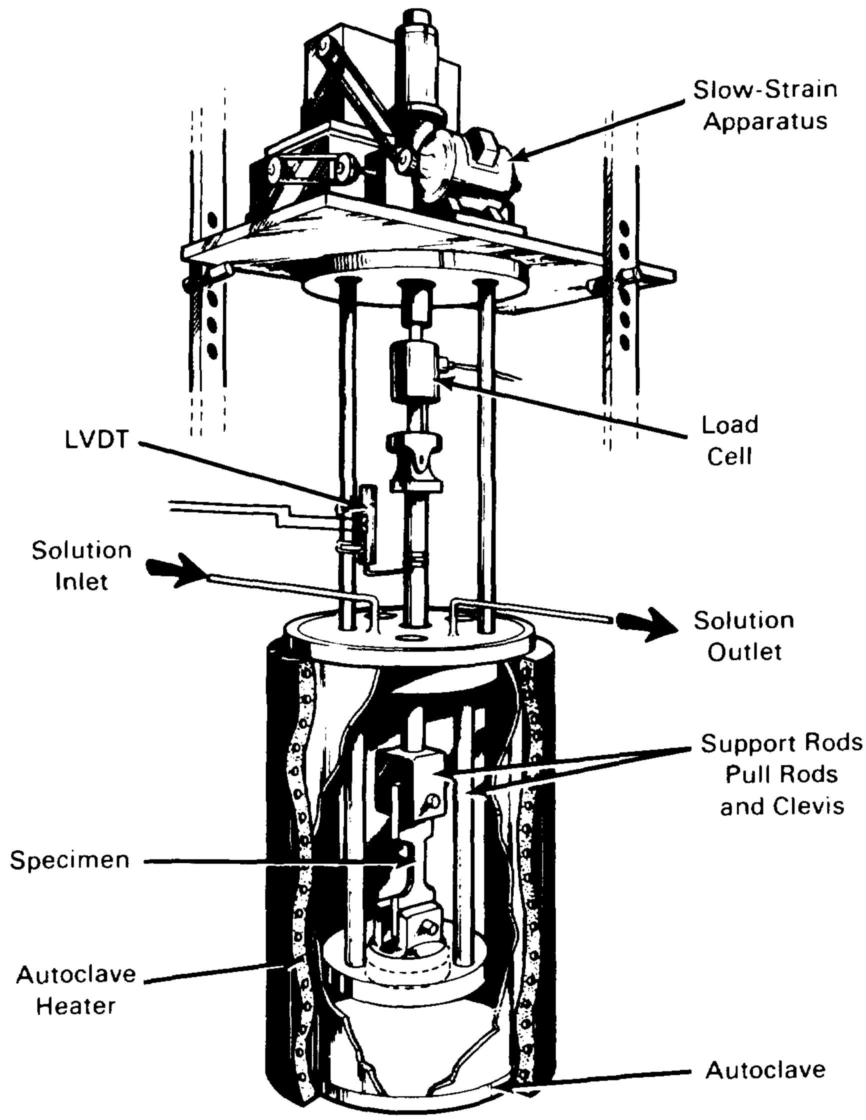

FIGURE 4. Slow-Strain-Rate Testing System, Unirradiated

For additional information on the use and applicability of SSR and corrosion fatigue tests, the reader is referred to the work of Payer et al,[5] Parkins,[6] Wei and Shim,[7] and Bamford.[8]

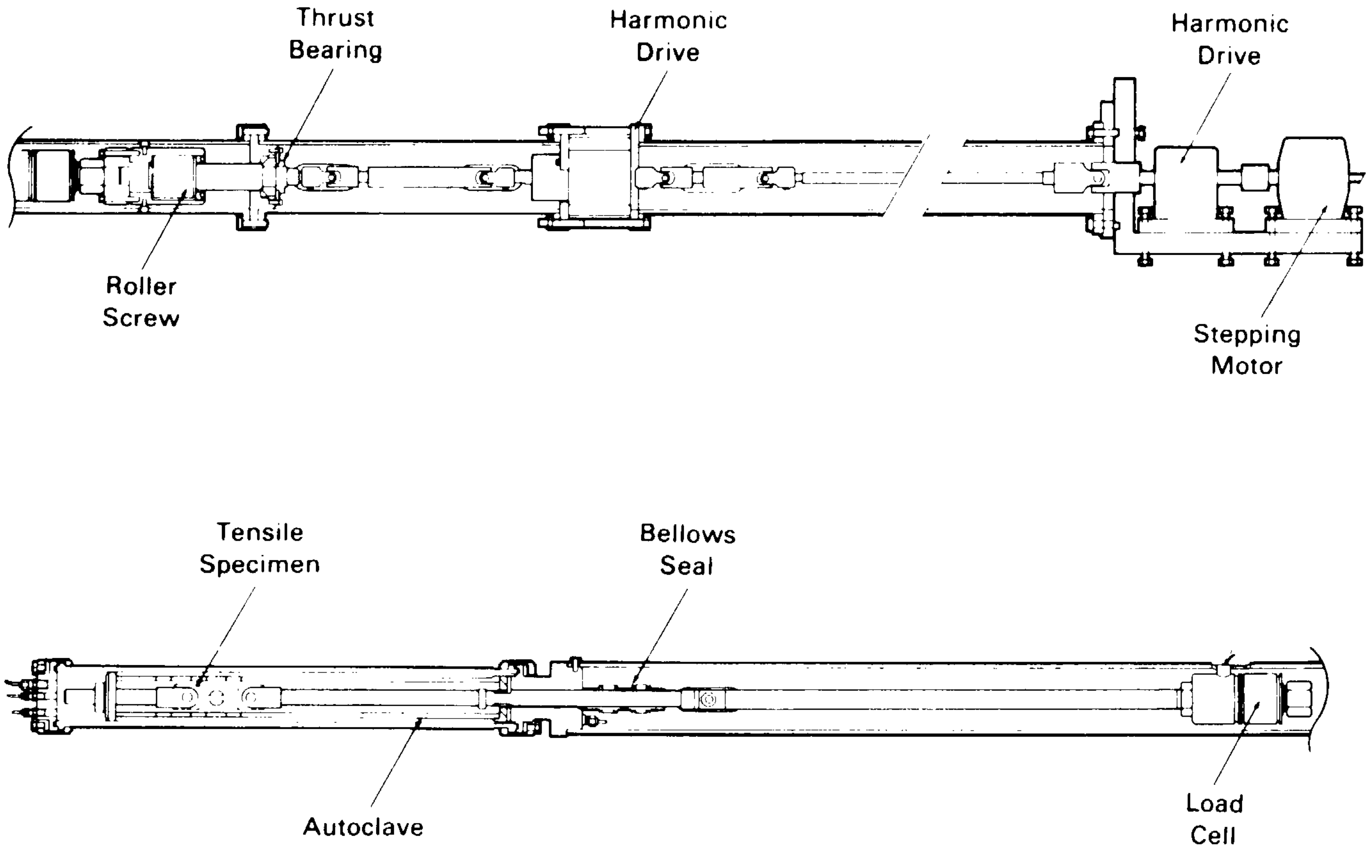

FIGURE 5. Slow-Strain-Rate Testing System, Irradiated

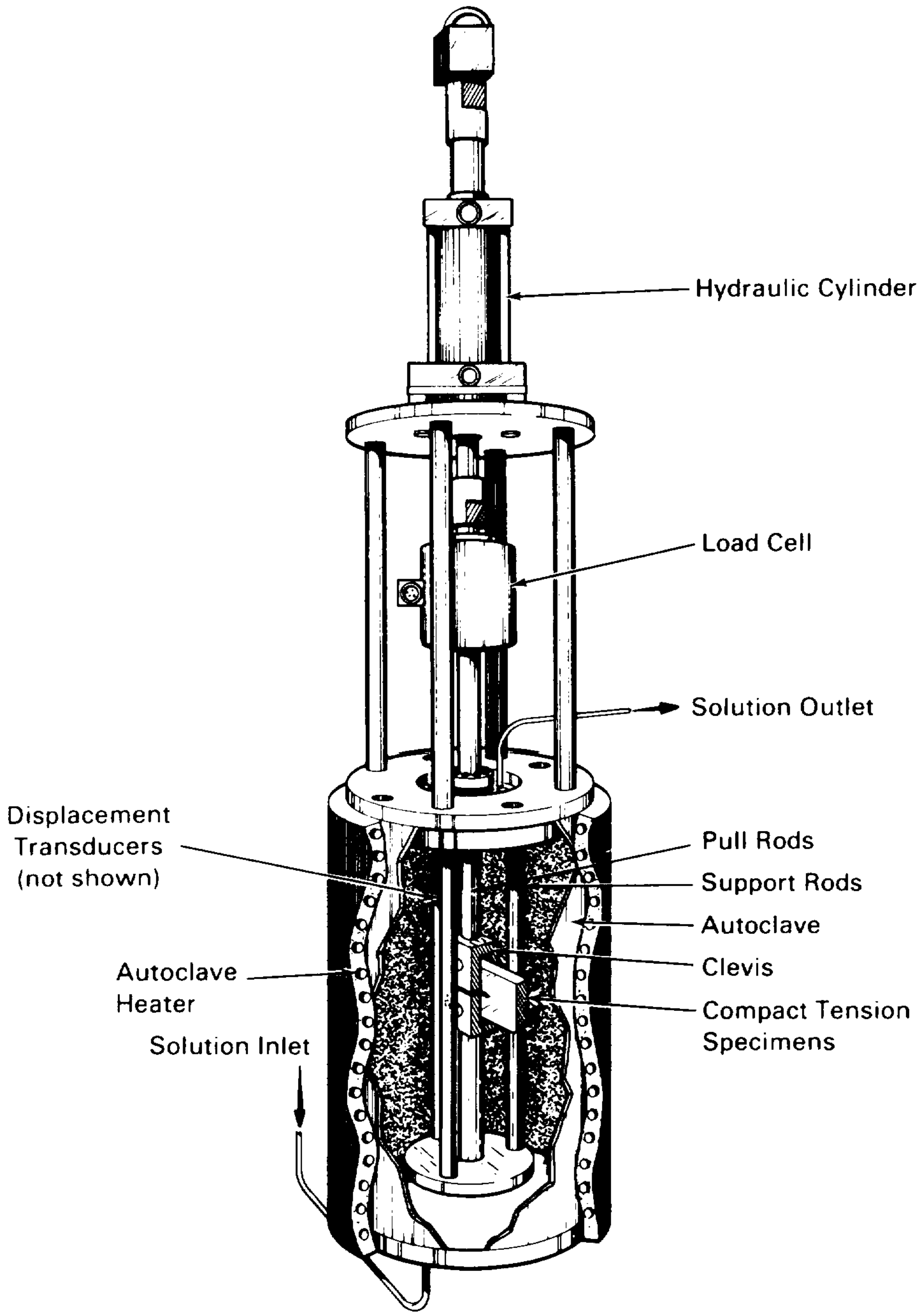

FIGURE 6. Corrosion Fatigue Test Facility

RESULTS AND DISCUSSION

A summary of all of the relevant corrosion and environmental-mechanical property data obtained under the Structural Barrier Task of the WPP and relating to brine-environment investigations over the fiscal years 1983-1984 is contained in this section. The raw data are summarized in Appendices A through D. Statistical treatments of the data are included where such insights prove helpful to data interpretation or to a determination of statistical significance; a compilation of the statistical summaries of the data is presented in Appendix E. The test results and discussions thereof are presented in the following order:

- general corrosion--intrusion brine
- general corrosion--moist salt tests
- irradiation corrosion--intrusion brine
- environmental-mechanical properties
  - slow-strain-rate tests
  - corrosion fatigue tests.

GENERAL CORROSION--INTRUSION BRINE

The general corrosion studies have been performed using flowing oxic (~1.5 ppm O_2) and anoxic (~50 ppb O_2) PBB2 feed brines at 150°C as the test media. The data obtained in these studies, expressed as linear metal corrosion rates, are tabulated in Appendix A. The maximum test duration attained was 21 months. The longest test duration attained for A216 steel was 8 months, as this material entered the test program later than any of the other materials. The materials exposed in these tests, and their maximum test duration, are presented in Table 3.

In general, the corrosion attack was found to be reasonably uniform, with little evidence of pitting attack; that is, there was no evidence of nonuniform attack progressing into the metal more than a tenth of a millimeter or so beyond the surface of the specimen. Pitting, or other nonuniform attack, obviously becomes a problem (relative to uniform attack) only when it proceeds

TABLE 3. Materials Exposed in General Corrosion/Intrusion Brine Corrosion Studies

Test Type	Material	Maximum Exposure Time, mo	Total Number[a] of Specimens Tested
Anoxic	A216 steel	8	15
	A27 cast steel	21	11
	A27 cast steel, normalized	17	10
	1025 wrought steel	20	11
	Ductile cast iron	21	7
	2-1/2% Cr, 1% Mo steel	21	8
	High-purity iron	17	6
Oxic	A216 steel	7	13
	A27 cast steel	21	10
	A27 cast steel, normalized	16	10
	1025 wrought steel	20	9
	Ductile cast iron	21	10
	2-1/2% Cr, 1% Mo steel	21	10
	High-purity iron	16	5

(a) Specimens yielding useful metal penetration data. Additional specimens, designated NA in the corrosion rate data columns of appendices A and B, were used for surface analysis investigations.

into the metal at a rate faster than uniform attack, and when such a rate is maintained for long time periods. This has not been observed in the present tests. The corrosion product film was always found to be magnetite (Fe_3O_4) by x-ray diffraction analysis. Anhydrite ($CaSO_4$) was frequently deposited on the specimen surfaces. The effect of this deposit on corrosion rates was not determined.

The corrosion data of Appendix A were statistically analyzed in order to test hypotheses concerning material differences, to examine trends in the data with respect to other variables, and to quantify random variabilities. In all such statistical analyses presented in this report, significant differences are interpreted as statistically significantly different with 95% confidence, unless otherwise noted.

An analysis of covariance was performed on the anoxic test data using $\log_{10}$(hours) as the covariate. The analysis revealed significant differences among the corrosion rates of different materials. The estimated average for each material is reported in Table 4. The A216 material has a significantly higher corrosion rate than all other materials (with 95% confidence). The high-purity iron corrosion rate is significantly higher than those of the A27 cast steel or 2-1/2% Cr, 1% Mo steel. The rates for the other materials are only significantly different from the A216 rate.

There was a significant log-linear trend across time; i.e., the corrosion rate decreased linearly with the logarithm of time. This trend was not significantly different for each material. Thus, the estimated rates as reported in Table 4 would change depending upon the number of hours tested but the comparisons would remain the same. The standard deviation, assumed to be the same for

TABLE 4. Comparison of Estimated Material Corrosion Rate Averages for General Corrosion in Anoxic Simulated Intrusion Brine PBB2 at 150°C

Material	Estimated Rate, μm/yr[(a)]	Standard Error	Comparison[(b)]
A216 steel	14.6	0.71	A
High-purity iron	9.8	1.11	B
1025 wrought steel	8.6	0.83	BC
Normalized cast A27	7.1	0.88	BC
Ductile cast iron	6.9	0.98	BC
A27 cast steel	5.3	0.82	C
2-1/2% Cr, 1% Mo steel	4.8	0.98	C
	$\hat{\sigma}$ = 2.73		

(a) Rates are estimated at the average time period (4480 hours).
(b) Materials that share the same letter (A, B, or C) are not significantly different with respect to corrosion rate at the 95% confidence level.

each material, is 2.73 μm/yr. The standard deviation reflects any unexplained variability, including specimen replication variability and deviations from the general log-linear time trend. The assumptions relating to the statistical analysis are presented in Appendix E.

A statistical analysis similar to that conducted on the anoxic data was performed on the oxic data. The estimated material corrosion rate averages and comparisons are reported in Table 5. The high-purity iron and A216 steel average corrosion rates are significantly higher than all other material rates. There is no significant difference between the A216 and high-purity iron average rates. Corrosion rates on 2-1/2% Cr, 1% Mo steel are significantly lower than all other materials except A27 cast steel.

There was a significant log-linear time trend such that the corrosion rate decreased linearly with an increase in $\log_{10}$ (hours). This trend was not significantly different for each material. Therefore, the estimated rates

TABLE 5. Comparison of Estimated Material Corrosion Rate Averages for General Corrosion in Oxic Simulated Intrusion Brine PBB2 at 150°C

Material	Estimated Rate, μm/yr[(a)]	Standard Error	Comparison[(b)]
A216 steel	25.2	0.68	A
High-purity iron	24.5	1.06	A
Normalized cast A27	17.1	0.76	B
1025 wrought steel	14.7	0.90	BC
Ductile cast iron	14.5	0.84	BC
A27 cast steel	12.2	0.84	CD
2-1/2% Cr, 1% Mo steel	10.1	0.84	D
	$\hat{\sigma}$ = 2.36		

(a) Rates are estimated at the average time period (4100 hours).
(b) Materials that share the same letter (A, B, C, or D) are not significantly different with respect to corrosion rate at the 95% confidence level.

reported in Table 5 would change depending upon the number of hours tested but the comparisons would remain the same. The estimated standard deviation of all of the oxic data is 2.36 μm/yr.

One outlying data value was detected using information from an analysis of the residuals and deleted from all statistical analyses. The deleted sample was P552 of the A216 material, which showed an unusually low corrosion rate. The coating on the sample was very adherent and could not be completely removed. This may have resulted in a misleadingly low rate.

The data of Tables 4 and 5 suggest that, given a repository environment of intrusion brine similar to that used in the present tests, controlled oxygen in the environment, a temperature of 150°C, and no significant effect of irradiation or processing parameters (such as welding), and no (currently unforeseen) initiation of significant nonuniform attack, A216 steel could be used in realistic thicknesses as a waste package overpack material. The average corrosion rates of A216 steel determined in the present tests are plotted with associated 95% confidence intervals in Figure 7. (The data from which these figures were derived are tabulated in Table E.1, Appendix E.) The highest corrosion rates found in this study were in the oxic brine test. The highest point of the upper 95% confidence limit lies at a (linearized) metal penetration rate of 32.3 μm/yr (1.27 mil/yr).

GENERAL CORROSION--MOIST SALT TESTS

Moist salt tests were performed to simulate the conditions eventually expected in a well sealed repository, i.e., an elevated-temperature waste package moistened by inclusion brine in an environment devoid of air-derived oxygen. The moist salt tests emphasized the A216 Grade WCA reference steel, but in some of the tests 1025 wrought steel and ductile cast iron were included to provide additional levels of comparison with intrusion-brine autoclave studies. In the moist salt tests two synthetic brine formulations were used as a basis for defining the corrosive environment: PBB1, representing an intrusion brine

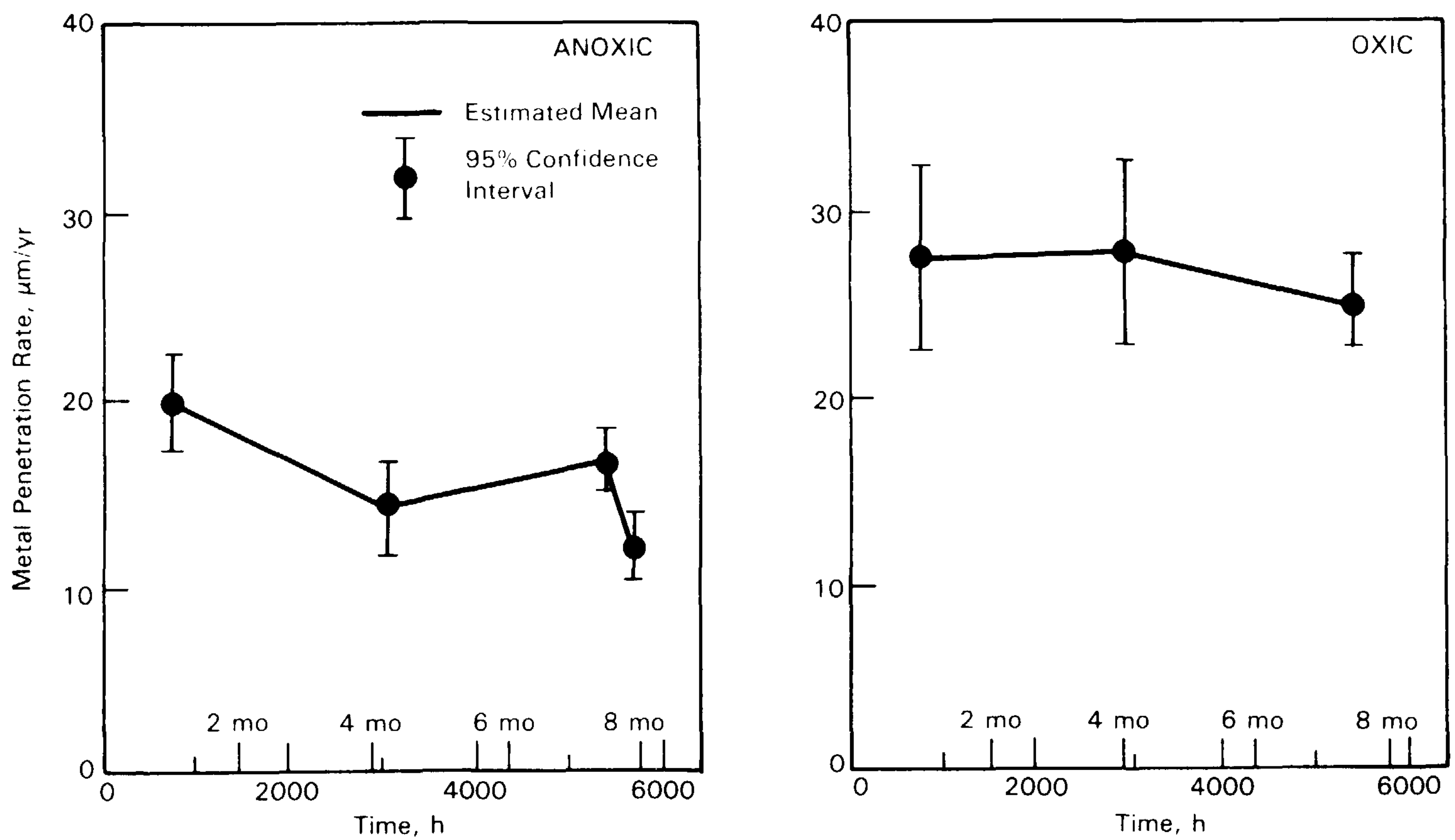

FIGURE 7. Estimated Means of Metal Penetration Rates and 95% Confidence Intervals About the Means--A216 Steel, 150°C, Brine PBB2, Unirradiated

composition; and PBB3, representing an inclusion brine composition. In one test, reagent-grade NaCl with water formed the test environment.

In the first series of tests, PBB3 in varying amounts was added to canisters containing specimens packed in dried PBB1. The dry PBB1 salt was made by thoroughly blending reagent-grade chemicals and drying the mixture for 18 h at 90°C before use. Sufficient PBB3 was added to the canisters to bring the water concentration of the salt masses to 5, 10, 20, 25, and 30% water. The sealed cans were placed in an oven at 150°C. Canisters were removed after one, two, and three months for specimen examination. (At a water concentration of 5%, the salt did not significantly differ in appearance or consistency from the dried salt; at 10% water some change in consistency was observed; at 20% water the salt was moist and "packable"; at 30% water the presence of a liquid phase was obvious by visual inspection, and the salt mass had a "slushy" consistency.)

The corrosion rates found after a 1-month exposure in canisters containing 20% and 30% water are shown in Figure 8. The corrosion rates found after a 3-month exposure are shown in Figure 9.[a]

The one-canister (30% water), 2-month test was performed primarily to obtain corrosion-product samples from the test specimens for x-ray diffraction and wet chemical analysis.

The corrosion-product hydrogen generated in the cans was routinely collected. An analysis of the gas revealed fairly pure hydrogen (89%), contaminated with N_2, He, Ar (from the welding glove box), CO_2, and hydrocarbon gases. Hydrogen pressure in the cans has been estimated to be as high as 20 atm at the end of a 3-month test.

The data that were used to generate the curves of Figures 8 and 9 were simply the averages of the corrosion rates of the four specimens contained in

(a) The raw data used as a basis for Figures 8 and 9 are given in Appendices B.1 and B.2; these tests are designated Moist Salt Test No. 2 and Moist Salt Test No. 3.

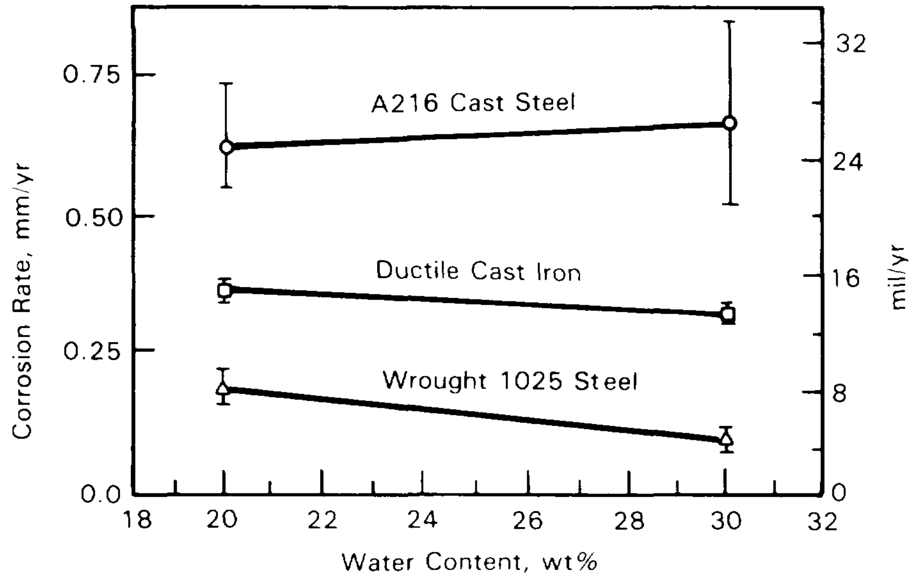

FIGURE 8. Corrosion Rates of Ferrous Materials in Dried Synthetic PBB1 Salt Moistened with PBB3 Brine; 1 Month Exposure at 150°C. Range of values for four specimens of each material represented by vertical bar at each data point. Data point is average of specimen values.

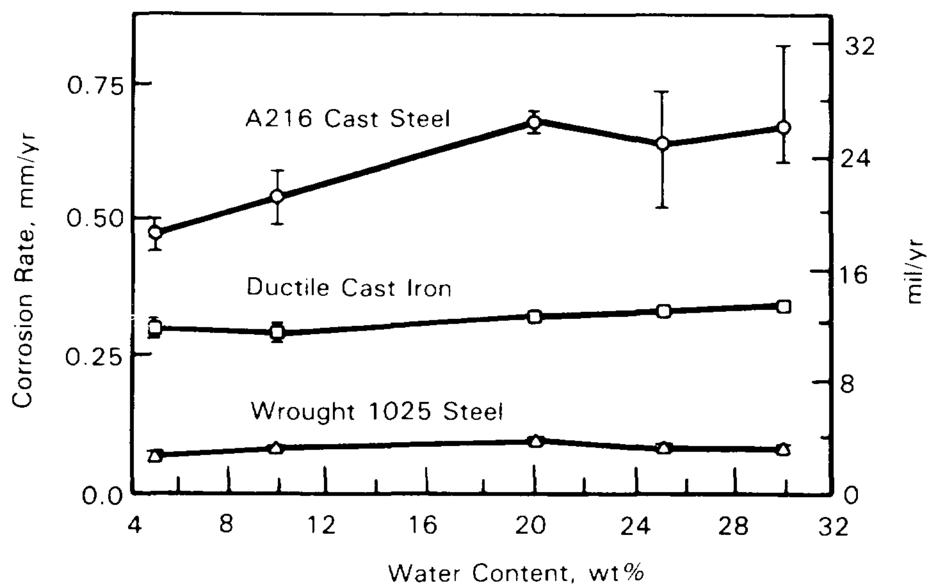

FIGURE 9. Corrosion Rates of Ferrous Materials in Dried Synthetic PBB1 Salt Moistened with PBB3 Brine; 3 Months Exposure at 150°C. Range of values for four specimens of each material represented by vertical bar at each data point. Data point is average of specimen values.

each can, with the range of values obtained from the four replicate specimens of each material shown at each point by a vertical bar. The estimated average rate, standard error, and 95% confidence limits on the corrosion rates of A216 steel in the 1-, 2-, and 3-month tests are presented in Table E.2, Appendix E. These data show, with 95% confidence, that under all conditions the A216 steel corrosion rate was significantly greater than those of the other two materials, and that the ductile cast iron rate was significantly higher than that of the 1025 wrought steel. The specimen-to-specimen corrosion rate variability was considerably higher for the A216 steel than for the other materials.

The penetration rates found after the 1- and 3-month exposures agreed well, suggesting constant linear corrosion rates over the test durations of the study. The rates found for penetration of all of the materials were far higher than those found in past autoclave tests, up to 30 times greater in the case of the A216 steel. On removal from the cans, specimens of both the A216 steel and the ductile cast iron were encased in soft layers of bluish-gray material, having a claylike texture, about 2 mm (0.08 in.) thick. After standing in air, the bluish-gray material rapidly showed evidence of the red-brown ferric ion. The wrought steel specimens, on the other hand, showed the magnetite (Fe_3O_4) film characteristic of specimens from the autoclave studies.

Further testing was undertaken to determine the reason for the high corrosion rates of A216 steel observed in the moist salt tests. The moist salt tests differed from autoclave tests in the following ways:

- a solid phase was present
- the tests were static
- the tests were highly anoxic
- the tests contained significant quantities of Mg^{2+}.

An additional observation was the low corrosion rates of 1025 wrought steel relative to the A216 steel. This finding initiated a question as to the importance of the microstructure, hence heat treatment, of the reference steel material, as the wrought (hot-rolled) material would be expected to be more homogeneous than the as-cast material given its thermal-mechanical history.

It was decided that tests would be initiated that would address primarily the questions of heat treatment and Mg^{2+} concentration.

A series of moist salt tests was therefore initiated in which specimens of as-cast, homogenized, and normalized A216 Grade WCA reference steel were exposed for 1 month at 150°C to three different environments, each with water added to the 20% by weight level by brine addition:

- dried NaCl with NaCl brine addition (0% Mg)
- dried PBB1 with PBB1 brine addition (0.042% Mg)
- dried PBB1 with PBB3 brine addition (1.7% Mg).

The results of these tests are presented in Table 6. The raw data may be found in Appendix B.3.

The effect of heat treatment on the reference steel is shown to be minimal, but the effect of environment is extremely large. The NaCl/NaCl and PBB1/PBB1 environments yield corrosion rates similar to those found in the autoclave studies. The PBB3 addition results in very high corrosion rates, similar to those found previously (Figures 8 and 9). The statistical treatment of the data shown in Table 6 is presented in Table E.3, Appendix E.

While it is not clear at present why the PBB1/PBB3 environment is so much more aggressive toward the steel than the NaCl/NaCl and PBB1/PBB1 environments, Mg^{2+} is strongly implicated in the formation of the claylike layer found on all specimens that exhibit rapid corrosion; that is, all but the 1025 wrought steel specimens in Figures 8 and 9, and all specimens in the PBB1/PBB3 test reported in Table 6. (All specimens in the two low-Mg^{2+} tests of Table 6 formed thin,

TABLE 6. Corrosion Rates of Reference A216 Grade WCA Steel in Moist Salt Environments 150°C, 1 month, 20% H_2O

Steel Treatment	Average Corrosion Rates,[a] mm/yr (mil/yr) NaCl/NaCl	PBB1/PBB1	PBB1/PBB3
As-cast	0.0046 (0.18)	0.011 (0.43)	0.58 (23)
Homogenized	0.0043 (0.17)	0.010 (0.41)	0.91 (36)
Normalized	0.0048 (0.19)	0.010 (0.40)	0.76 (30)

(a) Average of 4 specimens per heat treatment in each environment.

smooth Fe_3O_4 corrosion product films.) A specimen of the claylike layer scraped from a specimen from a 30% H_2O, PBB1/PBB3, 2-month exposure test showed a magnesium concentration of 5% to 7%, whereas the bulk salt mass showed a concentration of only 1.5%. A specimen of this claylike layer showed no crystallinity upon being dried and subjected to an XRD analysis. However, a steel specimen taken from the 20% H_2O, PBB1/PBB3 test (Table 6) showed evidence of a complex magnesium-containing ferrous hydroxide on its washed and dried surface, with no evidence of Fe_3O_4. It appears that Mg^{2+} may concentrate on or near the corroding steel surface, substitute in the ferrous hydroxide layer for Fe^{2+}, and interfere with the normally expected conversion of $Fe(OH)_2$ to magnetite. The $Fe(OH)_2$ layer appears to have little or no ability to protect the metal surface from corrosion.

Further evidence of the importance of Mg^{2+} in the environment is the general observation that corrosion rates increase with Mg^{2+} concentration. This observation is illustrated in Figure 10, which summarizes all of the as-cast A216 steel moist salt corrosion data contained in the present report. Attributing the corrosion observed to be strongly dependent on Mg^{2+} concentration assumes that the water concentration in the system over the range studied (5% to 30%) is not an overriding consideration. This appears to be a reasonable conclusion, as the lowest corrosion rates shown in Figure 10 (the NaCl/NaCl and PBB1/PBB1 tests) were both associated with relatively large amounts of water (20%).

The microstructure at the surface of a severely corroded specimen of as-cast A216 steel after 3 months exposure to a PBB1/PBB3 environment at 150°C is shown in Figure 11. The selective attack of the alpha phase, presumed to be anodic to the pearlite grains, which remain relatively unaffected, is clearly shown in the micrograph.

IRRADIATION-CORROSION--INTRUSION BRINE

All of the irradiation-corrosion studies described in this report are considered accelerated, in the sense that the irradiation intensity levels used in

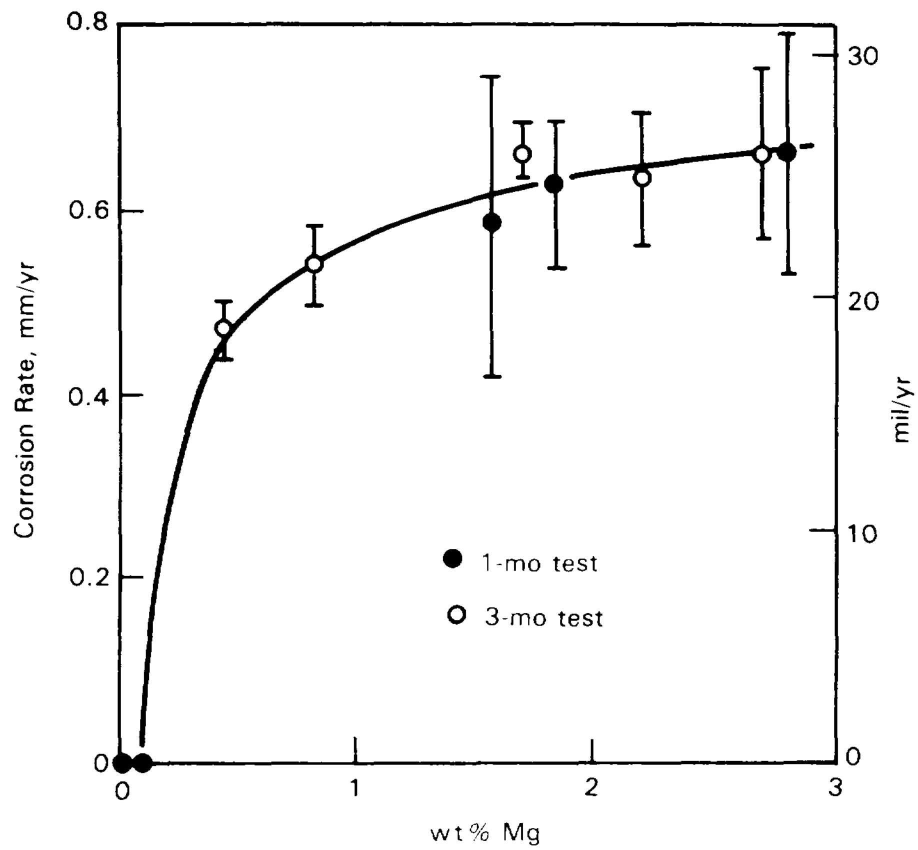

FIGURE 10. Dependence of Corrosion Rate on Mg Concentration (Mg concentration based on dry weight). Bands associated with data points (specimen groups) represent 95% confidence limits.

the tests were a factor of 10 to 1000 higher than those expected at the surface of a waste package containing spent fuel and having a thick steel overpack, i.e., <100 rad/h maximum.[3]

The corrosion rates of a variety of candidate ferrous materials were determined in 150°C PBB2 intrusion brine irradiated at both 1×10^5 rad/h and 2×10^3 rad/h. The brine was argon-sparged to reduce the dissolved O_2 level to ~50 ppb before it entered the autoclave systems. A summary of the materials exposed in these tests, and the maximum test durations, is presented in Table 7.

The corrosion rates observed at an irradiation intensity of 1×10^5 rad/h are shown in Figure 12, compared with data obtained from the unirradiated system. All of the available data are grouped within the scatter bands shown in

FIGURE 11. Microstructure at Surface of As-Cast A216 Steel Specimen, 3 Months Exposure, 150°C, PBB1/PBB3 Environment, 30% H_2O, 300X

TABLE 7. Materials Exposed in Irradiation-Corrosion Studies

Test Type	Material	Maximum Exposure Time, mo	Total Number of Specimens Tested[a]
1×10^5 rad/h	A216 steel	5	14
	A27 steel, normalized	15	7
	A27 steel	18	9
	1025 wrought steel	18	13
	Ductile cast iron	17	9
	2-1/2% Cr, 1% Mo steel	11	10
	High-purity iron	15	8
2×10^3 rad/h	A216 steel	7	14
	A27 steel, normalized	13	9
	1025 wrought steel	13	9
	Ductile cast iron	13	13
	High-purity iron	12	10

(a) Specimens yielding useful metal penetration data. Additional specimens, designated NA in the corrosion rate data columns of Appendix C, were used for surface analysis investigations.

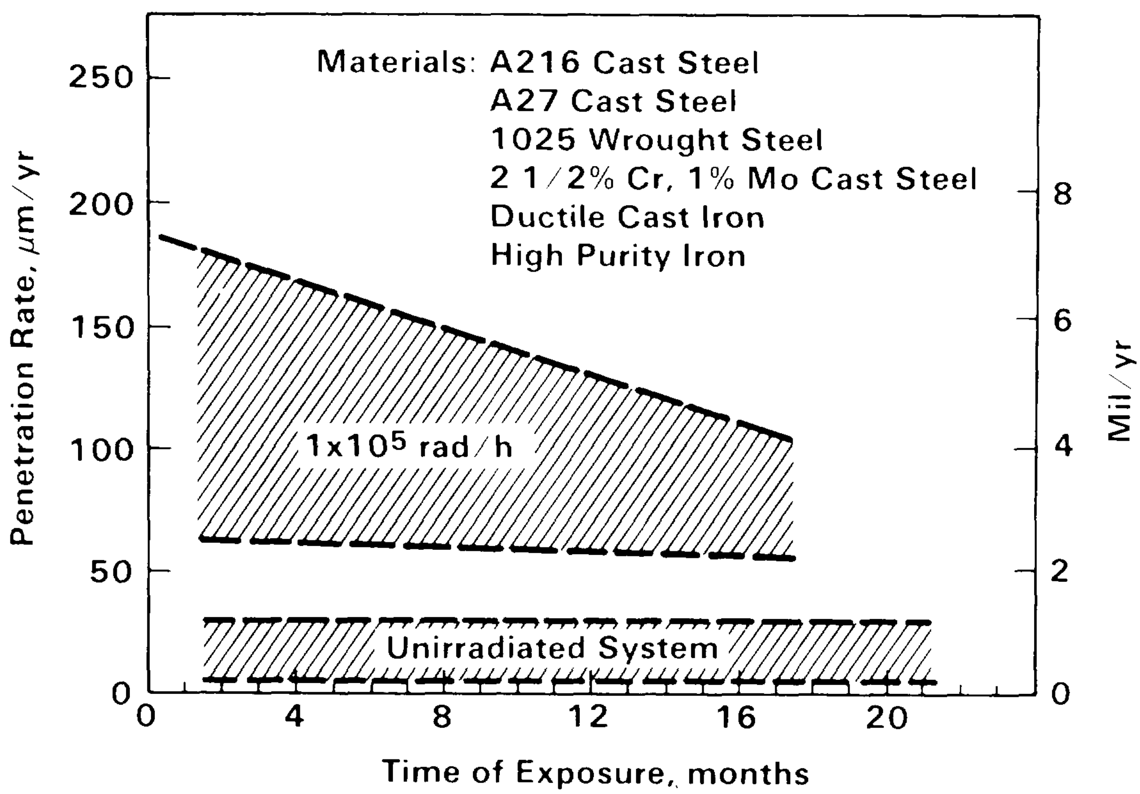

FIGURE 12. Penetration Rates of Ferrous Materials Obtained in 150°C PBB2 Irradiated at 1×10^5 rad/h Compared with Data from Unirradiated System

the figure. The irradiated-system corrosion rates are decreasing with time; but at the end of the test (18 months) an acceleration of a factor of ~4 is still present. The data obtained under the same test circumstances, but at an irradiation intensity of 2 x 10^3 rad/h, are presented in Figure 13, once again simply grouped within scatter bands. At this lower and more realistic level of irradiation intensity, the corrosion rates reverted to essentially the same level as those observed in the nonirradiated studies. All of the raw data associated with Figures 12 and 13 are presented in Appendix C.

The corrosion data of Appendix C were statistically analyzed in order to test hypotheses concerning the differences in behavior among materials, to examine trends in the data, and to quantify random variabilities. As before, significant differences were interpreted as being significantly different at the 95% confidence level.

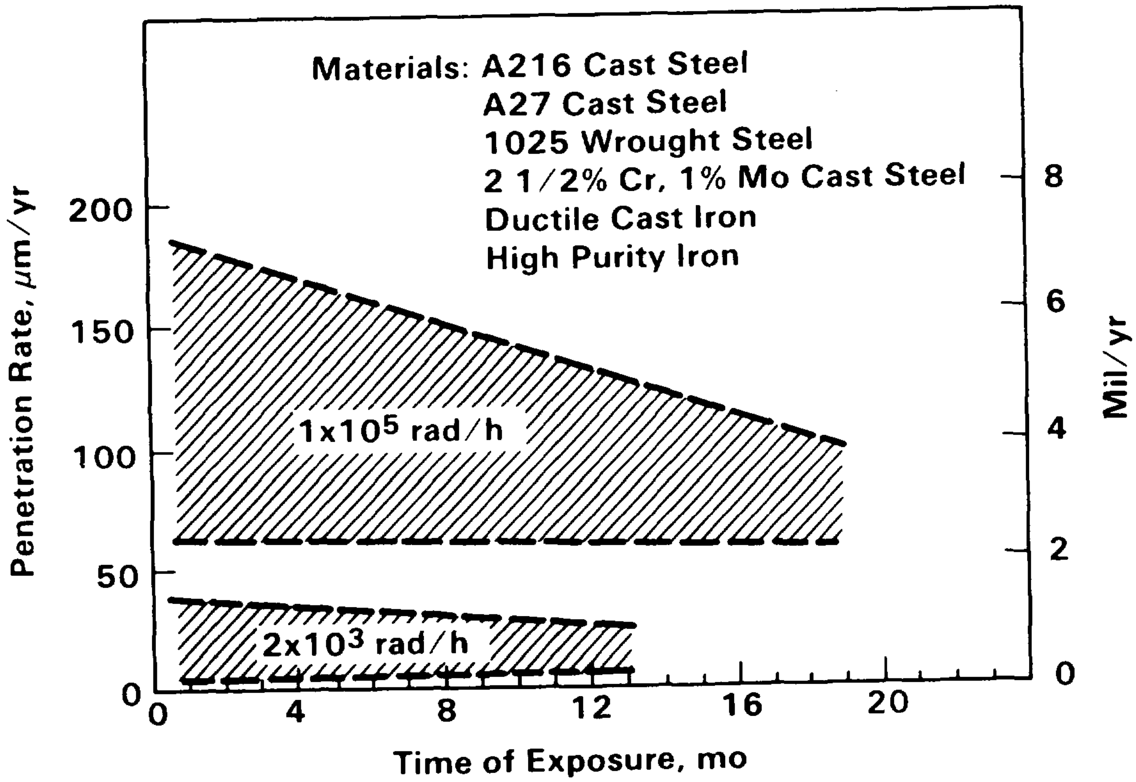

FIGURE 13. Penetration Rates of Ferrous Materials Obtained in 150°C PBB2 Irradiated at 1 x 10^5 rad/h and 2 x 10^3 rad/h

The test specimens in the irradiation-corrosion test autoclaves were arranged so that they lay horizontally and varied vertically in position. There appeared to be a location effect on the corrosion rates observed, in both the 2 x 10^3 rad/h test and the 1 x 10^5 rad/h test.

A statistical model[a] of the following form was used to test for material differences, time effects, and location effects in the 2 x 10^3 rad/h test:

$$\text{Rate} = \mu + M_i + L + H + H^2 + H^3 + L_i + H_i + H_i^2 + \varepsilon$$

where μ = overall corrosion rate mean

M_i = effect of the ith material

L = overall linear location effect

H = overall linear time effect in hours

H^2 = overall quadratic time effect

L_i = linear location effect for the ith material in addition to the overall location effect indicating a different location slope for each material

H_i^2 = linear time effect for the ith material in addition to the overall linear time effect indicating a different time slope for each material

H_i = quadratic time effect for the ith material in addition to the overall quadratic time effect

H^3 = cubic time effect

ε = random error.

Using this model, 97% of the total variability was explained in the 2 x 10^3 rad/h test. This model is not an attempt to provide a general corrosion model, but is only an approximation to the true model describing these data and is intended to be used only for the present statistical analysis. The underlying true model may be better characterized by some nonlinear mechanistic model. However, because this is an exercise in determining the significance of

(a) Statistical modeling of effects is a general technique widely used by statisticians to determine which experimental factors significantly affect experimental response variables.[9]

the effects of time, location, and materials and not an exercise in model development, the polynomial approximation was used. These statistical models should not be used to predict data values outside the range of these experimental data. Each of the terms in the above model was statistically significant. This means that the corrosion curves across time and location were different for some of the materials.

Material differences can be examined at various time and location combinations. Table 8 presents the estimated corrosion rate averages and comparisons of the materials for specimens located near the top, center, and bottom of the autoclave for 1300, 4360, and 9000 hours in the autoclave. At 1300 hours, the high-purity iron rate is significantly higher than that for other materials. The ductile cast iron corrosion rate is significantly lower than that of high-purity iron but significantly greater than 1025 wrought steel, A216, and normalized A27. Also, normalized A27 rates appear to be lower than the A216 and 1025 wrought steel rates except near the bottom of the autoclave.

At 4360 hours, the high-purity iron rate is significantly higher than other material rates. There are no significant differences among the rates of the other materials except near the bottom of the autoclave where the A216 steel rate is significantly lower than the normalized A27 rate.

At 9000 hours there are no significant differences among any of the material rates near the center and bottom of the autoclave. This is due to the fact that the corrosion rate for high-purity iron decreased over time at a much greater rate (slope) than for the other materials. The estimated rate for ductile cast iron is significantly higher than those for the high-purity iron and 1025 wrought steel near the top of the autoclave. Averages for A216 steel were not available in the 9000-hour range and estimates are not reported in Table 8. By examining Table 8, it can be seen that the high-purity iron rate is not affected by the location in the autoclave. On the other hand, A216 steel corrosion rates are greatly affected by location differences. It should be noted that the estimated averages at each time/location combination are in fact estimates. The uncertainty about each estimate is related to the number of

TABLE 8. Comparison[a] of Material Corrosion Rate Estimated Means at Various Combinations of Hours and Location in the 150°C, PBB2, 2×10^3 rad/h Test

Material	Hours	Location: Top Rate[b]	Top Comparison	Center Rate	Center Comparison	Bottom Rate	Bottom Comparison
High-purity iron	1300	48.4	A	48.4	A	48.4	A
Ductile cast iron		27.8	B	25.7	B	23.5	B
1025 wrought steel		17.9	CD	17.3	C	16.7	C
A216 steel		20.7	C	17.1	C	13.5	C
Normalized A27 steel		13.1	D	12.4	D	11.8	C
High-purity iron	4360	23.8	A	23.8	A	23.8	A
Ductile cast iron		16.5	B	14.3	B	12.2	BC
1025 wrought steel		12.9	B	12.3	B	11.7	BC
A216 steel		15.6	B	12.0	B	8.4	C
Normalized A27 steel		16.2	B	15.5	B	14.9	B
High-purity iron	9000	12.4	B	12.4	A	12.4	A
Ductile cast iron		21.3	A	19.2	A	17.1	A
1025 wrought steel		15.6	B	14.9	A	14.3	A
Normalized A27 steel		17.7	AB	17.1	A	16.4	A

(a) Materials that share the same letter (A, B, C, or D) within each time/location combination are not significantly different with respect to corrosion rate at the 95% confidence level.
(b) Rates are given in terms of μm/yr penetration.

actual data values of that material near that particular time/location combination. The estimates provide an understanding of how material comparisons change from time to time and location to location.

The 1×10^5 rad/h tests were performed in the same manner as the one irradiated at 2×10^3 rad/h, and a similar location effect was observed. The statistical model was similar, except that allowance was made for the observation that the time effect seemed to be linear across $\log_{10}$(hours) within the experimental time period. Again, this model is only an approximation to the true model. It may well be that the underlying true model is very similar to the true model for the data irradiated at 2×10^3 rad/h. The model[(a)] used was

$$\text{Rate} = \mu + M_i + L + H' + L_i + H_i' + \varepsilon$$

where μ = overall corrosion rate mean

M_i = effect of the ith material

L = overall linear location effect or slope

H' = overall log-linear time effect or slope

L_i = linear location effect for the ith material in addition to the overall location effect indicating a different location slope for each material

H_i' = log-linear time effect for the ith material in addition to the overall time effect indicating a different time slope for each material

ε = random error.

Using this model, 90% of the total variability of corrosion rates was explained. All effects represented by each of the terms in the above model were statistically significant. Thus, the corrosion curves across time and location are different for some of the materials. Material differences can be examined at various time and location combinations (Table 9).

Generally speaking, corrosion rates near the top of the autoclave were greater than rates near the bottom, as in the 2×10^3 rad/h test. The high-purity iron rates decreased more rapidly over time than the rates of the other materials. For shorter time periods, high-purity iron rates are higher than rates of other materials, but for longer time periods the high-purity iron

(a) Statistical modeling of effects is a general technique widely used by statisticians to determine which experimental factors significantly affect experimental response variables.[(9)]

rates are either not statistically different or lower than other material rates. The 2-1/2% Cr, 1% Mo steel was usually lowest except near the bottom of the autoclave at longer time periods.

The reason for the effect of sample location on corrosion rate in the irradiated autoclave tests is not known. Because the specimens near the top of the autoclave corroded, in general, at the highest rate, one might postulate that products of radiolysis have an effect on the corrosion rate, and that they are either swept away from the bottom of the autoclave by the ingress of fresh brine, or that they concentrate near the top of the autoclave because of gravitational segregation.

Two normalized cast A27 steel values were deleted from the statistical analyses. The deleted samples were P149 and P156. These two samples were replicate values run under the same test conditions. The difference between the two values was extremely large, significantly larger than the differences between other replicate values. Although the P156 corrosion rate is comparable to other rates from that material, the model that fit all other materials resulted in higher corrosion rates for shorter time periods, which suggests that the P156 rate should be much higher. The P149 specimen indeed resulted in a higher corrosion rate but it was much higher than would be expected. Rather than bias the results by eliminating only one of the two values or overestimating the variability by including both values, both were deleted.

The corrosion rates of A216 steel determined in the present irradiation-corrosion tests are plotted with the associated 95% confidence intervals in Figure 14. Comparison of the data of Figure 14 with those of Figure 7 shows essentially no difference between the rates found in unirradiated anoxic PBB2 and anoxic PBB2 irradiated at 2 x 10^3 rad/h. The statistical data on which Figure 14 is based are presented in Table E.4, Appendix E.

As in the case of unirradiated test coupons exposed to 150°C brine, the specimens exposed to irradiated brine formed a corrosion product layer consisting primarily of Fe_3O_4. The film is not tenacious; spallation is evident after exposures of 3 months in any 150°C brine environment. A specimen of A27 cast

TABLE 9. Comparison[a] of Material Corrosion Rate Estimated Means at Various Time/Location Combinations in the PBB2, 1 x 10^5 rad/h Test

Material	Hours	Top: Rate[b]	Top: Comparison	Center: Rate	Center: Comparison	Bottom: Rate	Bottom: Comparison
Pure iron	2000	185.0	A	148.3	A	111.6	A
A27 steel		147.7	B	120.4	B	93.0	AB
Ductile cast steel		141.7	B	118.9	AB	96.1	AB
A216 steel		141.5	B	108.2	B	74.9	B
Normalized A27 steel		140.7[c]	ABC	114.8[c]	ABC	89.2[c]	AB
1025 wrought steel		131.5	B	109.5	B	87.4	AB
2-1/2% Cr, 1% Mo		91.5	C	79.8	C	68.0	B
Pure iron	5000	137.1	A	100.4	AB	63.7	AB
A27 steel		132.5	AB	105.1	AB	77.7	AB
Ductile cast iron		128.5	AB	105.7	A	82.9	A
A216 steel		120.1	AB	86.8	BC	53.4	B
Normalized A27 steel		120.3	AB	94.6	ABC	69.0	AB
1025 wrought steel		114.1	B	92.1	AB	70.0	AB
2-1/2% Cr, 1% Mo		80.7	C	68.9	C	57.2	AB
Pure iron	10000	101.2	AB	64.5	B	27.8	C
A27 steel		121.0	A	93.7	A	66.3	AB
Ductile cast iron		118.7	A	95.8	A	73.0	A
A216 steel		104.0[c]	AB	70.7[c]	AB	37.4[c]	BC
Normalized A27 steel		105.2	AB	79.5	AB	53.9	ABC
1025 wrought steel		101.1	AB	79.0	AB	57.0	ABC
2-1/2% Cr, 1% Mo		72.5	B	60.8	B	49.0	ABC

(a) Materials that share the same letter (A, B, or C) within each time/location combination are not significantly different with respect to corrosion rate at the 95% confidence level.

(b) Rates are given in terms of μm/yr penetration.

(c) These averages are purely estimates. No data were available near this time period. Extrapolation of results to a time region unrepresented by data may produce erroneous results.

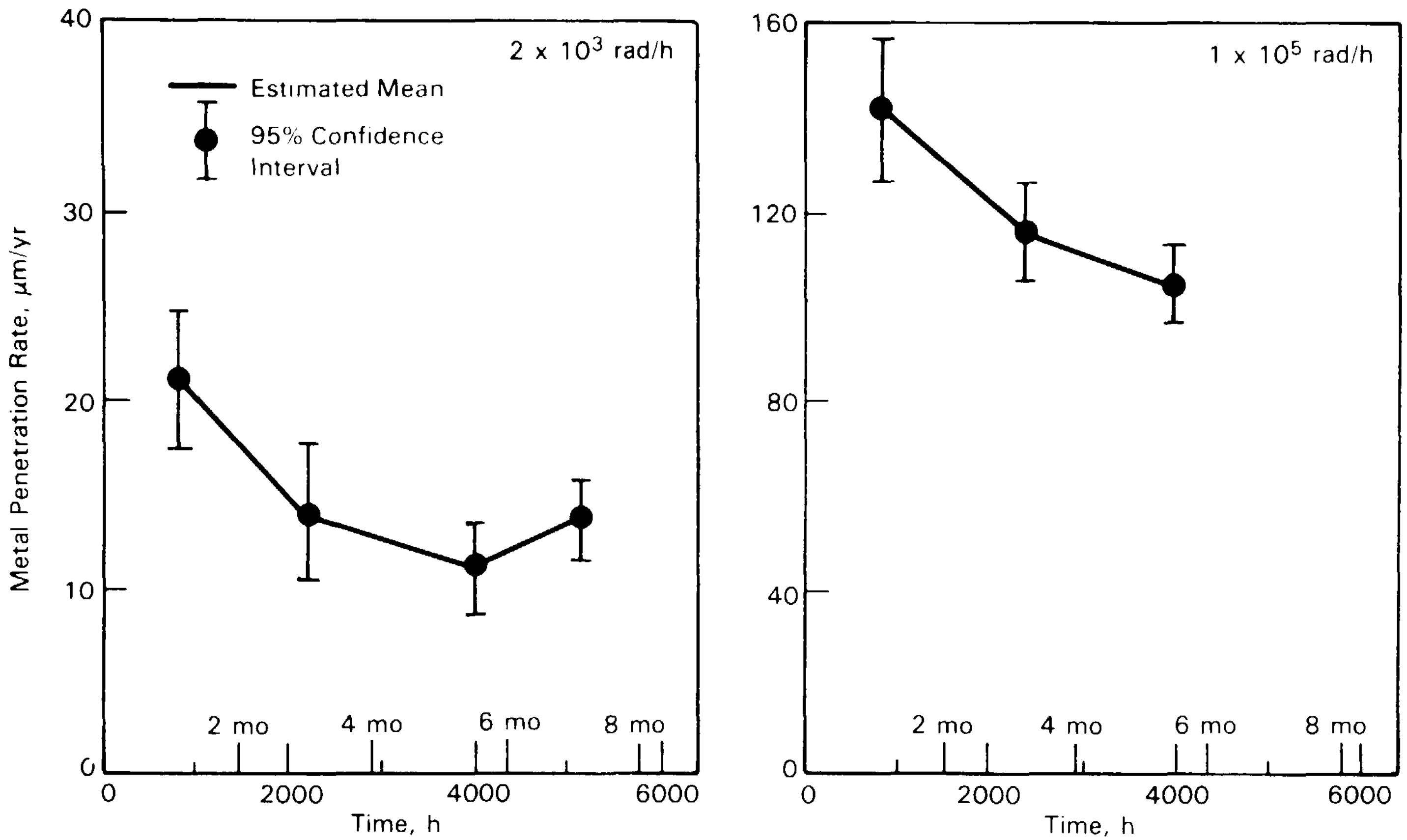

FIGURE 14. Estimated Means of Metal Penetration Rates and 95% Confidence Intervals About the Means--A216 Steel, 150°C, Brine PBB2, Irradiated at 2 x 10^3 rad/h and 1 x 10^5 rad/h

steel, removed from the autoclave after 11 months exposure to 150°C PBB2 at 1×10^5 rad/h is shown in Figure 15. This specimen exhibited a typical tendency, shown by specimens from both irradiated and nonirradiated corrosion tests, to "shed" its oxide film upon removal from test. The surfaces of the steel corrosion specimens seldom showed signs of significant nonuniform attack in these studies, in spite of the unprepossessing appearance of the specimens before stripping. And although the oxide is not strongly adherent, it obviously offers a certain amount of corrosion protection, as the corrosion rates observed generally decrease somewhat with time. A 45° taper-section view of a typical oxide film is provided in Figure 16. This film is much thinner than the one shown in Figure 15; it was formed in 150°C PBB2 at 2×10^3 rad/h during an exposure time of 6 months. The cracked, semi-adherent nature of the oxide is obvious from these micrographs.

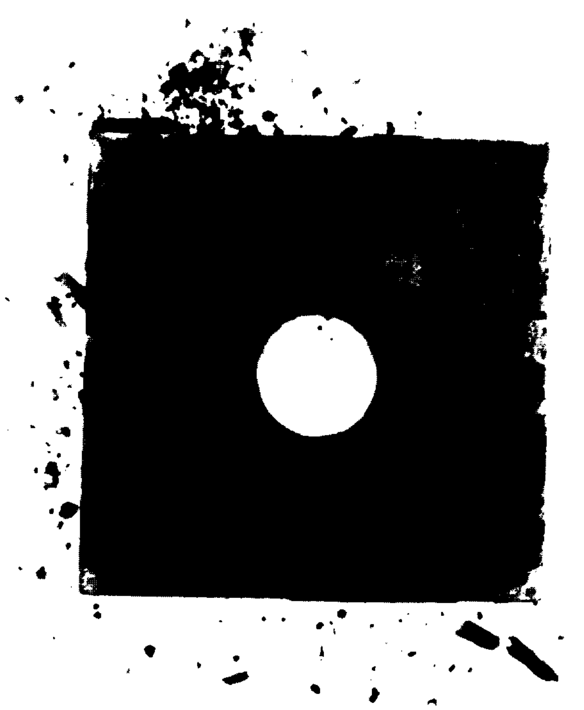

FIGURE 15. Specimen of A27 Steel Exposed to 150°C PBB2 at an Irradiation Intensity of 1×10^5 rad/h for 11 Months. Note ready spallation of Fe_3O_4 corrosion product.

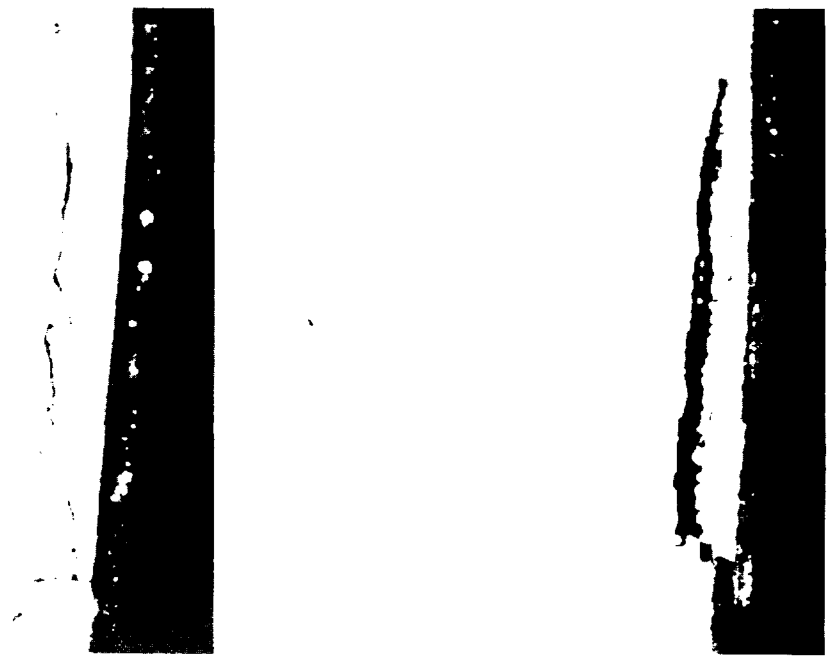

a) 10 µm   b) 10 µm

FIGURE 16. Scanning Electron Micrographs of Surface Film on a Specimen of ASTM A27 Cast Steel After 6 Months Exposure to PBB2 at 150°C and 2 x 10^3 rad/h

Evidence of nonuniform corrosion attack, especially the formation of deep pits that propagate into the metal at a rate faster than the more-or-less uniform regression of the metal surface, would pose serious problems to a waste package overpack, and, of course, to any candidate overpack material that evidenced such attack. A specimen of A216 steel was designed (Figure 17) to test whether, in an irradiation brine environment, the irradiated solutions residing within deep pits would exhibit a degree of aggression toward the steel different from that on or near the sample's free surface. The artificial pits were created by drilling. After an exposure of 4 months to 150°C PBB2 irradiated at 1 x 10^5 rad/h, the specimen was removed from test and carefully ground to its half-thickness (Figure 18). When the oxide was removed from the "pits," it was found that no unusual corrosion had occurred, i.e., the pits had not increased in diameter to any greater extent than would have been expected by the normal corrosion process, and there was no evidence of any localized corrosion within the pits.

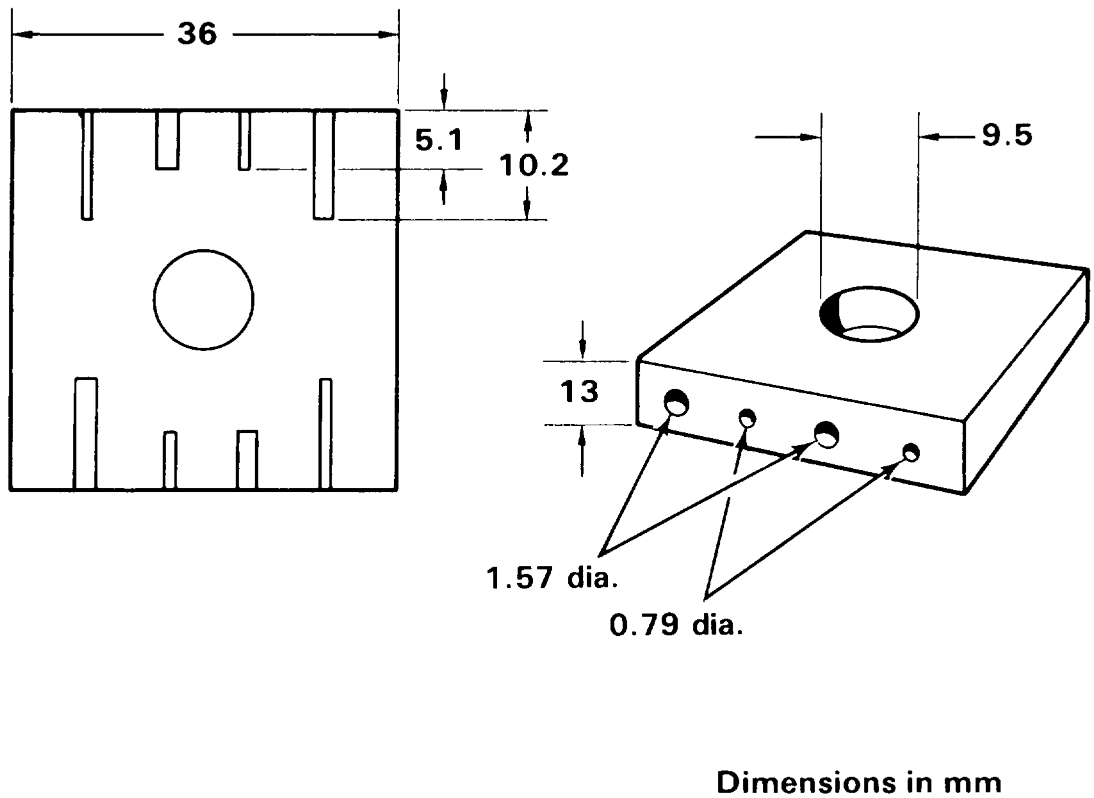

FIGURE 17. Pitting Corrosion Specimen

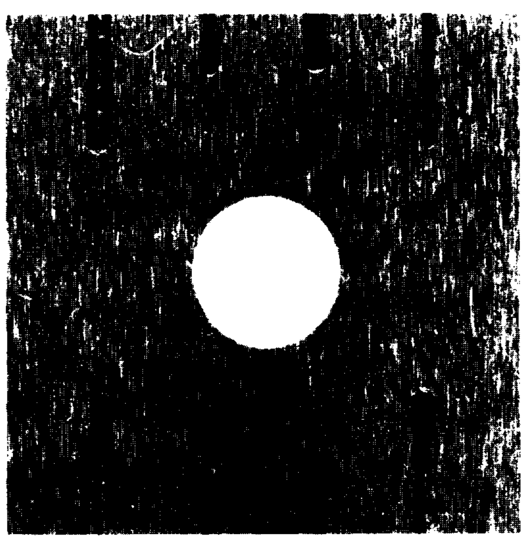

FIGURE 18. Artificially Pitted Specimen, Exposed 4 Months to 150°C PBB2 1 x 10^5 rad/h. After exposure, specimen was ground to half-thickness for pit examination.

This limited test, of course, does not necessarily preclude the possibility of self-propagating pits forming in A216 steel in a repository environment, but it offers some preliminary assurance that there is no such overt tendency.

ENVIRONMENTAL-MECHANICAL TESTING

Environmental-mechanical tests (i.e., SSR tests and corrosion fatigue tests) were performed to determine the resistance of candidate overpack materials to enviromentally assisted crack propagation, the important rate-limiting aspect of SCC if a flaw is (conservatively) expected to pre-exist. In the SSR test, flaws are produced during the straining and plastic deformation of the material; in the corrosion fatigue test, the flaw is of known geometry, permitting an estimate of the stress concentration existing at a crack tip.

Slow-Strain-Rate (SSR) Tests

SSR tests of wrought 1025 steel, A27 steel, and reference A216 Grade WCA cast steel have been performed in flowing (~35 mL/h) PBB2 and in air at 150°C. The results of these tests are summarized in Table 10. Limited tests of the reference cast steel have also been performed under irradiated conditions at 30°C and 90°C; these results are given in Table 11. A statistical evaluation of the data is included in Tables 10 and 11, with a more complete presentation in Appendix D.

The results of SSR tests on wrought 1025 steel are shown in Figure 19. These results are representative of those obtained from testing the other ferrous materials in slowly flowing (~35 mL/h) PBB2 at 150°C. The following observations can be made from an examination of the figure, and are supported by the statistical evaluation presented in Appendices D and E.

- Reduction of area was significantly reduced at the lower strain rate (2×10^{-7}/s) when tests were done in brine.
- Neither reduction of area nor elongation was affected by the brine when tests were done at a relatively high strain rate (1×10^{-4}/s).
- Reduction of area and elongation were about the same at 2×10^{-7}/s as at 1×10^{-4}/s when tests were done in air.

TABLE 10. Slow-Strain-Rate Test Results and Statistical Analyses. All tests performed at 150°C.

Material	Strain Rate	Reduction of Area (average values), %: Air (std. error)	Reduction of Area: PBB2 Brine (std. error)	Reduction of Area: Diff.[a]	Elongation (average values), %: Air (std. error)	Elongation: PBB2 Brine (std. error)	Elongation: Diff.[a]
Wrought 1025 steel (TL)[b]	1×10^{-4}/s	69.5 (3.12)	71.5 (3.12)	No	30.5 (1.14)	32.5 (1.14)	No
Wrought 1025 steel (LT)[b]		55.5 (3.12)	51.0 (2.55)	No	22.0 (1.14)	21.7 (0.93)	No
Cast A27 steel		53.0 (4.42)	49.0 (3.12)	No	22.0 (1.61)	24.5 (1.14)	No
2.5% Cr, 1% Mo steel		63.5 (3.12)	51.5 (3.12)	No	19.5 (1.40)	19.5 (1.40)	No
A216 cast steel		28.7 (2.55)	20.3 (2.21)	No	17.7 (0.93)	14.5 (0.80)	No
Wrought 1025 steel (TL)	2×10^{-7}/s	61.5 (3.12)	21.0 (3.12)	Yes	29.0 (1.14)	36.5 (1.14)	Yes
Wrought 1025 steel (LT)		52.0 (4.41)	28.5 (3.12)	Yes	24.0 (1.61)	17.5 (1.14)	Yes
Cast A27 steel		47.0 (3.12)	14.8 (1.97)	Yes	21.5 (1.14)	13.8 (0.72)	Yes
2.5% Cr, 1% Mo steel		60.0 (4.42)	32.5 (3.12)	Yes	19.0 (1.60)	15.5 (1.14)	No
A216 cast steel		25.7 (2.55)	16.5 (3.12)	Yes	19.0 (1.61)	12.7 (0.93)	Yes

(a) Refers to whether or not a significant difference exists between the average values, in air and brine environments, at the 95% confidence level.
(b) Specimens perpendicular to the rolling direction of the plate are designated "TL"; those parallel to the rolling direction are designated "LT."

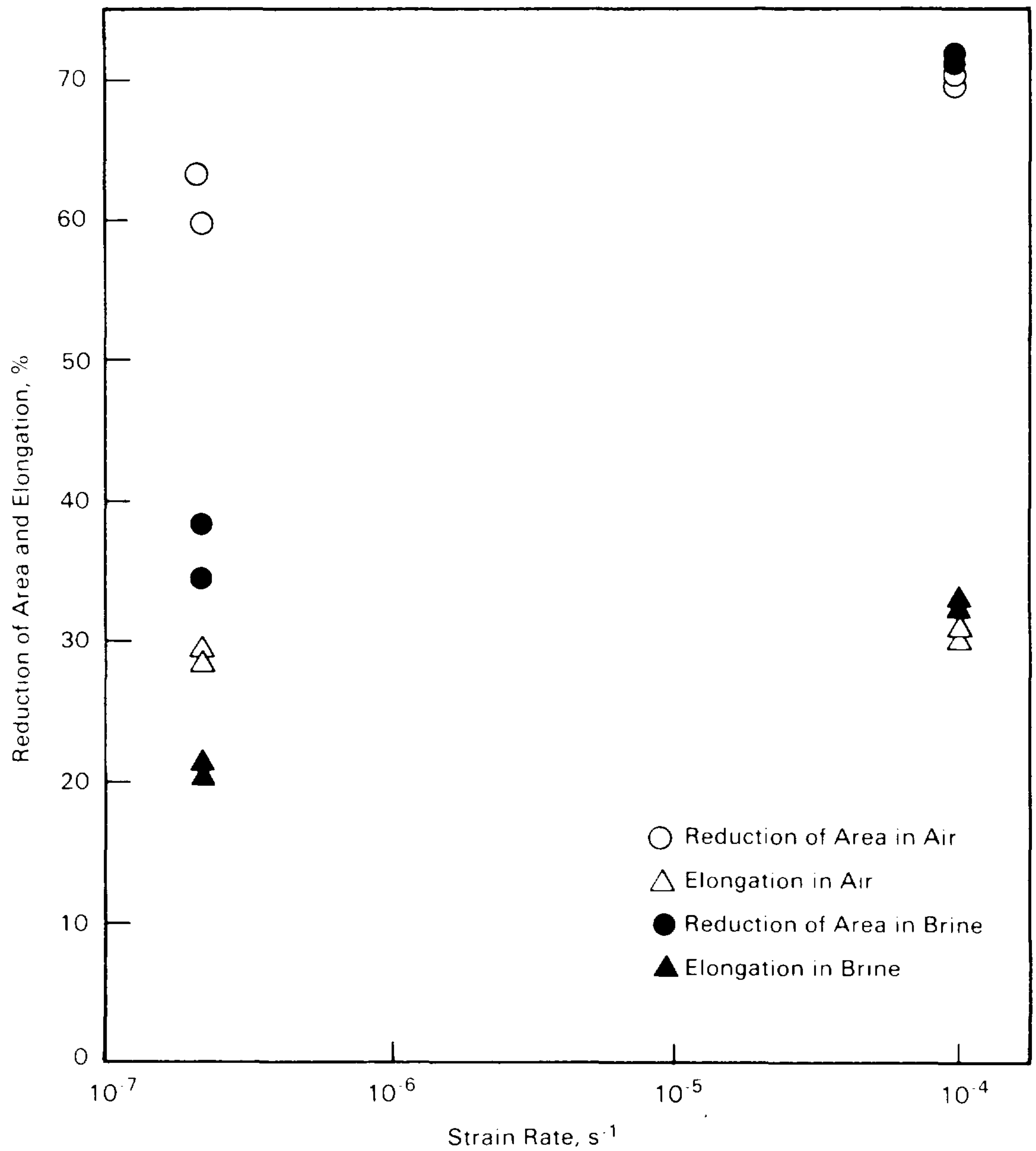

FIGURE 19. SSR Test Results for Wrought 1025 Steel in 150°C PBB2 and Air; Reduction of Area and Elongation Versus Strain Rate

Results of testing the ASTM A27 cast steel in brine and in air are given in Figures 20 through 23. The reduction of area was severely diminished at the lower strain rate, as shown in Figure 20. The degree of ductility decrease was similar to that of the 1025 steel. Reduction of area in air was not dependent on strain rate.

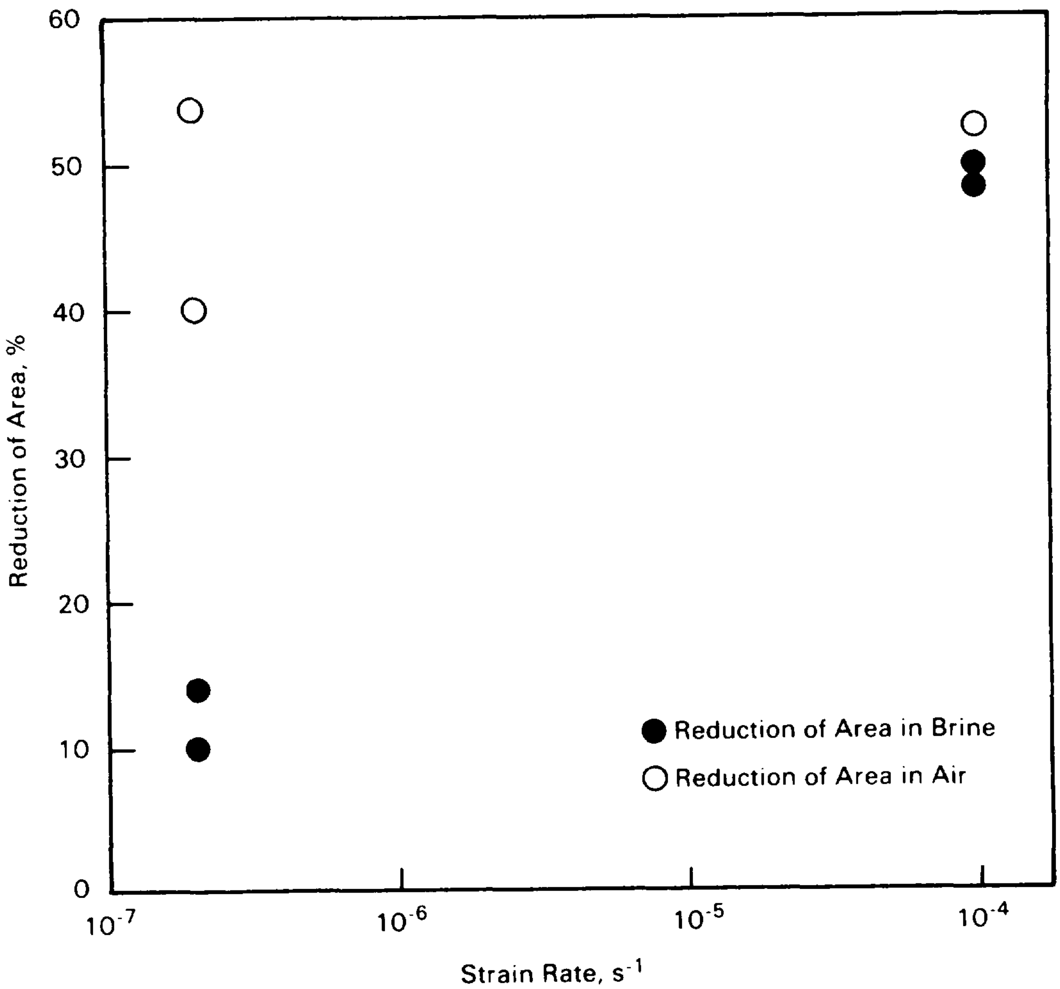

FIGURE 20. SSR Test Results for A27 Cast Steel in PBB2 and Air at 150°C; Reduction of Area Versus Strain Rate

The areas under the load-elongation plots were measured to determine the energy absorbed during deformation and fracture, as another means of determining susceptibility to environmentally assisted fracture. The total energy absorbed was significantly lower at the lower strain rate (Figure 21). The largest relative change was in the energy absorbed after maximum load.

Tests were conducted in PBB2 at different levels of dissolved oxygen to determine the environmental conditions under which the decrease in ductility occurred. As shown in Figure 22, the energy absorbed during deformation was

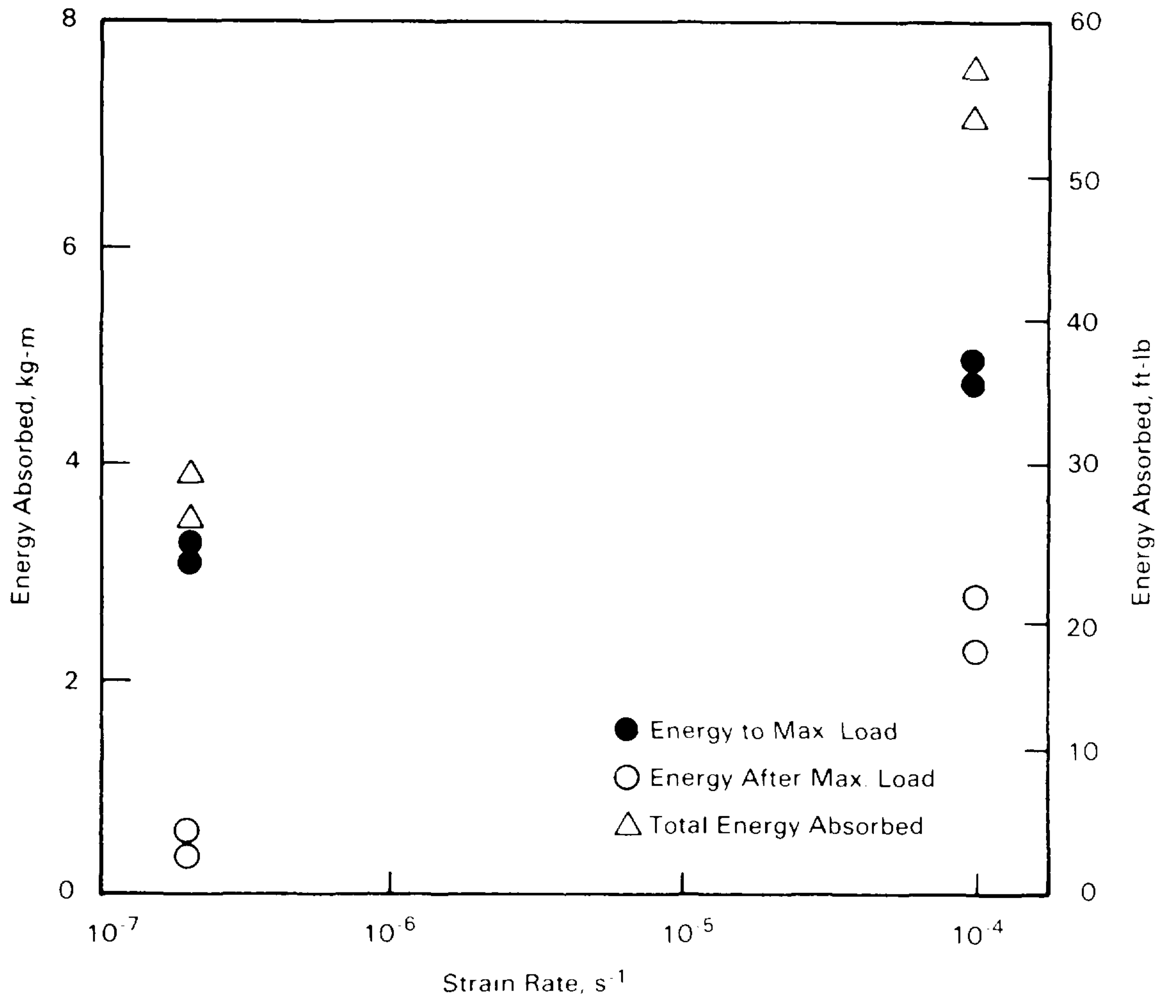

FIGURE 21. SSR Test Results for A27 Cast Steel in PBB2 at 150°C; Energy Absorbed During Deformation and Fracture Versus Strain Rate

not affected by changes in dissolved oxygen in tests in argon-sparged brine (approximately 0.1 ppm dissolved oxygen at inlet to autoclave), Ar-20% O_2-sparged brine (approximately 1 ppm dissolved oxygen at inlet), and oxygen-sparged brine (approximately 2 to 3 ppm dissolved oxygen at inlet). This indicates either that the mechanism responsible for the diminished ductility and corresponding low energy absorption is not affected by dissolved oxygen content, or that the dissolved oxygen levels used in the tests were not low enough to preclude operation of the mechanism.

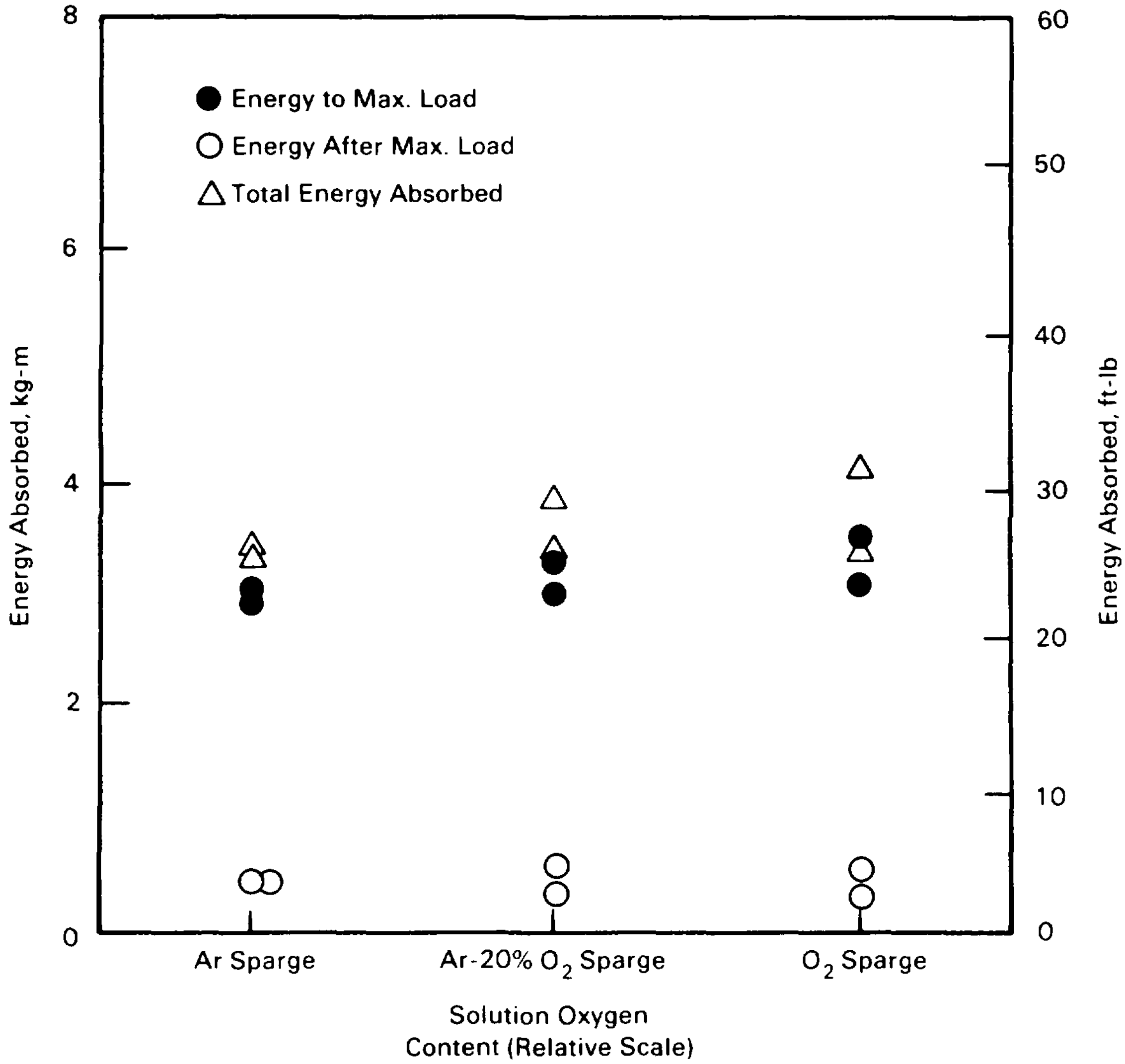

FIGURE 22. SSR Test Results for A27 Cast Steel in 150°C PBB2 Sparged with Ar, Ar-20% O_2, and O_2. Energy absorbed during deformation and fracture versus relative solution oxygen content. All tests shown were done at 2 x 10^{-7}/s.

A series of tests were made to determine whether ductility was diminished by straining the metal at a low strain rate in the presence of the brine or as a result of the longer exposure times when tests were done at the low strain rate. In this series of tests, two specimens were exposed to the PBB2 at 150°C for the normal duration of a test at 2 x 10^{-7}/s (approximately two weeks). The

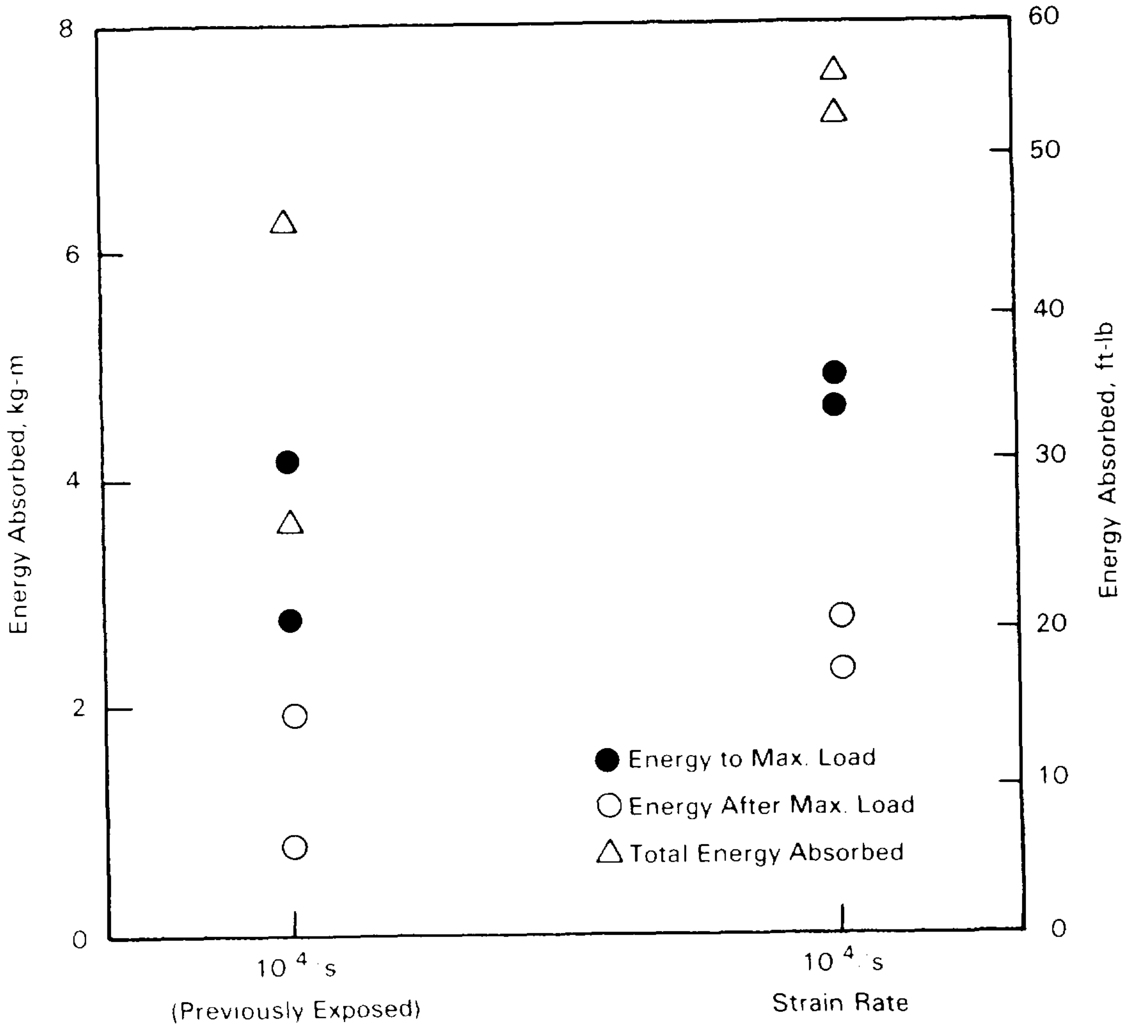

FIGURE 23. SSR Test Results for A27 Cast Steel in 150°C PBB2. Energy absorbed during deformation and fracture is shown for specimens exposed to the brine for two weeks before straining and for those tested in the usual manner. All tests shown were done at 1 x 10^{-4}/s.

specimens were then strained to failure at 1 x 10^{-4}/s. Results of these tests and of two tests performed in PBB2 at 1 x 10^{-4}/s in the usual manner are given in Figure 23.

It is clear from Figure 23 that the ductility was reduced by exposing the specimens to brine; however, the ductility was affected less than would be expected if the specimens were strained to failure at 2 x 10^{-7}/s (Figure 20).

TABLE 11. Results of Slow-Strain-Rate Tests of A216 Steel at 30°C and 90°C and Associated Statistical Analyses. The strain rate was 2×10^{-7}/s. In the irradiated test an irradiation intensity of 3×10^{5} rad/h was used.

Temperature, °C	Reduction of Area (average values), %		
	Air (std. error)	PBB2 (std. error)	Irradiated PBB2 (std. error)
30	25 (2.5)	16 (2.5)	15 (1.5)
90	39 (1.8)	23 (2.5)	15 (1.3)
	Elongation (average values), %		
	Air (std. error)	PBB2 (std. error)	Irradiated PBB2 (std. error)
30	20 (0.52)	16 (0.52)	14 (0.30)
90	22 (0.37)	16 (0.52)	14 (0.30)

As shown in Figure 23, the potential of the steel to absorb energy during deformation and fracture was reduced by exposing the specimens to brine, even in the absence of applied mechanical stresses. This indicates that SCC is probably not responsible for the observed changes in ductility, and suggests another mechanism, such as hydrogen embrittlement or dynamic strain aging, that may not depend on concurrent imposition of mechanical stress and exposure to an aggressive environment.

Scanning electron micrographs of typical A27 steel specimens strained to failure in air and in brine are given in Figures 24 through 26. It is not clear from examining these figures that there has been a change in fracture mode to correspond with the decreases in ductility. Severe pitting corrosion was observed on some specimens, especially in tests with high dissolved oxygen content (Figure 26). Minor surface cracks and secondary cracking were observed on some specimens (Figures 25 and 26). Crack-like defects occurred in some cases when porosity defects from the original casting opened as stress was applied. A good example of this phenomenon is shown in Figure 26.

SSR test results of the reference A216 cast steel are given in Figures 27 and 28. The reduction of area in air appears to decrease slightly with decreasing strain rate (Figure 27); however, this effect was found to be not statistically significant (Table 10). Reduction of area and elongation were lower in brine than in air at a strain rate of 2×10^{-7}/s, but not at a strain rate of 1×10^{-4}/s.

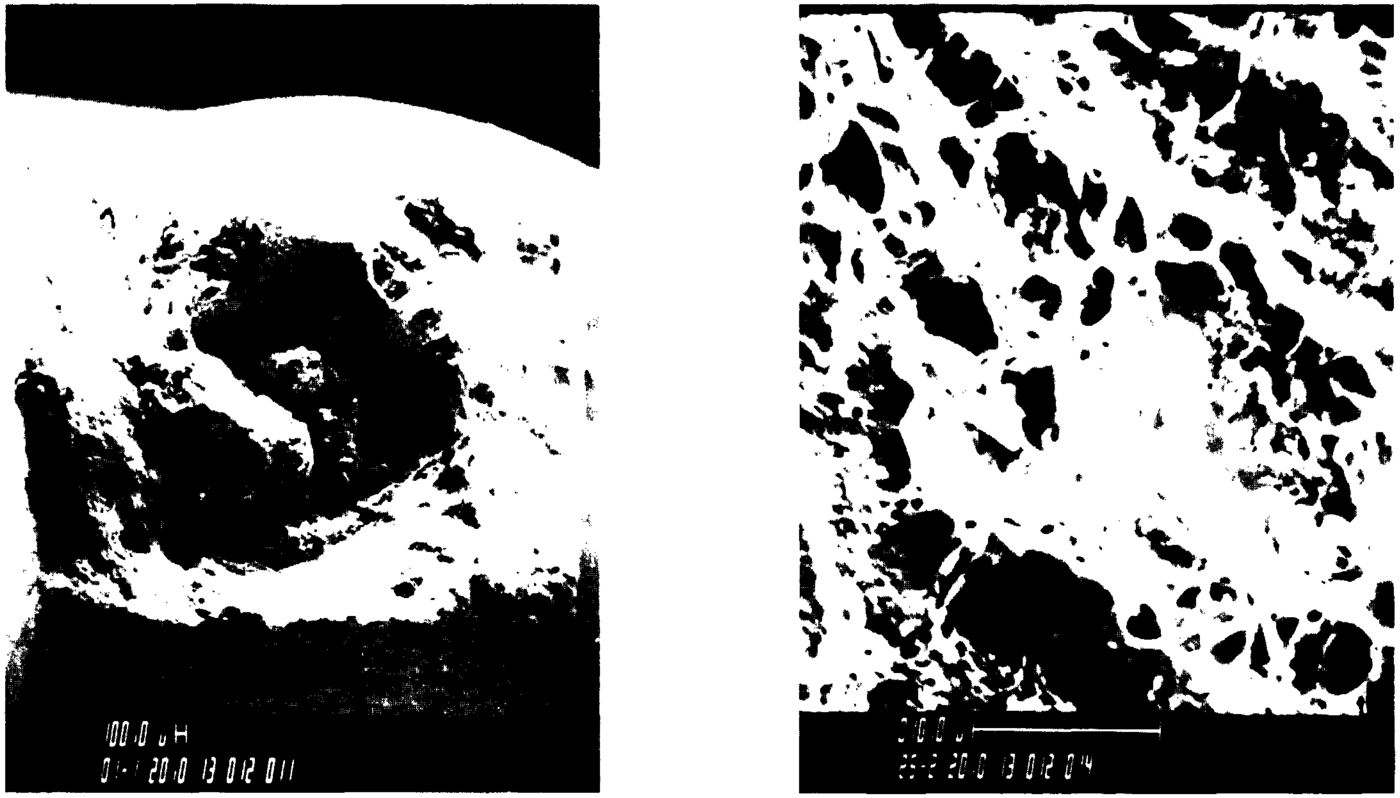

(a) (b)

FIGURE 24. SEM Micrographs of SSR Fracture Surface; Specimen Tested at 1 x 10^{-4}/s in 150°C Air. The Fracture Surface was typical of ductile fracture. (a) 15X; (b) 250X.

(a)

(b)

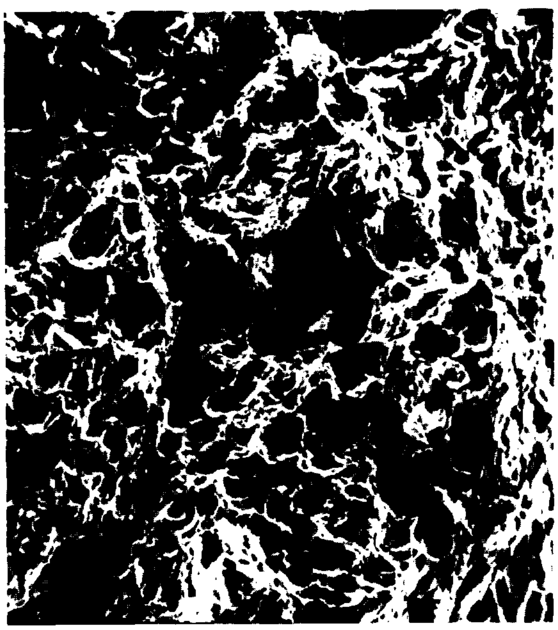

(c)

(d)

FIGURE 25. SEM Micrographs of SSR Fracture Surface; Specimen Tested in 150°C Brine Sparged with Argon. The strain rate was 2×10^{-7}/s. (a) 15X; (b) 150X; (c) 250X, center of fracture surface; (d) 200X, gage area near fracture surface.

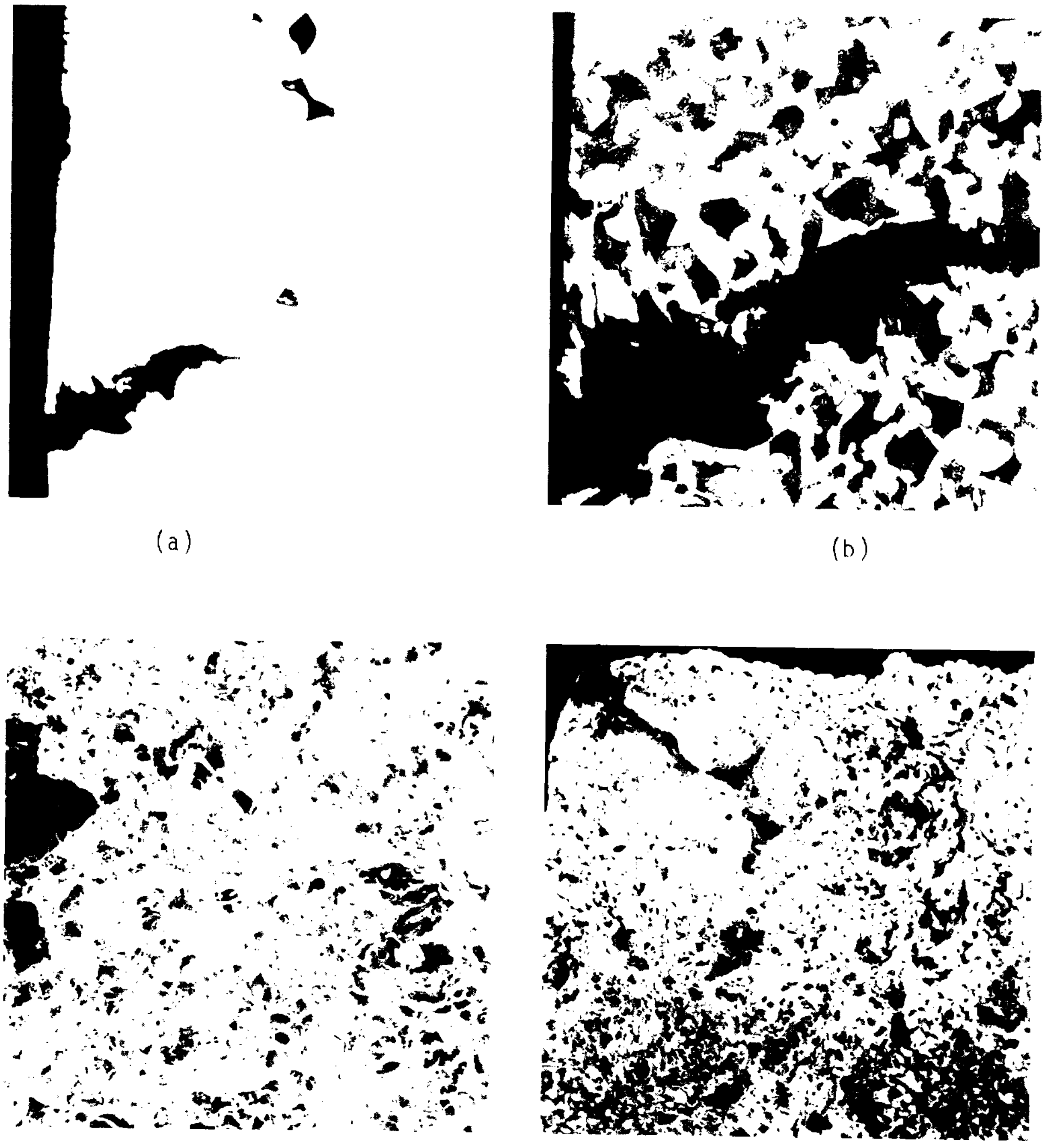

FIGURE 26. Metallographs and SEM Micrographs of a SSR Specimen. The specimen was tested in 150°C brine that was sparged with oxygen. The strain rate was 2×10^{-7}/s. (a) Metallograph, 100X, unetched; (b) metallograph, 250X, etched; (c) SEM micrograph, center of fracture surface, 250X; (d) edge of fracture surface, 80X.

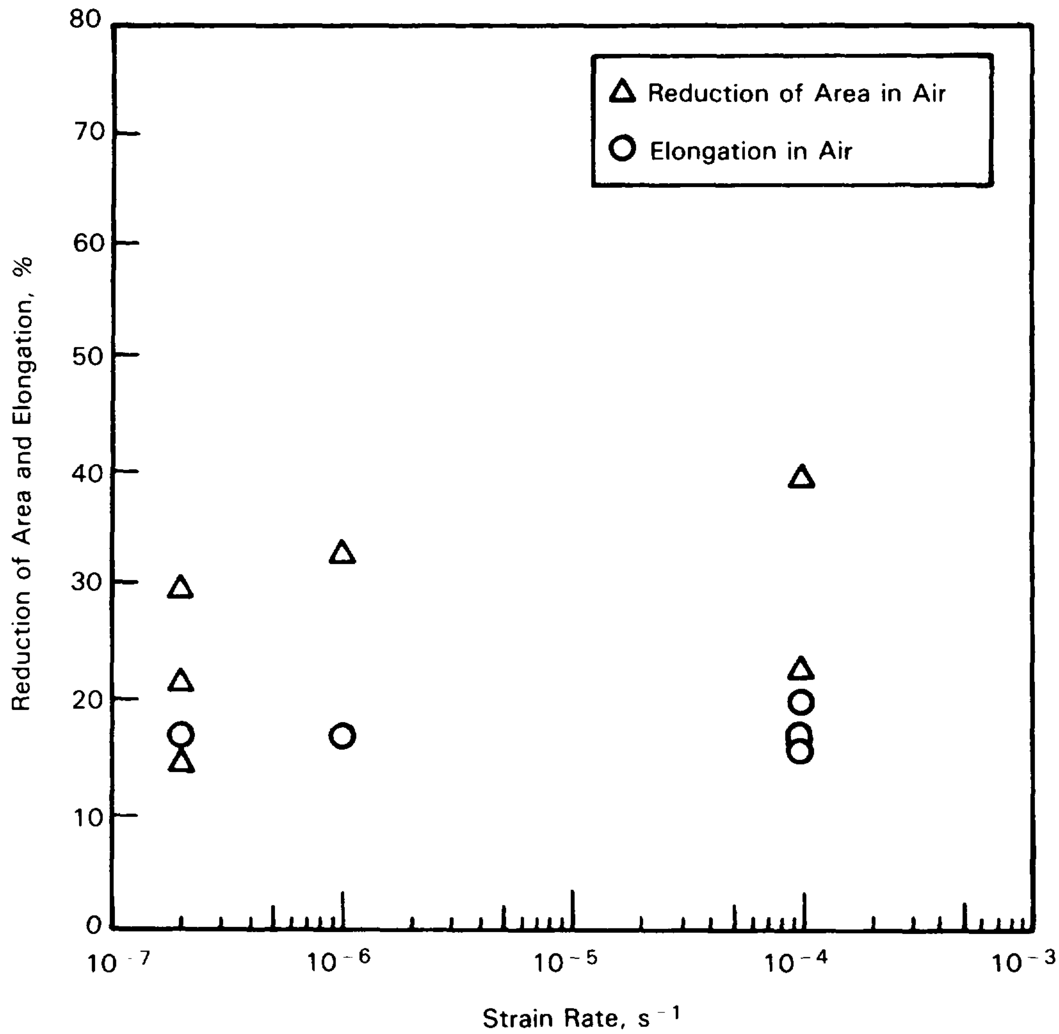

FIGURE 27. SSR Test Results for A216 Cast Steel in Air at 150°C; Reduction of Area and Elongation Versus Strain Rate

Some concluding statements are in order regarding the results of SSR tests on the A216 cast steel given in Table 11. If the effect of irradiation is considered to be independent of temperature, the reduction of area is higher in brine than in irradiated brine, at the 90% confidence level. Elongation is higher in brine than in irradiated brine at the 95% confidence level. Both reduction of area and elongation are higher in air than in brine or irradiated brine at the 95% confidence level.

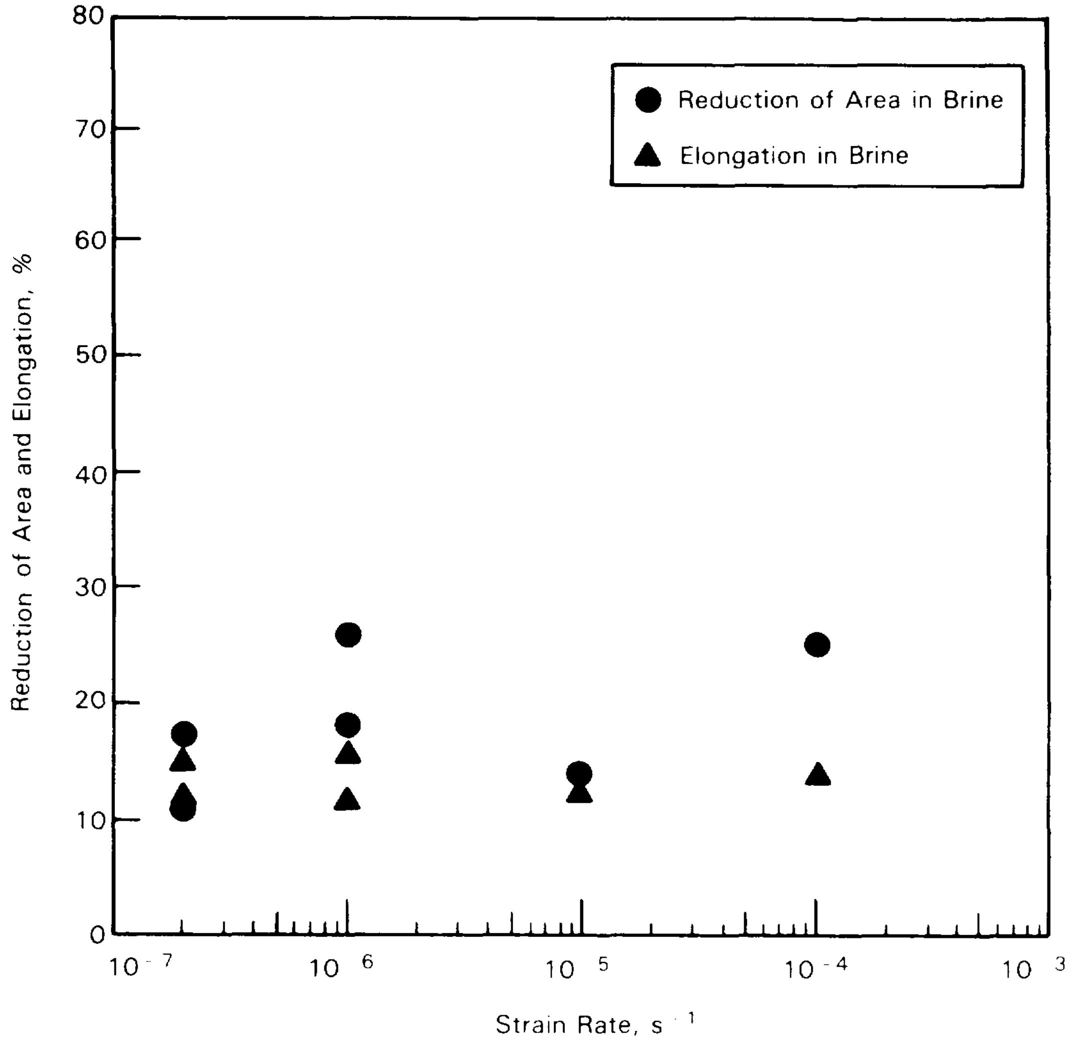

FIGURE 28. SSR Test Results for A216 Cast Steel in 150°C PBB2; Reduction of Area and Elongation versus Strain Rate

The effect of irradiation on reduction of area and elongation at 90°C is significant at the 95% confidence level, but reduction of area was not affected by irradiation at 30°C. The reasons for this temperature dependence are not known.

Data from these tests cannot be directly compared to the 150°C data because the brine in the lower-temperature tests was static and exposed to air.

Corrosion Fatigue Tests

Results of corrosion fatigue tests of 1025 wrought steel are given in Figure 29. Crack growth rates were clearly higher in deionized water than in air, and lower in brine than in air.

The decreased crack growth rates observed in brine were unexpected, but can be explained by buildup of material (salts and/or corrosion products) on the fracture faces and subsequent crack closure effects. If the crack cannot close completely on the low-load portion of the loading cycle, the repeated breaking of the corrosion-product film at the crack tip, obviously an imortant part of a corrosion fatigue test, cannot be properly effected and the test then approximates a statically loaded test.

Results of corrosion fatigue tests of the reference cast steel are given in Figures 30 through 32. As can be seen in Figure 30, the crack growth rate in deionized water is higher than in air. The crack growth rate was slightly increased by testing at a frequency of 0.1 Hz rather than 1 Hz (Figure 31).

The crack growth rate of the reference cast steel in PBB2 and in air is shown in Figure 32. The crack growth rate was clearly lower in the presence of the brine. This is in agreement with the results found for 1025 steel. Two tests were run for extended times (e.g., 2 x 10^6 cycles and 4 x 10^6 cycles at 0.1 Hz frequency) without measurable crack growth; these tests were done at stress intensities of 22 MPa $\sqrt{m}$ (20 ksi $\sqrt{in.}$), where crack growth was expected to be greater than 10^{-8} m/cycle.

The specimen that was cycled for over 4 x 10^6 cycles was subjected to a detailed metallographic examination, part of which is shown in Figures 33a and 33b. The following observations were made:

- The specimen was heavily oxidized, and heavy salt buildup occurred around the notch and pin areas.
- The precrack region appeared to be full of salt.
- Some areas of the specimen were pitted; particularly the plastic zone ahead of the crack tip.

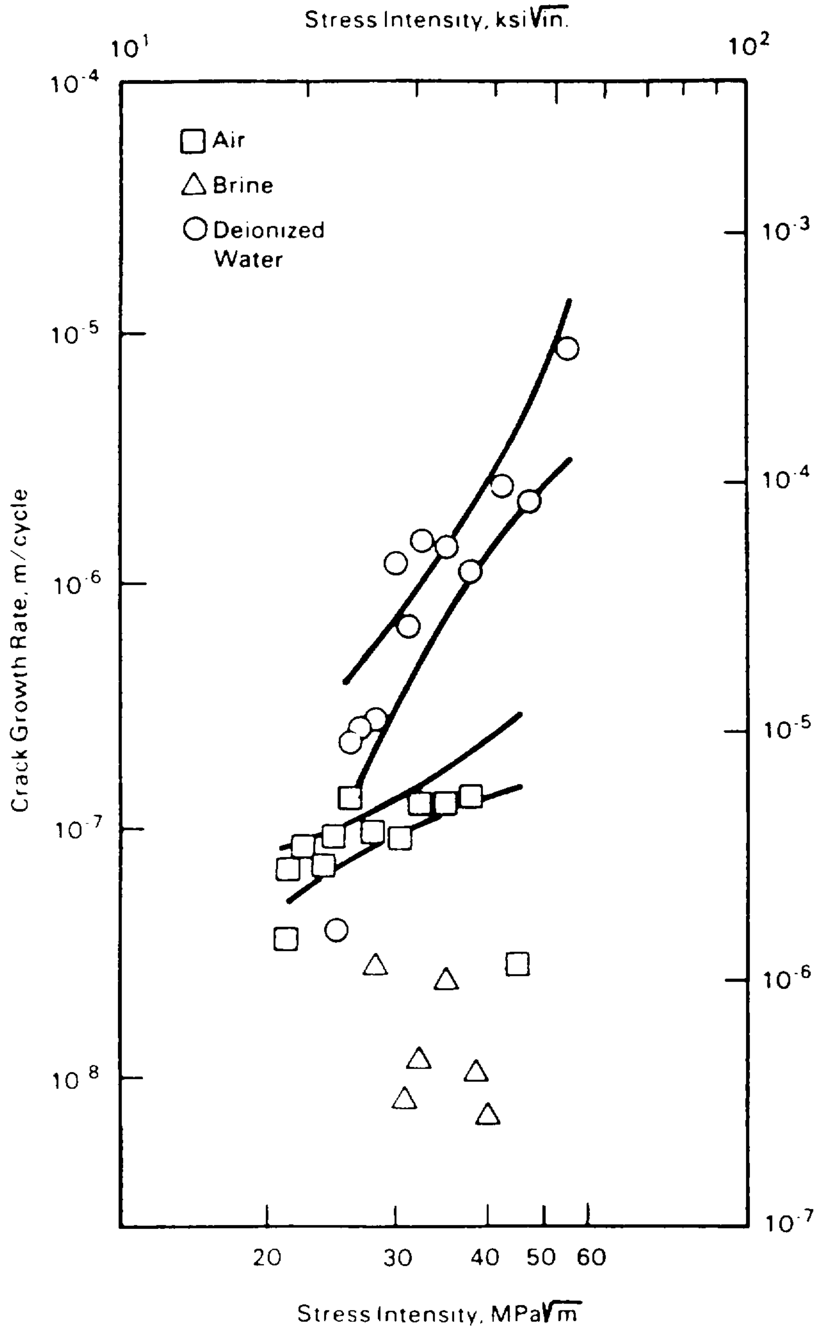

FIGURE 29. Corrosion Fatigue Test Results for 1025 Steel in Deionized Water, Air, and PBB2 at 150°C. The air test was done at 10 Hz; the others were done at 1 Hz. The solid lines represent 95% confidence bands about the regression line.

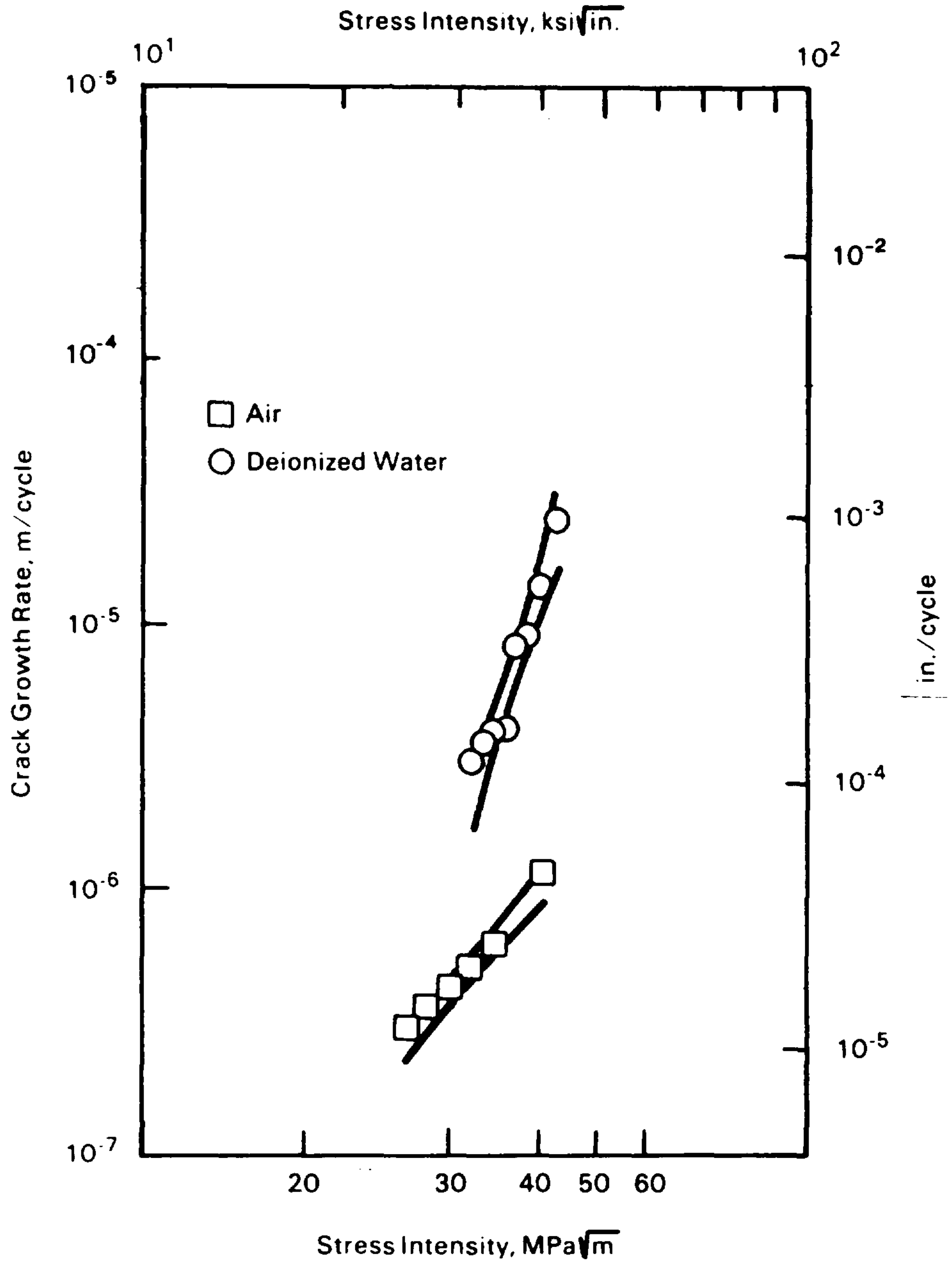

FIGURE 30. Corrosion Fatigue Test Results for A216 Cast Steel in Deionized Water and in Air at 150°C. The air test was done at 5 Hz; the deionized water test was done at 0.1 Hz. The solid lines represent 95% confidence bands about the regression line.

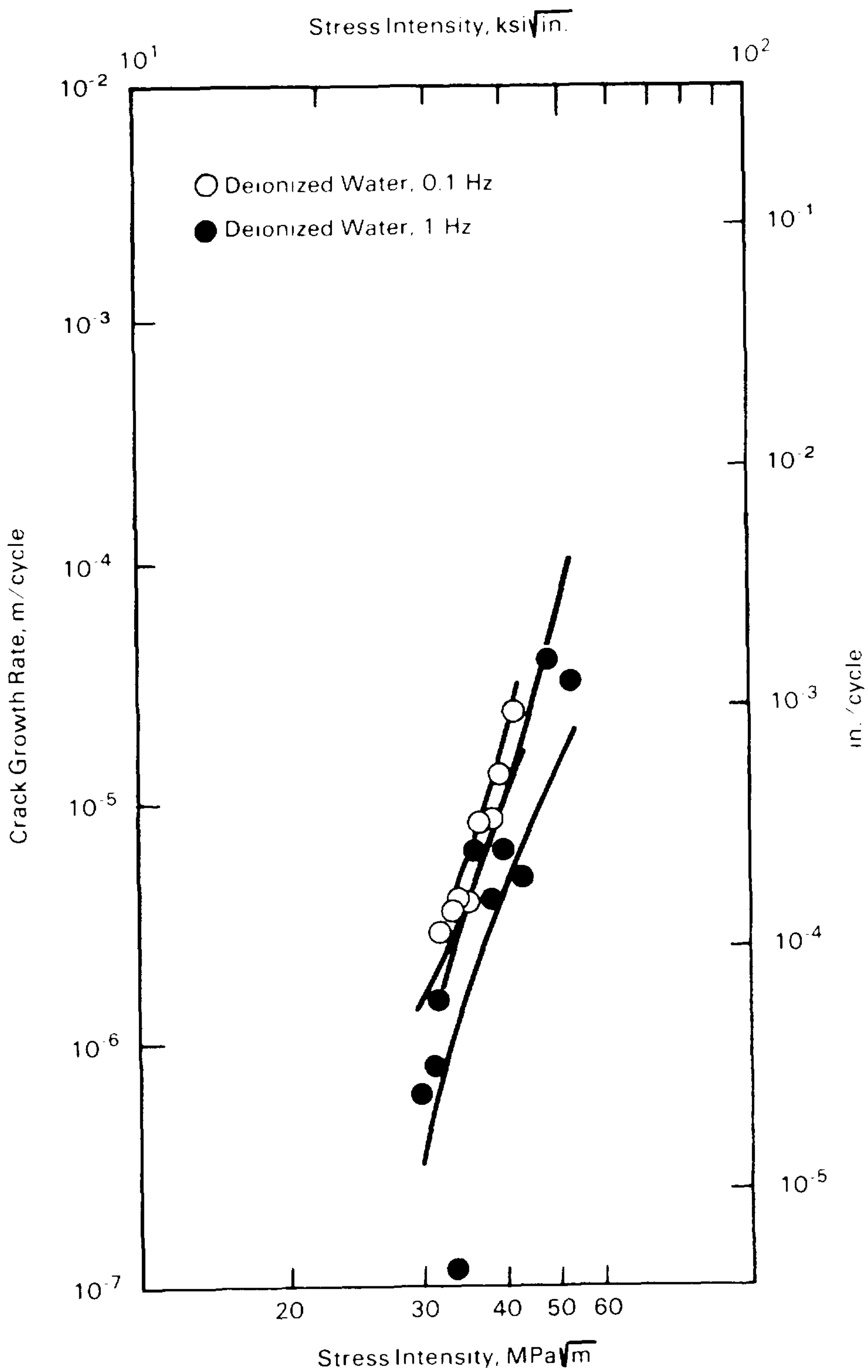

FIGURE 31. Corrosion Fatigue Test Results for A216 Cast Steel in 150°C Deionized Water at 0.1 Hz and 1 Hz. The solid lines represent 95% confidence bands about the regression line.

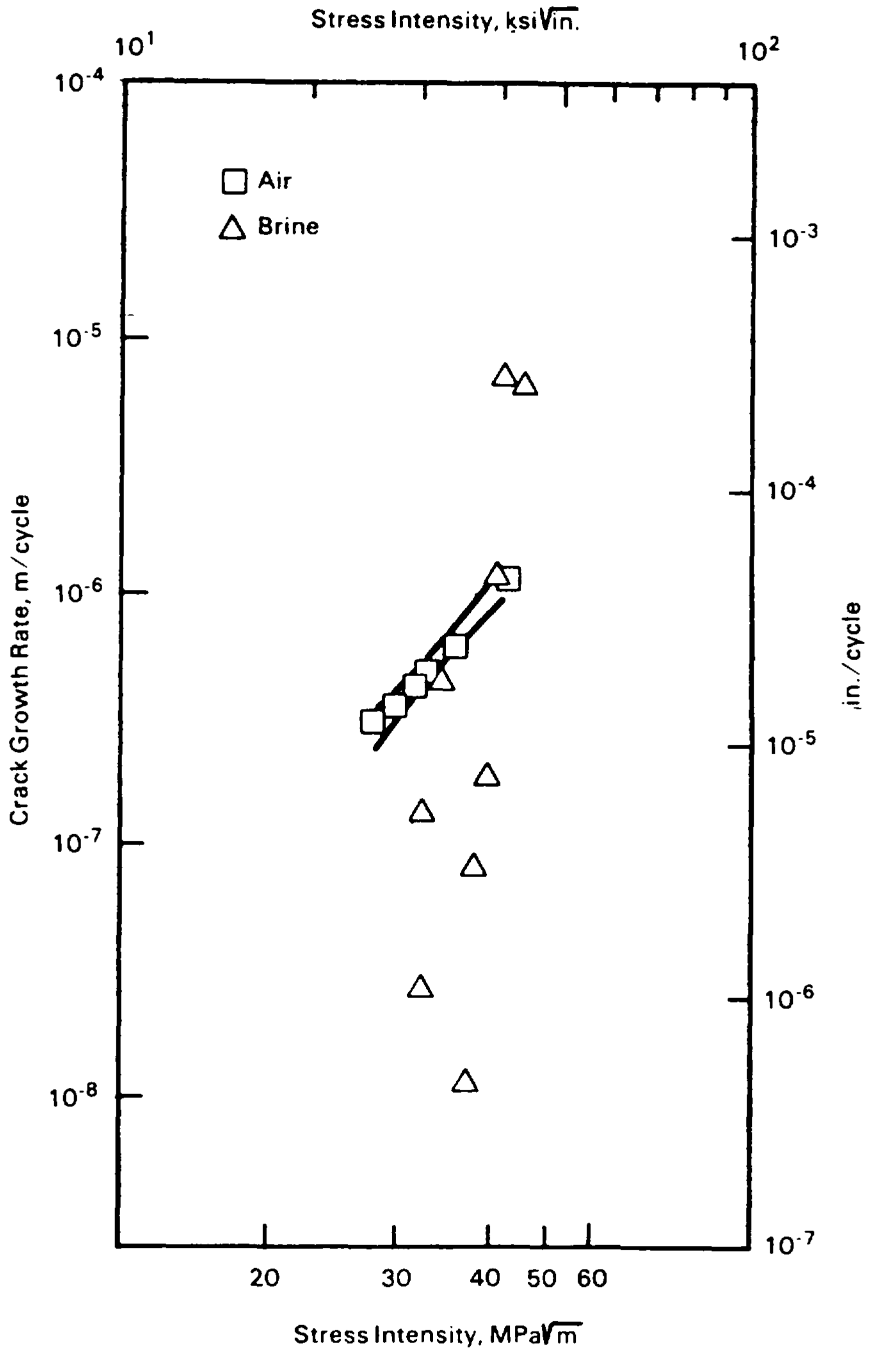

FIGURE 32. Corrosion Fatigue Test Results for A216 Cast Steel in PBB2 and in Air at 150°C. The solid lines represent 95% confidence bands about the regression line.

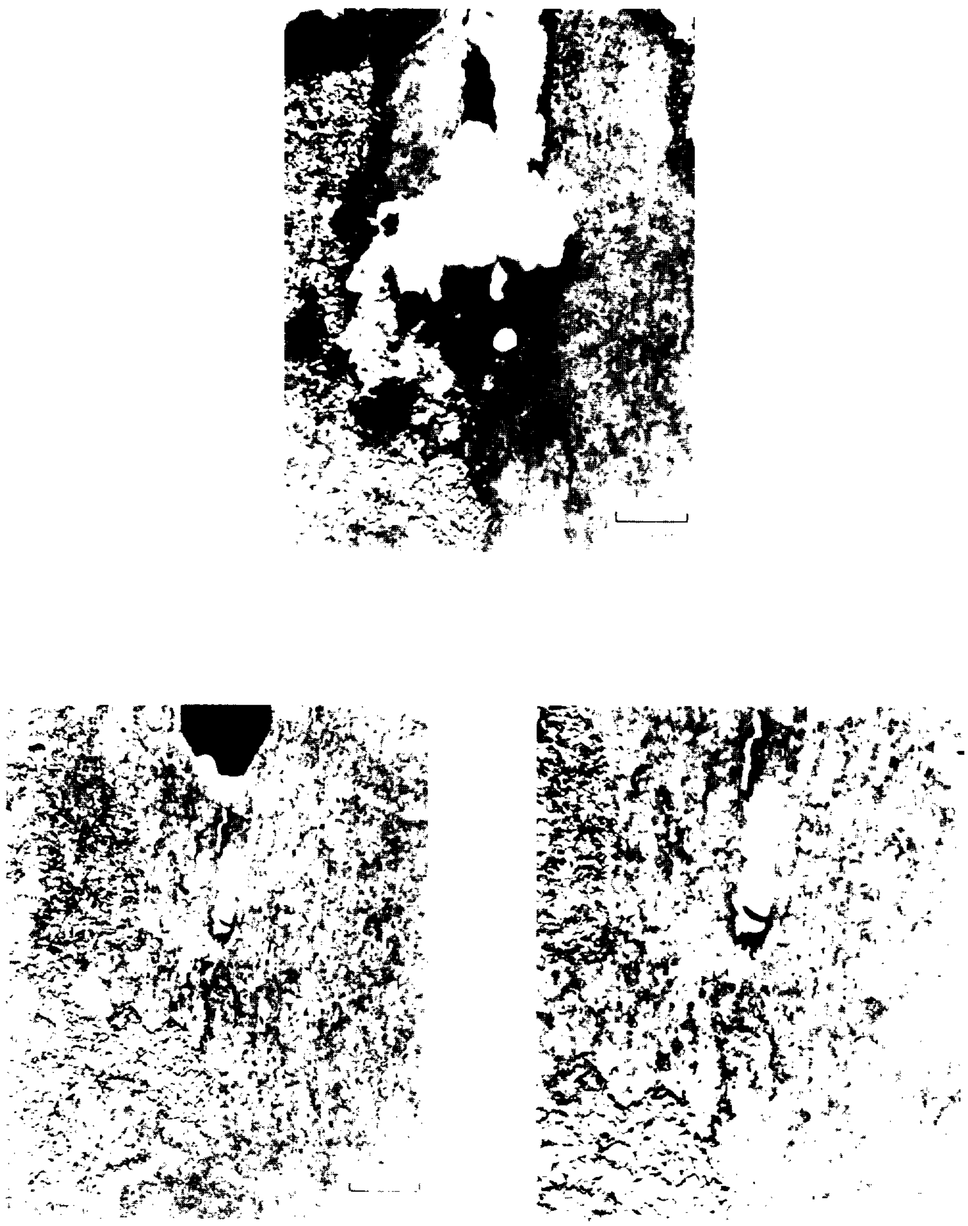

FIGURE 33a. Low-Magnification Photographs of the Machined Notch and Fatigue Crack of an A216 Cast Steel Corrosion Fatigue Specimen After Some Cleaning in Inhibited Acid Solution. This specimen was cycled for over 4×10^6 cycles with only a small amount of crack growth.

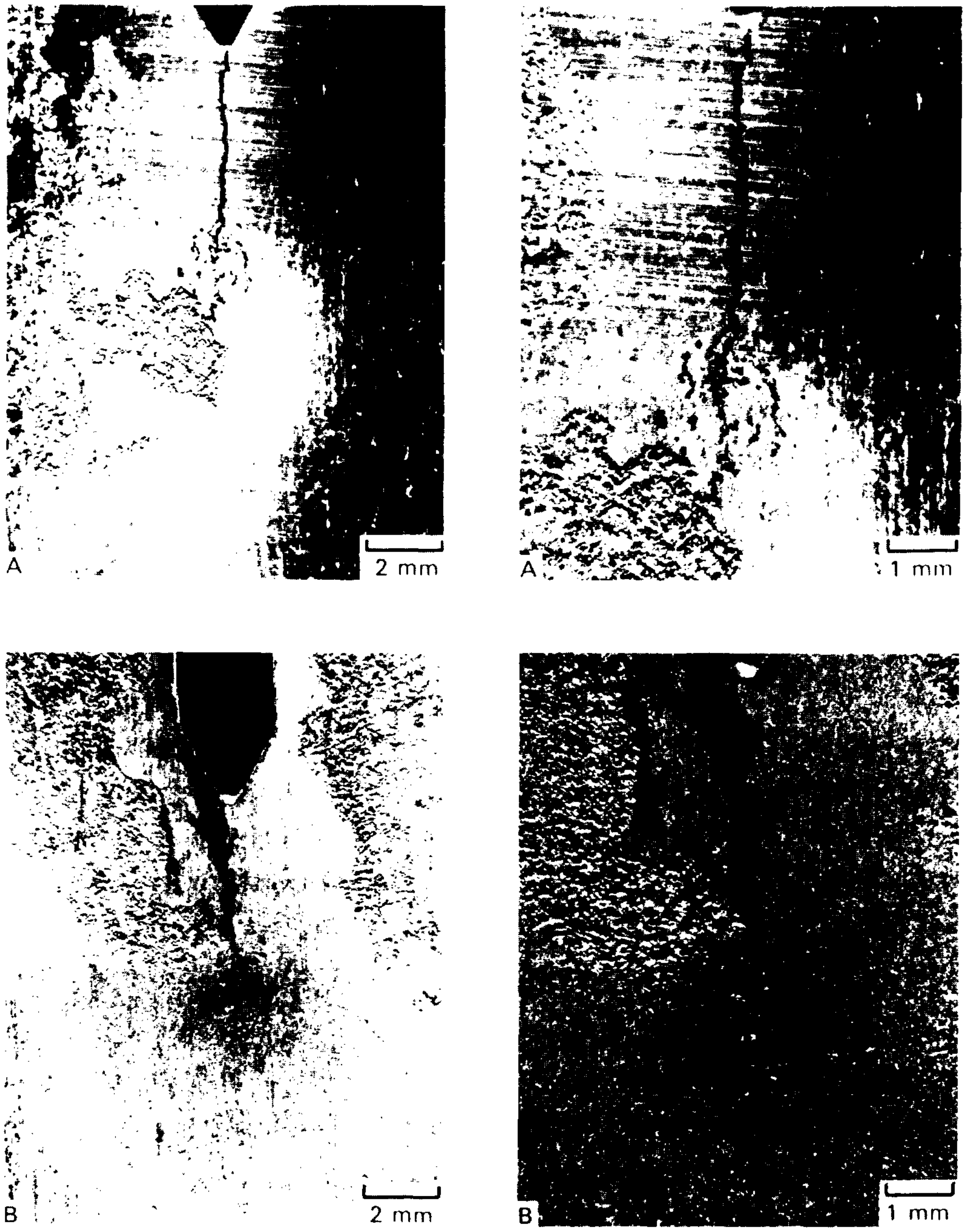

FIGURE 33b. Low-Magnification Photographs of the Machined Notch and Precrack After Thorough Cleaning. The top photos (A) and bottom photos (B) show the two sides of the same specimen. Note the presence of corrosion pits in the plastic zone.

- The crack (excluding the precrack) propagated along several grain boundaries, but not to such an extent that the cracking would be termed intergranular.
- A limited amount of crack branching occurred. It is also apparent from Figure 33 that corrosion products (gray areas) formed irregularly along the fracture surfaces, often extending into areas where the main crack did not propagate.

The specimen that was cycled for over 2 x 10^6 cycles without appreciable crack growth was cleaned, and a sample of the salt was removed from the fracture surface. X-ray diffraction analysis identified this sample as anhydrite, $CaSO_4$. It is possible that the fresh fracture surfaces provided preferred sites for nucleation of anhydrite crystals. A similar situation occurred on an irradiated SSR specimen. Crystals formed on the lower fracture surface and did not form elsewhere in the autoclave.

Corrosion fatigue testing performed to date has been conducted at low R ratios (i.e., ratio of minimum to maximum load). It is possible that higher crack growth rates will be obtained at higher R ratios, as higher R ratios tend to mitigate crack-wedging effects. Higher crack growth rates would permit the extrapolation of the environmental contribution to crack growth rate to long time periods, a conservative extrapolation that would be useful in design and lifetime predictions.

The corrosion fatigue data graphically presented in this section of the report may be found in tabular form in Appendix D.2.

The implications of the environmental-mechanical tests performed so far to the continued candidacy of mild steels to waste package barrier element applications are not clear. No severe problems have been uncovered in the tests. The SSR data show some effect of a brine environment on mechanical properties, but the effect does not appear to be serious. The corrosion fatigue tests have been complicated by anhydrite deposition in the region of the crack, frustrating the search for a stress-intensity threshold. Further testing, combined with a definition of the barrier material performance specifications, will be required before a judgment of material adequacy can be made on the basis of environmental-mechanical properties.

CONCLUSIONS

The principal technical conclusions derived from the corrosion and environmental-mechanical performance of iron-base alloys presented in the results and discussion section of this report are summarized below.

- The reference cast steel, ASTM A216 grade WCA, was found to corrode at a maximum rate of 3.2 cm (1.3 in.) per 1000 years in unirradiated 150°C PBB2 (Permian Basin intrusion brine), refreshed, and containing 1.5 ppm O_2. It, along with high-purity iron, corroded at a higher rate than any of the iron-base materials tested. The 2-1/2% Cr, 1% Mo steel showed the lowest corrosion rates.
- The imposition of a 1×10^5 rad/h ^{60}Co radiation field on the 150°C PBB2 environment increased the corrosion rates of all the ferrous materials studied by a factor of ~4. An irradiation intensity of 2×10^3 rad/h, on the other hand, caused no increase in corrosion rate over those found in the unirradiated study. Even the 2×10^3 rad/h test is considered to be an overtest, as the irradiation intensity is expected to be no higher than 100 rad/h with a spent fuel waste form.
- In both the 2×10^3 and the 1×10^5 rad/h irradiation-corrosion studies, the specimens located in the upper regions of the test autoclaves generally showed the highest corrosion rates. The reason for this is not known; it could be related to the direction of flow of incoming brine, bottom to top, or gravitational segregation of radiolysis products.
- In general, pitting attack was not a serious problem in the intrusion-brine autoclave corrosion tests, irradiated or unirradiated, or in the moist salt tests; but severe pitting attack was sometimes observed on environmental-mechanical property test specimens, especially in brine environments containing relatively high concentrations of oxygen (this observation is consistent with the generally accepted theories of pit formation under conditions in which

dissolved oxygen is available to the surface of corroding steel). The corrosion product was always found to be Fe_3O_4 on specimens tested in low-Mg intrusion brine.

- Ferrous materials exposed to moist salt environments that contained significant quantities of Mg^{2+} exhibited corrosion rates much higher (for A216 cast steel, a factor of ~30) than those found in simulated intrusion brine autoclave studies or low-Mg^{2+} moist salt test studies. It is inferred from the limited evidence available that Mg^{2+}, when present at concentrations above some undefined critical level, appears to inhibit the normal formation of semiprotective magnetite films from a ferrous hydroxide precursor, and thereby permits high corrosion rates.

- In slow-strain-rate studies, the ductility of 1025 wrought steel, A27 cast steel, and A216 cast steel was significantly lower in PBB2 than in air at 150°C. This effect was not observed at the highest strain rate used (1×10^{-4}/s).

- The reduction of area and elongation of as-cast A216 steel were lower in irradiated PBB2 at 30°C and 90°C than in unirradiated PBB2 at the same temperatures, except for the reduction of area at 30°C.

- There was no fractographic evidence found to indicate that stress-corrosion cracking was associated with the reduced ductility in the SSR tests.

- Fatigue crack growth rates of as-cast A27 steel and A216 steel were up to ten times higher in deionized water at 150°C than in air at the same temperature.

- Fatigue crack growth rates of A27 and A216 steels in PBB2 were less than a tenth of those in air or deionized water at 150°C. The reduced crack growth rates were probably caused by crack "wedging," resulting from the crystallization of anhydrite, or the formation of corrosion products, on the fracture surfaces.

- Of all the tests performed to date that simulate expected repository environments, only the moist salt general corrosion tests conducted using environments containing significant amounts of Mg^{2+} are cause for concern regarding the continuing consideration of mild steel for waste package overpack applications. If mild steels are to continue to be considered for waste package applications, the magnesium-rich, moist salt environment must be shown to be nonrepresentative of conditions expected in the repository; that is, it must be shown that 1) the concentration of water (or the reactant) expected in the salt at the waste package surface is far lower than the water (or other reactant) concentrations found to result in rapid corrosion rates in the present tests, and/or 2) the amount of reactant diffusing to the surface of the overpack is far smaller than that required to react with and perforate the overpack, or 3) either or both of these considerations is amenable to a practical engineering solution, such as use of impermeable, or highly absorbent, backfill materials. An assessment of these considerations was beyond the scope of the present study.

REFERENCES

1. R. E. Westerman. 1980. Investigation of Metallic, Ceramic, and Polymeric Materials for Engineered Barrier Applications in Nuclear Waste Packages. PNL-3484, Pacific Northwest Laboratory, Richland, Washington.

2. R. E. Westerman, J. L. Nelson, S. G. Pitman, W. L. Kuhn, S. J. Basham, and D. P. Moak. 1984. "Evaluation of Iron-Base Materials for Waste Package Containers in a Salt Repository." Presented at the International Symposium on the Scientific Basis for Nuclear Waste Management VII, November 1983, Boston, Massachusetts. Materials Research Society Symposia Proceedings, Volume 26, pp. 427-436.

3. U.S. Department of Energy. 1984. Draft Environmental Assessment, Deaf Smith County Site, Texas. DOE/RW0014, Office of Civilian Radioactive Waste Management, Washington, D.C., pp. 6-191.

4. J. H. Payer, W. E. Berry, and W. K. Boyd. 1976. "Constant Strain Rate Technique for Assessing Stress-Corrosion Susceptibility." In Stress Corrosion--New Approaches. ASTM STP 610, American Society for Testing and Materials, Philadelphia, Pennsylvania, pp. 82-93.

5. J. H. Payer, W. E. Berry, and W. K. Boyd. 1979. "Evaluation of Slow-Strain-Rate Stress Corrosion Test Results." Stress Corrosion Cracking--The Slow-Strain-Rate Technique. ASTM STP 665, American Society for Testing and Materials, Philadelphia, Pennsylvania, pp. 61-77.

6. R. N. Parkins. 1979. "Development of Strain-Rate Testing and Its Implications." Stress Corrosion Cracking--The Slow-Strain-Rate Technique. ASTM STP 665, American Society for Testing and Materials, Philadelphia, Pennsylvania, pp. 5-25.

7. R. P. Wei and G. Shim. 1983. "Fracture Mechanics and Corrosion Fatigue." Corrosion Fatigue: Mechanics, Metallurgy, Electrochemistry, and Engineering. ASTM STP 801, American Society for Testing and Materials, Philadelphia, Pennsylvania, pp. 5-25.

8. W. H. Bamford. 1983. "Implementing Corrosion-Fatigue Crack Growth Rate Data for Engineering Application." Corrosion Fatigue: Mechanics, Metallurgy, Electrochemistry, and Engineering. ASTM STP 801, American Society for Testing and Materials, Philadelphia, Pennsylvania, pp. 405-422.

9. J. Neter and W. Wasserman. 1974. Applied Linear Statistical Models. Irwin, Incorporated, pp. 685-720.

APPENDIX A

COMPILATION OF DATA FROM GENERAL CORROSION TESTS

APPENDIX A.1

COMPILATION OF DATA FROM GENERAL CORROSION TESTS

Anoxic Intrusion Brine Environment

Brine: PBB2

Oxygen Concentration: 0.05 ppm

Temperature: 150°C

Flow Rate: 35 mL/h

CALCULATION PROCEDURE

$$\text{Penetration rate } (\mu m/yr) = \frac{KW}{ATD}$$

where K = 8.76×10^7

W = mass loss, g

A = specimen area

T = exposure time, hr

D = density of metal, g/cm^3

GENERAL CORROSION, ANOXIC

SAMPLE ******		TIME **********			DIMENSIONS **********					WEIGHTS *******		CORROSION RATE *********
NUMBER	MATERIAL	START DATE	END DATE	TOTAL HR	LENGTH MM	WIDTH MM	HEIGHT MM	HOLE DI MM	AREA MM*MM	INITIAL GM	FINAL GM	MICRON/YR
N 71	A27 CAST STEEL	21-Sep-82	29-Oct-82	720	35.61	36.75	2.41	9.78	2890	23.6247	23.5924	17
N 76	A27 CAST STEEL	21-Sep-82	29-Oct-82	720	35.59	36.20	2.39	9.70	2840	22.9534	22.9251	15
N 74	A27 CAST STEEL	21-Sep-82	29-Oct-82	720	35.66	35.59	2.41	9.75	2810	22.6352	NA	NA
N 96	A27 CAST STEEL	16-Nov-82	22-Feb-83	2334	35.64	36.65	2.44	9.58	2890	23.3824	23.3516	5.1
N 98	A27 CAST STEEL	16-Nov-82	22-Feb-83	2334	35.64	35.76	2.46	9.70	2830	22.7324	22.7087	4.0
N 97	A27 CAST STEEL	16-Nov-82	18-Jul-83	4368	36.55	35.64	2.46	9.63	2890	23.3606	23.3261	3.1
N 72	A27 CAST STEEL	21-Sep-82	18-Jul-83	5358	35.59	35.71	2.51	9.86	2830	22.8621	22.8222	2.9
N 75	A27 CAST STEEL	21-Sep-82	18-Jul-83	5358	36.32	35.59	2.41	9.78	2860	23.0660	23.0371	2.1
N 99	A27 CAST STEEL	16-Nov-82	25-Sep-84	14426	36.58	35.64	2.46	9.60	2890	23.4736	23.3452	3.4
N 73	A27 CAST STEEL	21-Sep-82	25-Sep-84	15416	36.50	35.59	2.41	9.68	2880	23.3148	23.2610	1.4
N 106	A27 CAST STEEL	21-Sep-82	25-Sep-84	15416	35.33	35.64	6.35	9.60	3470	58.5858	58.5146	1.5
N 105	A27 CAST STEEL	21-Sep-82	25-Sep-84	15416	35.33	35.61	6.32	9.63	3460	58.7890	58.7432	0.96
N 195	1025 WROUGHT STEEL	16-Nov-82	22-Feb-83	2334	50.70	50.98	1.35	6.48	5400	28.4201	28.2534	15
N 194	1025 WROUGHT STEEL	16-Nov-82	22-Feb-83	2334	50.70	50.90	1.40	6.50	5410	28.2435	28.0930	13
N 199	1025 WROUGHT STEEL	16-Nov-82	22-Feb-83	2334	50.65	50.93	1.40	6.50	5410	28.5030	NA	NA
N 203	1025 WROUGHT STEEL	16-Nov-82	22-Feb-83	2334	50.75	50.83	1.42	6.43	5410	28.4749	28.4061	6.1
N 196	1025 WROUGHT STEEL	16-Nov-82	18-Jul-83	4368	50.57	50.90	1.35	6.48	5380	28.3440	28.1362	9.9
N 205	1025 WROUGHT STEEL	16-Nov-82	18-Jul-83	4368	50.60	51.03	1.40	6.45	5410	28.2503	28.1576	4.4
N 204	1025 WROUGHT STEEL	16-Nov-82	23-Oct-83	6744	50.75	50.93	1.45	6.45	5430	28.5232	28.3957	3.9
N 197	1025 WROUGHT STEEL	16-Nov-82	23-Oct-83	6744	50.60	50.88	1.35	6.50	5380	28.3483	28.0998	7.6
N 201	1025 WROUGHT STEEL	16-Nov-82	25-Sep-84	14426	50.70	50.90	1.40	6.43	5410	28.4289	28.0122	6.0
N 200	1025 WROUGHT STEEL	16-Nov-82	25-Sep-84	14426	50.85	50.65	1.45	6.43	5410	28.5272	28.1248	5.8
N 198	1025 WROUGHT STEEL	16-Nov-82	25-Sep-84	14426	50.75	50.75	1.40	6.45	5400	28.3617	27.9821	5.4
N 202	1025 WROUGHT STEEL	16-Nov-82	25-Sep-84	14426	50.60	50.95	1.42	6.43	5410	28.3310	28.0737	3.7
P 530	A216 CAST STEEL	29-Jan-84	29-Feb-84	696	35.56	35.53	1.47	9.80	2630	14.1605	14.1266	21
P 540	A216 CAST STEEL	29-Jan-84	29-Feb-84	696	35.56	35.56	1.45	9.83	2630	14.1427	14.1116	19
P 543	A216 CAST STEEL	29-Jan-84	01-Jun-84	2897	35.56	35.56	1.45	9.83	2630	13.9079	13.8190	13
P 536	A216 CAST STEEL	29-Jan-84	01-Jun-84	2897	35.56	35.53	1.52	9.83	2640	14.1525	14.0479	15
P 541	A216 CAST STEEL	29-Jan-84	25-Sep-84	5321	35.59	35.56	1.50	9.80	2640	14.2126	13.9803	18
P 544	A216 CAST STEEL	29-Jan-84	25-Sep-84	5321	35.56	35.56	1.47	9.83	2630	14.1028	13.8657	19
P 542	A216 CAST STEEL	29-Jan-84	25-Sep-84	5321	35.56	35.53	1.50	9.83	2640	14.2099	14.0452	13
P 539	A216 CAST STEEL	29-Jan-84	25-Sep-84	5321	35.56	35.53	1.50	9.80	2640	14.1792	13.9691	17
P 537	A216 CAST STEEL	29-Jan-84	25-Sep-84	5321	35.56	35.56	1.47	9.80	2630	14.2059	13.9946	17
P 538	A216 CAST STEEL	29-Jan-84	25-Sep-84	5321	35.56	35.53	1.50	9.83	2640	14.2216	14.0176	16
P 531	A216 CAST STEEL	29-Jan-84	25-Sep-84	5635	35.56	35.56	1.45	9.80	2630	14.1769	14.0294	11
P 532	A216 CAST STEEL	29-Jan-84	25-Sep-84	5635	35.56	35.56	1.47	9.80	2630	14.1358	13.9676	13
P 534	A216 CAST STEEL	29-Jan-84	25-Sep-84	5635	35.56	35.56	1.47	9.80	2630	14.1560	13.9944	12
P 535	A216 CAST STEEL	29-Jan-84	25-Sep-84	5635	35.59	35.56	1.50	9.80	2640	14.2159	14.0383	13
P 533	A216 CAST STEEL	29-Jan-84	25-Sep-84	5635	35.56	35.53	1.50	9.80	2640	14.1369	13.9989	10
N 132	2.5%CR,1%MO STEEL	21-Sep-82	29-Oct-82	720	50.75	50.83	2.54	9.68	5610	50.0453	49.9928	15
N 129	2.5%CR,1%MO STEEL	21-Sep-82	29-Oct-82	720	50.75	50.85	2.57	9.65	5610	50.3822	50.3378	12
N 134	2.5%CR,1%MO STEEL	21-Sep-82	29-Oct-82	720	50.75	50.67	2.54	9.63	5590	50.0711	50.0265	12
N 145	2.5%CR,1%MO STEEL	21-Sep-82	22-Feb-83	3054	50.75	50.27	6.30	9.60	6420	122.3762	122.3075	3.9
N 131	2.5%CR,1%MO STEEL	21-Sep-82	22-Feb-83	3054	50.75	50.65	2.57	9.60	5590	50.2814	50.2145	4.4
N 130	2.5%CR,1%MO STEEL	21-Sep-82	18-Jul-83	5358	50.75	50.85	2.54	9.68	5610	49.7153	49.6399	2.8
N 133	2.5%CR,1%MO STEEL	21-Sep-82	25-Sep-84	15416	50.72	50.72	2.49	9.68	5580	49.4924	49.4099	1.1
N 146	2.5%CR,1%MO STEEL	21-Sep-82	25-Sep-84	15416	50.75	50.04	6.30	9.58	6390	121.9614	121.8665	1.1
N 4	DUCTILE CAST IRON	21-Sep-82	29-Oct-82	720	35.59	35.51	2.49	9.63	2810	21.3383	21.3062	18
N 6	DUCTILE CAST IRON	21-Sep-82	29-Oct-82	720	35.56	35.48	2.49	10.01	2800	21.1782	21.1432	15
N 1	DUCTILE CAST IRON	21-Sep-82	29-Oct-82	720	35.48	35.61	2.57	10.03	2820	21.2905	21.2562	19
N 2	DUCTILE CAST IRON	21-Sep-82	22-Feb-83	3054	35.48	35.79	2.49	10.03	2820	21.3013	21.2603	5.3

GENERAL CORROSION, ANOXIC

SAMPLE		TIME			DIMENSIONS					WEIGHTS		CORROSION RATE
NUMBER	MATERIAL	START DATE	END DATE	TOTAL HR	LENGTH MM	WIDTH MM	HEIGHT MM	HOLE DI MM	AREA MM*MM	INITIAL GM	FINAL GM	MICROM/YR
N 5	DUCTILE CAST IRON	21-Sep-82	22-Feb-83	3054	35.69	35.48	2.51	10.08	2810	21.2090	21.1800	3.8
N 3	DUCTILE CAST IRON	21-Sep-82	18-Jul-83	5358	35.56	35.48	2.49	10.01	2800	21.1864	21.1519	2.6
N 37	DUCTILE CAST IRON	21-Sep-82	25-Sep-84	15416	35.51	35.61	6.27	10.08	3460	53.1663	53.0795	1.8
N 38	DUCTILE CAST IRON	21-Sep-82	25-Sep-84	15416	35.53	35.51	6.27	10.06	3450	52.8825	52.7506	2.8
P 159	A27 NORM. CAST	13-Apr-83	27-Jul-83	2472	35.36	35.59	1.52	8.99	2650	13.9877	13.9409	8.0
P 160	A27 NORM. CAST	13-Apr-83	27-Jul-83	2472	35.59	35.36	1.52	9.37	2640	13.9602	13.9096	8.6
P 161	A27 NORM. CAST	13-Apr-83	27-Jul-83	2472	35.69	35.31	1.52	9.04	2650	13.1458	NA	NA
P 170	A27 NORM. CAST	13-Apr-83	23-Oct-83	4632	35.56	35.26	1.52	9.09	2640	13.8680	NA	NA
P 169	A27 NORM. CAST	13-Apr-83	23-Oct-83	4632	35.36	35.51	1.52	9.30	2640	13.8299	13.7532	7.0
P 162	A27 NORM. CAST	13-Apr-83	23-Oct-83	4632	35.66	35.41	1.52	9.07	2660	14.2361	14.1807	5.0
P 163	A27 NORM. CAST	13-Apr-83	25-Sep-84	12314	35.66	35.31	1.52	9.09	2650	14.0403	13.8945	5.0
P 167	A27 NORM. CAST	13-Apr-83	25-Sep-84	12314	35.26	35.64	1.55	9.09	2650	13.9798	13.8472	4.5
P 168	A27 NORM. CAST	13-Apr-83	25-Sep-84	12314	35.59	35.38	1.55	9.30	2650	14.1967	14.1114	2.9
P 164	A27 NORM. CAST	13-Apr-83	25-Sep-84	12314	35.36	35.71	1.52	9.02	2660	14.0388	13.8902	5.1
P 165	A27 NORM. CAST	13-Apr-83	25-Sep-84	12314	35.48	35.31	1.55	9.04	2640	13.9119	13.8320	2.7
P 166	A27 NORM. CAST	13-Apr-83	25-Sep-84	12314	35.48	35.28	1.52	9.07	2630	13.9304	13.8534	2.6
FE 16	PURE IRON	13-Apr-83	27-Jul-83	2472	31.72	31.80	1.52	9.50	2120	11.1006	11.0617	8.3
FE 17	PURE IRON	13-Apr-83	27-Jul-83	2472	31.67	31.78	1.45	9.50	2100	10.3843	NA	NA
FE 15	PURE IRON	13-Apr-83	27-Jul-83	2472	31.72	31.75	1.35	9.53	2080	9.9142	9.8372	17
FE 20	PURE IRON	13-Apr-83	23-Oct-83	4632	31.80	31.75	1.60	9.50	2130	11.7145	11.6385	8.6
FE 19	PURE IRON	13-Apr-83	23-Oct-83	4632	31.72	31.78	1.55	9.50	2120	11.2522	NA	NA
FE 18	PURE IRON	13-Apr-83	23-Oct-83	4632	31.75	31.75	1.63	9.50	2130	11.6657	11.6133	5.9
FE 22	PURE IRON	13-Apr-83	25-Sep-84	12314	31.72	31.72	1.60	9.53	2120	11.3481	11.1618	8.0
FE 21	PURE IRON	13-Apr-83	25-Sep-84	12314	31.83	31.72	1.57	9.50	2130	10.8926	10.7027	8.1

APPENDIX A.2

COMPILATION OF DATA FROM GENERAL CORROSION STUDIES

Oxic Intrusion Brine Environment

Brine: PBB2

Oxygen Concentration: 1.5 ppm

Temperature: 150°C

Flow Rate: 35 ml/h

SAMPLE ******		TIME **********			DIMENSIONS **********					WEIGHTS *******		CORROSION RATE *********
NUMBER	MATERIAL	START DATE	END DATE	TOTAL HR	LENGTH MM	WIDTH MM	HEIGHT MM	HOLE DI MM	AREA MM*MM	INITIAL GMS	FINAL GMS	MICROM/YR
N 86	A27 CAST STEEL	29-Nov-82	04-Jan-83	833	35.64	36.45	2.44	9.63	2880	23.3066	23.2698	17
N 84	A27 CAST STEEL	29-Nov-82	04-Jan-83	833	36.50	35.64	2.46	9.65	2890	23.4355	23.4004	16
N 102	A27 CAST STEEL	29-Nov-82	04-Jan-83	833	35.64	35.86	2.46	9.73	2840	22.7667	22.7334	16
N 85	A27 CAST STEEL	29-Nov-82	11-Apr-83	2993	35.66	36.30	2.46	9.63	2870	23.2613	23.1524	14
N 85A	A27 CAST STEEL	11-Apr-83	25-Sep-84	12597	35.66	36.30	2.46	9.63	2870	23.1524	22.8182	10
N 100	A27 CAST STEEL	29-Nov-82	11-Apr-83	2993	36.02	35.64	2.46	9.73	2850	22.9329	22.8396	12
N 100A	A27 CAST STEEL	11-Apr-83	25-Sep-84	12597	36.02	35.64	2.46	9.73	2850	22.8396	22.4572	12
N 101	A27 CAST STEEL	29-Nov-82	27-Jul-83	5273	35.64	36.45	2.44	9.63	2880	22.9511	22.7870	12
N 109	A27 CAST STEEL	29-Nov-82	25-Sep-84	15168	35.64	36.58	6.35	9.58	3570	60.4843	60.0833	8.3
N 110	A27 CAST STEEL	29-Nov-82	25-Sep-84	15168	35.46	35.64	6.35	9.63	3480	58.9604	58.5144	9.4
N 233	1025 WROUGHT STEEL	11-Jan-83	11-Apr-83	2160	50.78	50.75	1.42	6.40	5400	28.4219	NA	NA
N 231	1025 WROUGHT STEEL	11-Jan-83	11-Apr-83	2160	50.83	50.67	1.42	6.38	5400	28.3906	28.1752	21
N 231A	1025 WROUGHT STEEL	11-Apr-83	25-Sep-84	12597	50.83	50.67	1.42	6.38	5400	28.1752	27.2444	15
N 232	1025 WROUGHT STEEL	11-Jan-83	11-Apr-83	2160	50.77	50.75	1.45	6.38	5410	28.4652	28.2806	18
N 232A	1025 WROUGHT STEEL	11-Apr-83	25-Sep-84	12597	50.77	50.75	1.45	6.38	5410	28.2806	27.5422	12
N 236	1025 WROUGHT STEEL	11-Jan-83	27-Jul-83	4440	50.67	50.80	1.45	6.38	5410	28.3038	28.0103	14
N 235	1025 WROUGHT STEEL	11-Jan-83	27-Jul-83	4440	50.70	50.62	1.42	6.38	5390	28.3431	NA	NA
N 234	1025 WROUGHT STEEL	11-Jan-83	27-Jul-83	4440	50.65	50.75	1.45	6.40	5400	28.2699	28.0165	12
N 239	1025 WROUGHT STEEL	11-Jan-83	25-Sep-84	14167	50.75	50.67	1.42	6.43	5400	28.5170	27.8805	9.3
N 237	1025 WROUGHT STEEL	11-Jan-83	25-Sep-84	14167	50.90	50.65	1.40	6.45	5400	28.0328	27.2562	11
N 238	1025 WROUGHT STEEL	11-Jan-83	25-Sep-84	14167	50.57	50.77	1.40	6.40	5390	28.3417	27.6231	11
P 554	A216 CAST STEEL	10-Feb-84	12-Mar-84	736	35.53	35.53	1.45	9.83	2620	14.1613	14.1157	26
P 548	A216 CAST STEEL	10-Feb-84	12-Mar-84	736	35.56	35.56	1.47	9.80	2630	14.0967	14.0477	28
P 547	A216 CAST STEEL	10-Feb-84	12-Jun-84	2908	35.56	35.56	1.42	9.80	2620	13.9013	13.7125	28
P 552	A216 CAST STEEL	10-Feb-84	12-Jun-84	2908	35.56	35.53	1.45	9.80	2630	14.2178	14.1155	15 *
P 553	A216 CAST STEEL	10-Feb-84	25-Sep-84	5384	35.56	35.53	1.45	9.80	2630	14.0262	13.7562	21
P 549	A216 CAST STEEL	10-Feb-84	25-Sep-84	5384	35.56	35.56	1.47	9.80	2630	14.1001	13.7626	27
P 555	A216 CAST STEEL	10-Feb-84	25-Sep-84	5384	35.56	35.53	1.45	9.83	2630	14.2015	13.9046	23
P 556	A216 CAST STEEL	10-Feb-84	25-Sep-84	5384	35.53	35.53	1.47	9.83	2630	14.1989	13.9224	22
P 550	A216 CAST STEEL	10-Feb-84	25-Sep-84	5384	35.56	35.56	1.45	9.80	2630	14.1494	13.7644	30
P 546	A216 CAST STEEL	10-Feb-84	25-Sep-84	5384	35.56	35.56	1.47	9.78	2630	14.1911	13.9147	22
P 545	A216 CAST STEEL	10-Feb-84	25-Sep-84	5384	35.59	35.56	1.47	9.78	2640	14.1928	13.8553	27
P 557	A216 CAST STEEL	10-Feb-84	25-Sep-84	5384	35.56	35.56	1.45	9.83	2630	14.0682	13.7042	29
P 551	A216 CAST STEEL	10-Feb-84	25-Sep-84	5384	35.56	35.56	1.47	9.83	2630	14.2304	13.9240	24
N 135	2.5%CR,1%MO STEEL	29-Nov-82	04-Jan-83	833	50.80	50.80	2.57	9.58	5620	50.3722	50.3063	16
N 124	2.5%CR,1%MO STEEL	29-Nov-82	04-Jan-83	833	50.65	50.80	2.57	9.60	5600	49.9923	49.9261	16
N 125	2.5%CR,1%MO STEEL	29-Nov-82	04-Jan-83	833	50.70	50.75	2.59	9.60	5610	50.1093	50.0409	16
N 126	2.5%CR,1%MO STEEL	29-Nov-82	11-Apr-83	2993	50.24	50.77	2.57	9.55	5550	49.9404	49.7779	11
N 126A	2.5%CR,1%MO STEEL	11-Apr-83	25-Sep-84	12597	50.24	50.77	2.57	9.55	5550	49.7779	49.4045	6.0
N 123	2.5%CR,1%MO STEEL	29-Nov-82	11-Apr-83	2993	50.80	50.75	2.57	9.60	5610	50.2894	50.1253	11
N 123A	2.5%CR,1%MO STEEL	11-Apr-83	25-Sep-84	12597	50.80	50.75	2.57	9.60	5610	50.1253	49.7606	5.8
N 127	2.5%CR,1%MO STEEL	29-Nov-82	27-Jul-83	5273	50.62	50.80	2.59	9.58	5600	50.0822	49.8797	7.6
N 144	2.5%CR,1%MO STEEL	29-Nov-82	25-Sep-84	15168	50.04	50.77	6.35	9.65	6410	121.8027	121.3478	5.2
N 143	2.5%CR,1%MO STEEL	29-Nov-82	25-Sep-84	15168	50.17	50.75	6.35	9.65	6420	122.0594	121.5350	6.0
N 7	DUCTILE CAST IRON	29-Nov-82	04-Jan-83	833	35.56	35.51	2.49	10.08	2800	21.0249	20.9762	23
M 997	DUCTILE CAST IRON	29-Nov-82	04-Jan-83	833	38.02	38.02	2.51	10.13	3190	21.1089	21.0642	19
M 995	DUCTILE CAST IRON	29-Nov-82	04-Jan-83	833	37.90	38.05	2.54	10.03	3190	21.1834	21.1359	20
M 998	DUCTILE CAST IRON	29-Nov-82	11-Apr-83	2993	35.56	35.51	2.49	10.11	2800	21.1549	21.0359	16
M 998A	DUCTILE CAST IRON	11-Apr-83	25-Sep-84	12597	35.56	35.51	2.49	10.11	2800	21.0359	20.6702	12
M 996	DUCTILE CAST IRON	29-Nov-82	11-Apr-83	2993	35.89	38.05	2.54	10.03	3030	21.5231	21.3810	17
M 996A	DUCTILE CAST IRON	11-Apr-83	25-Sep-84	12597	35.89	38.05	2.54	10.03	3030	21.3810	21.0319	10

*Considered to be an outlier in statistical analysis.

GENERAL CORROSION, OXIC

SAMPLE ******		TIME **********			DIMENSIONS **********					WEIGHTS *******		CORROSION RATE
		START	END	TOTAL	LENGTH	WIDTH	HEIGHT	HOLE DI	AREA	INITIAL	FINAL	*********
NUMBER	MATERIAL	DATE	DATE	HR	MM	MM	MM	MM	MM*MM	GMS	GMS	MICROM/YR
M 999	DUCTILE CAST IRON	29-Nov-82	27-Jul-83	5273	35.51	35.76	2.54	10.06	2820	21.3352	21.2015	10
N 36	DUCTILE CAST IRON	29-Nov-82	25-Sep-84	15168	35.94	35.48	6.27	10.03	3490	53.4249	53.0232	8.5
N 35	DUCTILE CAST IRON	29-Nov-82	25-Sep-84	15168	35.53	35.48	6.27	9.53	3460	53.8016	52.5538	9.5
P 173	A27 NORM CAST	22-Apr-83	27-Jul-83	2280	35.38	35.69	1.55	9.04	2660	14.2520	NA	NA
P 172	A27 NORM CAST	22-Apr-83	27-Jul-83	2280	35.26	35.56	1.52	9.02	2640	13.9371	13.8577	15
P 171	A27 NORM CAST	22-Apr-83	27-Jul-83	2280	35.59	35.28	1.52	9.07	2640	13.9654	13.8864	15
P 174	A27 NORM CAST	22-Apr-83	27-Oct-83	4488	35.38	35.64	1.52	9.04	2650	14.0405	13.8468	18
P 176	A27 NORM CAST	22-Apr-83	27-Oct-83	4488	35.28	35.53	1.50	9.35	2630	13.8020	NA	NA
P 175	A27 NORM CAST	22-Apr-83	27-Oct-83	4488	35.59	35.28	1.50	9.58	2620	13.7546	13.5306	21
P 179	A27 NORM CAST	22-Apr-83	25-Sep-84	11739	35.69	35.36	1.52	9.32	2650	13.9721	13.5475	15
P 178	A27 NORM CAST	22-Apr-83	25-Sep-84	11739	35.26	35.53	1.52	9.07	2640	13.9045	13.5162	14
P 180	A27 NORM CAST	22-Apr-83	25-Sep-84	11739	35.28	35.53	1.50	9.09	2630	13.7664	13.3039	17
P 181	A27 NORM CAST	22-Apr-83	25-Sep-84	11739	35.53	35.26	1.52	9.09	2640	13.9206	13.5532	13
P 177	A27 NORM CAST	22-Apr-83	25-Sep-84	11739	35.33	35.69	1.52	9.09	2650	13.8904	13.5287	13
P 182	A27 NORM CAST	22-Apr-83	25-Sep-84	11739	35.26	35.56	1.52	9.32	2630	13.8774	13.4983	14
FE 24	PURE IRON	22-Apr-83	27-Jul-83	2280	31.80	31.80	1.57	9.50	2130	11.2362	11.1323	24
FE 25	PURE IRON	22-Apr-83	27-Jul-83	2280	31.70	31.75	1.50	9.53	2110	10.7699	NA	NA
FE 23	PURE IRON	22-Apr-83	27-Jul-83	2280	31.72	31.78	1.52	9.50	2110	10.8128	10.6957	27
FE 27	PURE IRON	22-Apr-83	27-Oct-83	4488	31.70	31.65	1.45	9.50	2090	10.5162	NA	NA
FE 26	PURE IRON	22-Apr-83	27-Oct-83	4488	31.60	31.72	1.50	9.53	2100	10.5406	10.3081	28
FE 30	PURE IRON	22-Apr-83	25-Sep-84	11739	31.67	31.55	1.52	9.53	2090	11.2723	10.8069	21
FE 28	PURE IRON	22-Apr-83	25-Sep-84	11739	31.65	31.70	1.37	9.50	2080	9.8976	9.4655	20

APPENDIX B

COMPILATION OF DATA FROM MOIST SALT STUDIES

APPENDIX B.1

COMPILATION OF DATA FROM MOIST SALT STUDIES

Moist Salt Test Number 2

Temperature: 150°C

Salt/brine combination: PBB1/PBB3

Magnesium concentrations reported on dry weight basis

Test start date: 3-5-84

Test end date: 6-4-84

Total time: 2178 hours

Sample Number	Material Type	Salt/Brine Combination	Water Concentration (wt%)	Magnesium Concentration (wt%)	Total Time (hr)	Coupon Length (mm)	Coupon Width (mm)	Coupon Thickness (mm)	Coupon Area (mm^2)	Initial Weight (gms)	Final Weight (gms)	Corrosion Rate (mm/yr)
CANISTER A												
N552	AISI 1025	PBB1/PBB3	5	0.42	2178	15.494	15.367	1.397	562.42	2.5885	2.5220	0.0605
N561	"	↓	↓	↓	↓	15.494	15.469	1.422	567.41	2.6227	2.5453	0.0699
N566	"	↓	↓	↓	↓	15.469	15.443	1.397	564.14	2.5408	2.4656	0.0682
N645	Ductile	↓	↓	↓	↓	15.545	15.342	1.499	569.58	2.4474	2.0973	0.315
N646	Cast Iron	↓	↓	↓	↓	15.291	15.392	1.575	567.37	2.4594	2.1198	0.307
N664	"	↓	↓	↓	↓	15.265	15.316	1.524	560.81	2.4567	2.1548	0.276
P650	A216 WCA	↓	↓	↓	↓	15.342	15.342	1.016	533.10	1.8408	1.3374	0.484
P652	(as cast)	↓	↓	↓	↓	15.215	15.316	1.016	528.10	1.8566	1.4141	0.429
P653	"	↓	↓	↓	↓	15.240	15.316	1.016	528.92	1.8463	1.3422	0.488
P665	"	↓	↓	↓	↓	15.265	15.240	1.016	527.26	1.8459	1.3323	0.499
P670	"	↓	↓	↓	↓	15.316	15.342	1.016	532.25	1.8493	1.3614	0.470
P674	"	↓	↓	↓	↓	15.316	15.316	1.016	531.40	1.8539	1.3952	0.442
CANISTER B												
N547	AISI 1025	PBB1/PBB3	10	0.81	2178	15.494	15.443	1.422	566.53	2.5947	2.5084	0.0782
N548	"	↓	↓	↓	↓	15.367	15.392	1.422	560.54	2.5656	2.4973	0.0625
N554	"	↓	↓	↓	↓	15.519	15.265	1.397	559.81	2.5737	2.4704	0.0945
N639	Ductile	↓	↓	↓	↓	15.342	15.265	1.524	561.68	2.4548	2.1163	0.309
N650	Cast Iron	↓	↓	↓	↓	15.240	15.443	1.524	564.22	2.4527	2.1322	0.291
N663	"	↓	↓	↓	↓	15.342	15.418	1.524	566.84	2.4563	2.1644	0.264
P639	A216 WCA	↓	↓	↓	↓	15.367	15.265	1.016	531.40	1.8626	1.3472	0.497
P646	(as cast)	↓	↓	↓	↓	15.265	15.367	1.041	532.93	1.8357	1.2472	0.566
P656	"	↓	↓	↓	↓	15.265	15.392	1.016	532.21	1.8634	1.3047	0.538
P660	"	↓	↓	↓	↓	15.367	15.316	1.016	533.07	1.8634	1.2503	0.589
P673	"	↓	↓	↓	↓	15.265	15.392	1.016	532.21	1.8427	1.3411	0.483
P687	"	↓	↓	↓	↓	15.291	15.418	1.016	533.91	1.8419	1.2853	0.534

Sample Number	Material Type	Salt/Brine Combination	Water Concentration (wt%)	Magnesium Concentration (wt%)	Total Time (hr)	Coupon Length (mm)	Coupon Width (mm)	Coupon Thickness (mm)	Coupon Area (mm²)	Initial Weight (gms)	Final Weight (gms)	Corrosion Rate (mm/yr)
CANISTER C												
N544	AISI 1025	PBB1/PBB3	20	1.7	2176	15.418	15.342	1.397	559.03	2.5742	2.4625	0.102
N550	"	↓	↓	↓	↓	15.418	15.316	1.422	559.69	2.5861	1.4975	0.0810
N570	"					15.418	15.469	1.422	564.84	0.6024	2.5049	0.0885
N637	Ductile					15.367	15.316	1.524	564.24	2.4537	2.0997	0.321
N643	Cast Iron					15.443	15.265	1.575	568.20	2.4557	2.1098	0.312
N651	"					15.291	15.367	1.575	566.53	2.4557	2.1042	0.318
P635	A216 WCA					15.265	15.392	1.016	[illegible]	1.6378	1.1237	0.667
P644	(as cast)					15.291	15.418	1.016	533.91	1.8620	1.1883	0.646
P662	"					15.316	15.316	1.016	531.40	1.8590	1.1781	0.656
P666	"					15.088	15.418	1.016	[illegible]	1.8065	1.1176	[illegible]
P667	"					15.367	15.342	1.016	533.92	1.8517	1.1632	0.661
P672	"					15.265	15.291	1.016	[illegible]	1.8493	1.1355	0.691
CANISTER D												
N551	AISI 1025	PBB1/PBB3	25	2.2	2176	15.494	15.418	1.397	564.14	2.6000	2.5201	0.0725
N553	"	↓	↓	↓	↓	15.519	15.443	1.422	567.38	2.5874	2.4931	0.0851
N568	"					15.519	15.469	1.422	568.26	2.6309	2.5393	0.0826
N640	Ductile					15.392	15.291	1.499	562.71	2.4414	2.0861	0.323
N644	Cast Iron					15.342	15.316	1.549	564.93	2.4493	2.0833	0.332
N654	"					15.265	15.392	1.524	563.36	2.4426	1.0742	0.335
P642	A 216 WCA					15.215	15.265	1.016	526.45	1.8205	1.1375	0.665
P645	(as cast)					15.392	15.443	0.991	536.51	1.8477	1.0735	0.739
P651	"					15.316	15.469	1.016	536.40	1.8650	1.2208	0.615
P659	"					15.240	15.367	1.016	530.58	1.8508	1.3128	0.519
P669	"					15.291	15.240	1.016	528.11	1.8218	1.1757	0.627
P686	"					15.418	15.291	1.016	533.91	1.8450	1.1965	0.622

Sample Number	Material Type	Salt/Brine Combination	Water Concentration (wt%)	Magnesium Concentration (wt%)	Total Time (hr)	Coupon Length (mm)	Coupon Width (mm)	Coupon Thickness (mm)	Coupon Area (mm^2)	Initial Weight (gms)	Final Weight (gms)	Corrosion Rate (mm/yr)
CANISTER E												
N545	AISI 1025	PBB1/PBB3	30	2.78		15.443	15.469	1.422	565.69	2.6155	2.5268	0.0803
N563						15.443	15.367	1.397	560.71	2.6049	2.5271	0.0711
N573						15.316	15.291	1.422	555.44	2.5695	2.4734	0.0887
N649	Ductile					15.342	15.367	1.549	566.66	2.4543	2.0793	0.339
N662	Cast Iron					15.367	15.392	1.524	566.81	2.4606	2.0782	0.346
N666	"					15.215	15.342	1.524	559.99	2.4327	2.0702	0.332
P643	A216 WCA					15.316	15.418	0.911	533.20	1.8563	1.2095	0.621
P658	(as cast)					15.291	15.367	1.016	532.25	1.8460	1.0694	0.747
P661	"					15.265	15.342	1.016	530.58	1.8466	1.2289	0.596
P668	"					15.291	15.392	1.016	533.07	1.8372	1.2244	0.589
P679	"					15.342	15.316	1.016	532.25	1.8585	1.2186	0.616
P685	"					15.265	15.316	1.016	529.74	1.8405	1.0064	0.806

APPENDIX B.2

COMPILATION OF DATA FROM MOIST SALT STUDIES

Moist Salt Test Number 3

Temperature: 150°C

Salt/brine combination: PBB1/PBB3

Magnesium concentrations reported on dry weight basis.

Test start date: 5-10-84

(Canister EE is an ongoing test.)

Sample Number	Material Type	Salt/Brine Combination	Water Concentration (wt%)	Magnesium Concentration (wt%)	Total Time (hr)	Coupon Length (mm)	Coupon Width (mm)	Coupon Thickness (mm)	Coupon Area (mm^2)	Initial Weight (gms)	Final Weight (gms)	Corrosion Rate (mm/yr)
CANISTER EE												
N558	AISI 1025	PBB1/PBB3	20	1.7	--	15.392	15.519	1.397	564.10	2.6004	--	-
N560	"				--	15.392	15.494	1.397	563.26	2.5732	--	-
N565	"				--	15.392	15.443	1.397	561.55	2.5967	--	-
N636	Ductile				--	15.342	15.291	1.499	561.03	2.4535	--	-
N638	Cast Iron				--	15.316	15.265	1.499	559.28	2.4473	--	-
N668	"				--	15.469	15.291	1.473	563.69	2.4490	--	-
P637	A216 WCA				--	15.215	15.316	1.016	528.10	1.8429	--	-
P641	(as cast)				--	15.265	15.392	1.016	532.21	1.8510	--	-
P654	"				--	15.265	15.392	1.016	532.21	1.8374	--	-
P655	"				--	15.291	15.342	0.991	529.90	1.8325	--	-
P671	"				--	15.316	15.291	1.016	530.59	1.8584	--	-
P678	"				--	15.265	15.342	1.016	530.58	1.8359	--	-
CANISTER F												
N543	AISI 1025	PBB1/PBB3	30	2.7	1659	15.443	15.443	1.397	563.27	2.5855	2.5242	0.0731
N562	"					15.443	15.519	1.397	562.46	2.6187	2.5598	0.0699
N574						15.392	15.494	1.397	563.26	2.5732	2.5029	0.0839
N647	Ductile					15.342	15.519	1.473	567.10	2.4417	2.1564	0.338
N648	Cast Iron					15.443	15.342	1.499	566.15	2.4540	2.1680	0.339
N665	"					15.291	15.316	1.499	560.15	2.4573	2.1698	0.345
P638	A216 WCA					15.240	15.342	0.991	528.24	1.8424	1.2318	0.777
P647	(as cast)					15.342	15.342	1.016	533.10	1.8320	1.2029	0.793
P648	"					15.291	15.392	0.991	531.53	1.8376	1.2844	0.700
P676	"					15.265	15.342	0.889	522.81	1.6211	1.1346	0.626
P688	"					15.265	15.342	1.016	530.58	1.8453	1.4064	0.556
P690	"					15.291	15.291	1.016	529.77	1.8410	1.2955	0.692

Sample Number	Material Type	Salt/Brine Combination	Water Concentration (wt%)	Magnesium Concentration (wt%)	Total Time (hr)	Coupon Length (mm)	Coupon Width (mm)	Coupon Thickness (mm)	Coupon Area (mm^2)	Initial Weight (gms)	Final Weight (gms)	Corrosion Rate (mm/yr)
CANISTER G												
N546	AISI 1025	PBB1/PBB3	20	1.7	767	15.418	15.570	1.397	566.70	2.5992	2.5138	0.219
N559	"					15.392	15.570	1.397	565.81	2.5867	2.5249	0.159
N571	"					15.494	15.494	1.397	566.71	2.5991	2.5286	0.181
N653	Ductile					15.291	15.342	1.499	561.03	2.4572	2.3282	0.334
N656	Cast Iron					15.392	15.494	1.499	569.56	2.4545	2.3043	0.383
N661	"					15.443	15.291	1.499	564.42	2.4587	2.3136	0.374
P636	A216 WCA					15.265	15.342	1.016	530.58	1.8414	1.6437	0.542
P640	(as cast)					15.291	15.240	0.991	526.58	1.8275	1.5854	0.668
P663	"					15.265	15.342	1.016	530.58	1.8473	1.6399	0.568
P664	"					15.316	15.418	1.016	534.74	1.8558	1.5904	0.722
P680	"					15.265	15.316	1.016	529.74	1.8615	1.6232	0.654
P682	"					15.342	15.316	0.838	521.34	1.5017	1.3088	0.538
CANISTER H												
N564	AISI 1025	PBB1/PBB3	30	2.7	767	15.418	15.443	1.397	562.43	2.6088	2.5736	0.0911
N567	"					15.469	15.443	1.346	560.99	2.5092	2.4716	0.0974
N569	"					15.469	15.392	1.397	562.42	2.5855	2.5371	0.125
N641	Ductile					15.291	15.418	1.499	563.58	2.4503	2.3133	0.353
N657	Cast Iron					15.265	15.443	1.499	563.54	2.4525	2.3297	0.317
N667	"					15.342	15.367	1.473	561.99	2.4468	2.3226	0.321
P649	A216 WCA					15.291	15.291	0.991	528.24	1.8414	1.5430	0.821
P675	(as cast)					15.342	15.392	0.991	533.20	1.8330	1.5932	0.654
P677	"					15.265	15.367	1.016	531.40	1.8574	1.6643	0.528
P683	"					15.291	15.316	1.016	530.59	1.8268	1.5319	0.808
P684	"					15.316	15.316	0.991	529.87	1.8340	1.6174	0.594
P689	"					15.316	15.392	0.914	527.62	1.6681	1.4546	0.588

APPENDIX B.3

COMPILATION OF DATA FROM MOIST SALT STUDIES

Moist Salt Test Number 4

Temperature: 150°C

Material: A216 Grade WCA (various heat treatments)

Magnesium concentrations reported on dry weight basis.

Test start date: 8-16-84

(Canisters F and G are ongoing tests.)

Sample Number	Material Type	Salt/Brine Combination	Water Concentration (wt%)	Magnesium Concentration (wt%)	Total Time (hr)	Coupon Length (mm)	Coupon Width (mm)	Coupon Thickness (mm)	Coupon Area (mm^2)	Initial Weight (gms)	Final Weight (gms)	Corrosion Rate (mm/yr)
CANISTER D												
Q366	As Cast	NaCl/NaCl	20	0	759.5	15.469	15.443	1.499	570.45	2.7287	2.7270	0.00425
Q367	"					15.469	15.519	1.499	573.03	2.7439	2.7422	0.00423
Q428	"					15.570	15.418	1.499	573.02	2.7015	2.6994	0.00538
Q570	"					15.392	15.570	1.499	572.13	2.7282	2.7263	0.00488
Q621	Normalized					15.494	15.291	1.524	567.67	2.7603	2.7585	0.00466
Q623	"					15.418	15.342	1.524	566.84	2.7615	2.7590	0.00661
Q625	"					15.392	15.418	1.524	568.54	2.7960	2.7944	0.00400
Q627	"					15.469	15.316	1.524	567.68	2.7803	2.7787	0.00401
Q754	Homogenized					15.469	15.265	1.499	564.41	2.7407	2.7395	0.00312
Q760	"					15.392	15.291	1.499	562.71	2.7389	2.7376	0.00352
Q762	"					15.392	15.291	1.499	562.71	2.7002	2.6977	0.00652
Q767	"					15.418	15.316	1.499	564.42	2.7012	2.6997	0.00390
CANISTER E												
Q433	As Cast	PBB1/PBB1	20	0.042	759.5	15.469	15.443	1.524	572.00	2.7670	2.7623	0.0121
Q489	"					15.545	15.443	1.499	573.02	2.7360	2.7311	0.0126
Q493	"					15.418	15.519	1.499	571.29	2.7411	2.7369	0.0108
Q505	"					15.443	15.494	1.499	571.30	2.7458	2.7425	0.00835
Q611	Normalized					15.418	15.316	1.524	565.96	2.7958	2.7922	0.00934
Q617	"					15.392	15.316	1.524	565.09	2.7620	2.7584	0.00949
Q618	"					15.418	15.291	1.524	565.11	2.7920	2.7868	0.0135
Q622	"					15.418	15.316	1.524	565.96	2.7978	2.7948	0.00791
Q752	Homogenized					15.469	15.291	1.499	565.29	2.7185	2.7147	0.00987
Q756	"					15.469	15.291	1.499	565.29	2.7140	2.7106	0.00896
Q758	"					15.418	15.342	1.499	565.30	2.7345	2.7303	0.0109
Q763	"					15.367	15.342	1.499	563.59	2.7302	2.7257	0.0117

Sample Number	Material Type	Salt/Brine Combination	Water Concentration (wt%)	Magnesium Concentration (wt%)	Total Time (hr)	Coupon Length (mm)	Coupon Width (mm)	Coupon Thickness (mm)	Coupon Area (mm^2)	Initial Weight (gms)	Final Weight (gms)	Corrosion Rate (mm/yr)
CANISTER F												
Q419	As Cast	PBB1/PBB3	20	1.7	--	15.519	15.494	1.499	573.88	2.7285	--	--
Q549	"				--	15.443	15.494	1.499	571.30	2.7413	--	--
Q553	"				--	15.418	15.519	1.499	571.29	2.7410	--	--
Q579	"				--	15.519	15.418	1.524	572.84	2.7535	--	--
Q610	Normalized				--	15.342	15.494	1.499	567.86	2.7490	--	--
Q612	"				--	15.418	15.291	1.524	565.11	2.7658	--	--
Q614	"				--	15.342	15.342	1.524	564.28	2.7836	--	--
Q620	"				--	15.418	15.367	1.524	567.69	2.7874	--	--
Q759	Homogenized				--	15.570	15.291	1.524	570.23	2.7463	--	--
Q764	"				--	15.392	15.316	1.499	563.55	2.7172	--	--
Q768	"				--	15.443	15.291	1.499	564.42	2.7305	--	--
Q769	"				--	15.443	15.316	1.499	565.27	2.7254	--	--
CANISTER G												
Q401	As Cast	PBB1/PBB1	20	0.042	--	15.519	15.469	1.499	573.03	2.7508	--	--
Q424	"				--	15.469	15.494	1.499	572.18	2.7455	--	--
Q477	"				--	15.519	15.570	1.499	576.47	2.7400	--	--
Q569	"				--	15.494	15.418	1.499	570.45	2.7417	--	--
Q616	Normalized				--	15.367	15.367	1.524	565.97	2.7974	--	--
Q619	"				--	15.392	15.342	1.524	565.97	2.7979	--	--
Q624	"				--	15.418	15.316	1.524	565.96	2.7533		
Q628	"				--	15.443	15.367	1.524	568.53	2.7925	--	--
Q750	Homogenized				--	15.469	15.291	1.499	565.29	2.7369	--	--
Q755	"				--	15.443	15.291	1.499	564.42	2.7240	--	--
Q761	"				--	15.392	15.316	1.499	563.55	2.7192	--	--
Q766	"				--	15.469	15.265	1.499	564.41	2.7301	--	--

Sample Number	Material Type	Salt/Brine Combination	Water Concentration (wt%)	Magnesium Concentration (wt%)	Total Time (hr)	Coupon Length (mm)	Coupon Width (mm)	Coupon Thickness (mm)	Coupon Area (mm^2)	Initial Weight (gms)	Final Weight (gms)	Corrosion Rate (mm/yr)
CANISTER H												
Q369	As Cast	PBB1/PBB3	20	1.7	759.5	15.570	15.469	1.499	574.76	2.7446	2.4599	0.728
Q526	"	↓	↓	↓	↓	15.469	15.545	1.499	573.91	2.7407	2.5243	0.554
Q598	"	↓	↓	↓	↓	15.469	15.443	1.499	570.45	2.7538	2.5630	0.491
Q609	"	↓	↓	↓	↓	15.469	15.545	1.499	573.91	2.7606	2.5510	0.536
Q613	Normalized	↓	↓	↓	↓	15.418	15.291	1.524	565.11	2.7870	2.5413	0.638
Q615	"	↓	↓	↓	↓	15.418	15.316	1.524	565.96	2.7928	2.5217	0.703
Q626	"	↓	↓	↓	↓	15.494	15.291	1.524	567.67	2.7907	2.5133	0.717
Q629	"	↓	↓	↓	↓	15.443	15.316	1.524	566.80	2.7543	2.3666	1.004
Q751	Homogenized	↓	↓	↓	↓	15.469	15.316	1.499	566.14	2.7380	2.3095	1.111
Q753	"	↓	↓	↓	↓	15.469	15.291	1.499	565.29	2.7248	2.3899	0.870
Q757	"	↓	↓	↓	↓	15.494	15.316	1.499	566.98	2.7253	2.4467	0.722
Q765	"	↓	↓	↓	↓	15.443	15.291	1.499	564.42	2.7408	2.3673	0.972

APPENDIX C

COMPILATION OF DATA FROM IRRADIATION-CORROSION STUDIES

APPENDIX C

COMPILATION OF DATA FROM IRRADIATION-CORROSION STUDIES

Irradiation intensities: 2×10^3 rad/h and 1×10^5 rad/h

Brine: PBB2

Oxygen concentration: 0.05 ppm

Temperature: 150°C

Flow rate: 35 mL/h

IRRADIATION CORROSION

SAMPLE		TIME		IRRADIATION		DIMENSIONS					WEIGHTS		CORROSION RATE
NUMBER	MATERIAL	START DATE	END DATE	TOTAL HR	RATE KR/H	LENGTH MM	WIDTH MM	HEIGHT MM	HOLE DI MM	AREA MM*MM	INITIAL GM	FINAL GM	MICRON/YR
N 703	1025 WROUGHT STEEL	19-May-83	NA	NA	2	35.51	35.59	1.42	9.60	2630	12.9402	NA	NA
N 700	1025 WROUGHT STEEL	19-May-83	27-Jun-83	840	2	35.43	35.46	1.42	9.93	2600	12.9963	NA	NA
N 711	1025 WROUGHT STEEL	19-May-83	27-Jun-83	840	2	35.46	35.43	1.40	9.88	2600	12.5151	12.4698	23
N 705	1025 WROUGHT STEEL	19-May-83	27-Jun-83	840	2	35.43	35.48	1.42	9.88	2610	13.0363	12.9976	20
N 710	1025 WROUGHT STEEL	19-May-83	22-Aug-83	2160	2	35.51	35.51	1.42	9.88	2620	13.0815	13.0155	13
N 701	1025 WROUGHT STEEL	19-May-83	22-Aug-83	2160	2	35.59	35.59	1.42	9.86	2630	13.2162	13.1483	13
N 706	1025 WROUGHT STEEL	19-May-83	22-Aug-83	2160	2	35.56	35.53	1.42	9.88	2620	13.1970	13.1367	12
N 709	1025 WROUGHT STEEL	19-May-83	12-Dec-83	4344	2	35.43	35.43	1.37	9.86	2600	12.6161	12.4867	13
N 702	1025 WROUGHT STEEL	19-May-83	12-Dec-83	4344	2	35.56	35.61	1.42	9.75	2630	13.2193	NA	NA
N 707	1025 WROUGHT STEEL	19-May-83	19-Sep-84	9443	2	35.56	35.59	1.42	9.63	2630	13.2114	12.9599	11
N 704	1025 WROUGHT STEEL	19-May-83	19-Sep-84	9443	2	35.46	35.48	1.42	9.91	2610	13.0634	12.7771	13
N 708	1025 WROUGHT STEEL	19-May-83	19-Sep-84	9443	2	35.43	35.46	1.42	9.91	2610	12.9912	12.7142	13
P 518	A216 CAST STEEL	23-Dec-83	NA	NA	2	35.56	35.56	1.55	9.78	2650	14.0877	NA	NA
P 529	A216 CAST STEEL	23-Dec-83	24-Jan-84	768	2	35.56	35.56	1.60	9.78	2660	14.1837	14.1587	14
P 515	A216 CAST STEEL	23-Dec-83	24-Jan-84	768	2	35.56	35.56	1.55	9.78	2650	14.1927	14.1391	29
P 527	A216 CAST STEEL	23-Dec-83	13-Apr-84	2180	2	35.56	35.56	1.55	9.78	2650	14.0262	13.9605	13
P 516	A216 CAST STEEL	23-Dec-83	13-Apr-84	2180	2	35.56	35.56	1.55	9.78	2650	14.1614	14.0771	16
Q 118	A216 CAST STEEL	20-Apr-84	19-Sep-84	2919	2	35.59	35.56	12.73	9.27	NA	117.9610	117.6411	NA
Q 117	A216 CAST STEEL	20-Apr-84	19-Sep-84	2919	2	35.53	35.53	12.75	9.37	NA	117.9316	117.5986	NA
P 517	A216 CAST STEEL	23-Dec-83	06-Jul-84	3974	2	35.56	35.56	1.57	9.78	2650	14.0504	13.9148	14
P 522	A216 CAST STEEL	23-Dec-83	06-Jul-84	3974	2	35.56	35.56	1.55	9.78	2650	14.1328	14.0363	10
P 528	A216 CAST STEEL	23-Dec-83	06-Jul-84	3974	2	35.56	35.56	1.60	9.78	2660	14.2335	14.1522	8.6
P 525	A216 CAST STEEL	23-Dec-83	06-Jul-84	3974	2	35.56	35.56	1.57	9.78	2650	14.1888	14.0916	10
P 520	A216 CAST STEEL	23-Dec-83	06-Jul-84	3974	2	35.56	35.56	1.55	9.78	2650	14.1655	14.0562	12
P 523	A216 CAST STEEL	23-Dec-83	19-Sep-84	5099	2	35.53	35.56	1.55	9.78	2650	14.1345	13.9814	13
P 521	A216 CAST STEEL	23-Dec-83	19-Sep-84	5099	2	35.56	35.56	1.55	9.78	2650	14.1310	13.9794	13
P 519	A216 CAST STEEL	23-Dec-83	19-Sep-84	5099	2	35.56	35.56	1.52	9.78	2640	14.1540	13.9675	15
P 526	A216 CAST STEEL	23-Dec-83	19-Sep-84	5099	2	35.53	35.56	1.60	9.78	2650	14.1513	13.9995	13
P 524	A216 CAST STEEL	23-Dec-83	19-Sep-84	5099	2	35.56	35.56	1.55	9.75	2650	14.0488	13.8854	14
P 312	A27 NORM. CAST	19-May-83	NA	NA	2	35.56	35.53	1.47	9.55	2640	13.7615	NA	NA
P 313	A27 NORM. CAST	19-May-83	27-Jun-83	840	2	35.53	35.56	1.47	9.53	2640	13.8145	13.7878	13
P 305	A27 NORM. CAST	19-May-83	27-Jun-83	840	2	35.43	35.48	1.50	9.55	2630	13.8482	13.8222	13
P 317	A27 NORM. CAST	19-May-83	27-Jun-83	840	2	35.53	35.46	1.50	9.55	2630	13.7554	NA	NA
P 309	A27 NORM. CAST	19-May-83	27-Jun-83	840	2	35.56	35.53	1.50	9.55	2640	13.8958	NA	NA
P 316	A27 NORM. CAST	19-May-83	22-Aug-83	2160	2	35.53	35.56	1.50	9.55	2640	13.7960	13.7345	12
P 306	A27 NORM. CAST	19-May-83	22-Aug-83	2160	2	35.43	35.53	1.50	9.53	2630	13.7144	13.6607	11
P 311	A27 NORM. CAST	19-May-83	22-Aug-83	2160	2	35.51	35.56	1.47	9.55	2640	13.8500	13.7830	13
P 315	A27 NORM. CAST	19-May-83	12-Dec-83	4344	2	35.53	35.53	1.50	9.55	2640	13.8815	13.7335	14
P 307	A27 NORM. CAST	19-May-83	12-Dec-83	4344	2	35.51	35.43	1.50	9.53	2630	13.8120	NA	NA
P 310	A27 NORM. CAST	19-May-83	19-Sep-84	9443	2	35.56	35.53	1.47	9.58	2640	13.7044	13.4135	13
P 314	A27 NORM. CAST	19-May-83	19-Sep-84	9443	2	35.53	35.51	1.50	9.55	2640	13.8350	13.4950	15
P 308	A27 NORM. CAST	19-May-83	19-Sep-84	9443	2	35.53	35.43	1.47	9.53	2630	13.5507	13.2847	12
N 23	DUCTILE CAST IRON	19-May-83	NA	NA	2	35.69	35.48	2.51	9.53	2820	21.4427	NA	NA
N 34	DUCTILE CAST IRON	19-May-83	27-Jun-83	840	2	35.46	35.46	2.51	10.13	2790	21.0555	20.9805	36
N 20	DUCTILE CAST IRON	19-May-83	27-Jun-83	840	2	35.89	35.48	2.51	10.06	2830	21.4476	NA	NA
N 24	DUCTILE CAST IRON	19-May-83	27-Jun-83	840	2	35.48	35.71	2.51	9.96	2820	21.4402	21.3735	31
N 30	DUCTILE CAST IRON	19-May-83	27-Jun-83	840	2	35.81	35.48	2.49	10.21	2810	21.2209	21.1481	34
N 26	DUCTILE CAST IRON	19-May-83	27-Jun-83	840	2	35.51	35.79	2.51	10.03	2820	21.4703	21.4101	28
N 21	DUCTILE CAST IRON	19-May-83	22-Aug-83	2160	2	35.46	35.51	2.51	10.06	2800	21.2250	21.1442	15
N 33	DUCTILE CAST IRON	19-May-83	22-Aug-83	2160	2	35.61	35.48	2.51	10.06	2810	21.2272	21.1261	19
N 27	DUCTILE CAST IRON	19-May-83	22-Aug-83	2160	2	35.48	35.56	2.51	10.03	2800	21.2906	21.1910	18

IRRADIATION CORROSION

SAMPLE ******			TIME **********	IRRADIATION ***********		DIMENSIONS **********					WEIGHTS *******		CORROSION RATE *********
NUMBER	MATERIAL	START DATE	END DATE	TOTAL HR	RATE KR/H	LENGTH MM	WIDTH MM	HEIGHT MM	HOLE DI MM	AREA MM*MM	INITIAL GM	FINAL GM	MICRON/YR
N 22	DUCTILE CAST IRON	19-May-83	12-Dec-83	4344	2	35.53	35.31	2.49	9.53	2790	21.1462	21.0014	13
N 32	DUCTILE CAST IRON	19-May-83	12-Dec-83	4344	2	35.48	35.48	2.51	10.06	2800	21.1250	20.9304	18
N 25	DUCTILE CAST IRON	19-May-83	19-Sep-84	9443	2	35.48	35.74	2.51	10.01	2820	21.3277	20.9377	16
N 28	DUCTILE CAST IRON	19-May-83	19-Sep-84	9443	2	35.48	35.56	2.51	10.06	2800	21.1163	20.6844	18
N 31	DUCTILE CAST IRON	19-May-83	19-Sep-84	9443	2	35.59	35.48	2.51	10.11	2800	21.1073	20.6382	20
N 29	DUCTILE CAST IRON	19-May-83	19-Sep-84	9443	2	35.48	35.76	2.51	10.03	2820	21.4648	21.0114	19
P 350	PURE IRON	29-Jun-83	NA	NA	2	32.08	31.42	1.83	9.45	2160	13.0374	NA	NA
P 347	PURE IRON	29-Jun-83	23-Aug-83	1320	2	31.72	31.90	1.75	9.45	2160	13.0277	NA	NA
P 352	PURE IRON	29-Jun-83	23-Aug-83	1320	2	31.78	31.72	1.91	9.45	2170	13.7406	13.6162	48
P 341	PURE IRON	29-Jun-83	23-Aug-83	1320	2	31.55	31.88	1.96	9.45	2180	14.0906	13.9677	48
P 351	PURE IRON	29-Jun-83	12-Dec-83	3504	2	31.85	31.67	1.65	9.42	2140	11.7003	11.5112	28
P 342	PURE IRON	29-Jun-83	12-Dec-83	3504	2	31.45	31.75	1.96	9.35	2160	14.0242	13.8434	27
P 348	PURE IRON	29-Jun-83	06-Jul-84	7478	2	31.70	32.18	1.55	9.55	2140	11.3819	11.1057	19
P 345	PURE IRON	29-Jun-83	06-Jul-84	7478	2	31.70	32.18	1.91	9.47	2200	13.8486	13.5960	17
P 349	PURE IRON	29-Jun-83	06-Jul-84	7478	2	31.88	31.75	1.91	9.35	2190	13.9183	13.6544	18
P 346	PURE IRON	29-Jun-83	06-Jul-84	7478	2	32.08	31.88	1.85	9.30	2200	13.3129	13.0438	18
P 343	PURE IRON	29-Jun-83	06-Jul-84	7478	2	31.60	31.95	1.78	9.40	2160	12.9896	12.6974	20
P 344	PURE IRON	29-Jun-83	19-Sep-84	8461	2	31.90	31.95	1.91	9.40	2200	13.9446	13.6825	16
N 253	1025 WROUGHT STEEL	26-Oct-82	NA	NA	100	35.38	35.66	1.47	9.60	2630	13.3240	NA	NA
N 250	1025 WROUGHT STEEL	26-Oct-82	30-Nov-82	784	100	35.43	35.66	1.45	9.58	2630	13.0148	12.8319	99
N 251	1025 WROUGHT STEEL	26-Oct-82	30-Nov-82	784	100	35.74	35.51	1.45	9.63	2640	13.2756	13.0136	140
N 256	1025 WROUGHT STEEL	26-Oct-82	30-Nov-82	784	100	35.69	35.46	1.45	9.70	2630	13.2662	12.9739	160
N 261	1025 WROUGHT STEEL	01-Dec-82	03-Mar-83	2160	100	35.41	35.56	1.45	9.65	2620	13.2239	12.5706	130
N 262	1025 WROUGHT STEEL	01-Dec-82	03-Mar-83	2160	100	35.43	35.56	1.40	9.60	2620	13.0250	12.3606	130
N 260	1025 WROUGHT STEEL	01-Dec-82	03-Mar-83	2160	100	35.46	35.59	1.42	9.63	2620	13.2804	12.6105	130
N 252	1025 WROUGHT STEEL	26-Oct-82	03-Mar-83	2944	100	35.53	35.64	1.50	9.60	2650	13.3769	12.8114	81
N 257	1025 WROUGHT STEEL	26-Oct-82	20-Jul-83	5296	100	35.53	35.69	1.47	9.63	2650	13.2404	11.8354	120
N 259	1025 WROUGHT STEEL	26-Oct-82	20-Jul-83	5296	100	35.69	35.56	1.45	9.58	2640	13.2583	12.3356	74
N 255	1025 WROUGHT STEEL	26-Oct-82	22-Nov-83	7576	100	35.69	35.51	1.45	9.65	2640	13.2741	12.2153	59
N 248	1025 WROUGHT STEEL	26-Oct-82	22-Nov-83	7576	100	35.56	35.74	1.47	9.65	2650	13.2516	11.3232	110
N 254	1025 WROUGHT STEEL	26-Oct-82	22-Nov-83	7576	100	35.66	35.59	1.45	9.58	2640	13.2803	NA	NA
N 249	1025 WROUGHT STEEL	26-Oct-82	27-Feb-84	9298	100	35.66	35.59	1.45	9.65	2640	13.2324	11.9401	59
N 258	1025 WROUGHT STEEL	26-Oct-82	17-Sep-84	13245	100	35.61	35.48	1.47	9.63	2640	13.2607	10.9057	75
N 175	2.5%CR,1%MO STEEL	26-Oct-82	30-Nov-82	784	100	35.53	35.53	6.35	9.60	3480	58.5172	58.2838	96
N 174	2.5%CR,1%MO STEEL	26-Oct-82	30-Nov-82	784	100	35.59	35.56	6.35	9.58	3480	58.6257	58.4449	74
N 176	2.5%CR,1%MO STEEL	26-Oct-82	30-Nov-82	784	100	35.53	35.53	6.35	9.63	3470	58.5346	58.2339	120
N 148	2.5%CR,1%MO STEEL	01-Dec-82	03-Mar-83	2160	100	35.56	34.67	2.57	9.58	2760	23.3026	22.8631	82
N 149	2.5%CR,1%MO STEEL	01-Dec-82	03-Mar-83	2160	100	35.43	35.51	2.59	9.60	2820	23.8301	23.3444	89
N 150	2.5%CR,1%MO STEEL	01-Dec-82	03-Mar-83	2160	100	35.46	35.51	2.59	9.58	2820	23.8226	23.3641	84
N 155	2.5%CR,1%MO STEEL	26-Oct-82	03-Mar-83	2944	100	35.74	35.53	2.59	9.58	2840	24.0379	23.5718	62
N 153	2.5%CR,1%MO STEEL	26-Oct-82	20-Jul-83	5296	100	35.53	35.15	2.59	9.55	2800	23.6058	22.8341	58
N 156	2.5%CR,1%MO STEEL	26-Oct-82	20-Jul-83	5296	100	35.53	35.46	2.54	9.55	2820	23.4895	22.5061	74
N 154	2.5%CR,1%MO STEEL	26-Oct-82	22-Nov-83	7576	100	35.53	35.48	2.57	9.55	2820	23.4938	22.1677	69
P 924	A216 CAST STEEL	06-Mar-84	NA	NA	100	35.61	35.56	1.60	9.45	2670	14.7218	NA	NA
P 920	A216 CAST STEEL	06-Mar-84	09-Apr-84	815	100	35.66	35.53	1.55	9.73	2650	14.4975	14.1343	190
P 932	A216 CAST STEEL	06-Mar-84	09-Apr-84	815	100	35.64	35.51	1.50	9.58	2650	14.4731	14.2863	97
P 923	A216 CAST STEEL	06-Mar-84	25-Jun-84	2393	100	35.64	35.53	1.55	9.53	2660	14.3426	13.6209	130
P 930	A216 CAST STEEL	06-Mar-84	25-Jun-84	2393	100	35.56	35.64	1.57	9.55	2660	14.5399	13.9650	100
P 926	A216 CAST STEEL	06-Mar-84	25-Jun-84	2393	100	35.61	35.53	1.55	9.50	2650	14.4754	13.8164	120
P 921	A216 CAST STEEL	06-Mar-84	25-Jun-84	2393	100	35.53	35.64	1.55	9.75	2650	14.4789	13.6616	140
Q 121	A216 CAST STEEL	20-Apr-84	17-Sep-84	3132	100	35.61	35.56	12.75	9.40	NA	117.9500	116.6844	NA

IRRADIATION CORROSION

SAMPLE			TIME	IRRADIATION		DIMENSIONS					WEIGHTS		CORROSION RATE
NUMBER	MATERIAL	START DATE	END DATE	TOTAL HR	RATE KR/H	LENGTH MM	WIDTH MM	HEIGHT MM	HOLE DI MM	AREA MM*MM	INITIAL GM	FINAL GM	MICROM/YR
Q 119	A216 CAST STEEL	20-Apr-84	17-Sep-84	3132	100	35.61	35.59	12.73	9.50	NA	117.9537	116.2482	NA
P 933	A216 CAST STEEL	06-Mar-84	17-Sep-84	3947	100	35.56	35.64	1.52	9.50	2660	14.4312	13.7865	69
P 928	A216 CAST STEEL	06-Mar-84	17-Sep-84	3947	100	35.56	35.64	1.57	9.58	2660	14.6320	13.7130	98
P 927	A216 CAST STEEL	06-Mar-84	17-Sep-84	3947	100	35.56	35.64	1.52	9.68	2650	14.6920	13.6941	110
P 922	A216 CAST STEEL	06-Mar-84	17-Sep-84	3947	100	35.66	35.53	1.55	9.58	2660	14.7769	13.7572	110
P 919	A216 CAST STEEL	06-Mar-84	17-Sep-84	3947	100	35.64	35.53	1.52	9.58	2650	14.4251	13.1022	140
P 925	A216 CAST STEEL	06-Mar-84	17-Sep-84	3947	100	35.61	35.56	1.52	9.80	2650	14.2810	13.3098	100
P 931	A216 CAST STEEL	06-Mar-84	17-Sep-84	3947	100	35.66	35.53	1.52	9.63	2650	14.5640	13.7429	87
P 929	A216 CAST STEEL	06-Mar-84	17-Sep-84	3947	100	35.56	35.64	1.55	9.53	2660	14.5015	13.5816	98
N 104	A27 CAST STEEL	26-Oct-82	NA	NA	100	36.04	35.64	6.35	9.65	3530	59.8908	NA	NA
N 83	A27 CAST STEEL	26-Oct-82	30-Nov-82	784	100	35.61	36.83	2.44	9.68	2900	23.6034	NA	NA
N 82	A27 CAST STEEL	26-Oct-82	30-Nov-82	784	100	35.61	35.86	2.44	9.60	2830	23.0058	22.8021	100
N 103	A27 CAST STEEL	26-Oct-82	30-Nov-82	784	100	35.66	35.41	6.35	9.55	3480	58.8981	58.4599	180
N 66	A27 CAST STEEL	26-Oct-82	03-Mar-83	2944	100	35.64	35.79	2.44	9.63	2830	22.9468	21.9903	130
N 108	A27 CAST STEEL	26-Oct-82	03-Mar-83	2944	100	35.51	35.61	6.35	9.68	3480	59.0103	57.7520	140
N 69	A27 CAST STEEL	26-Oct-82	03-Mar-83	2944	100	35.61	36.65	2.46	9.68	2890	23.3693	22.6845	90
N 70	A27 CAST STEEL	26-Oct-82	20-Jul-83	5296	100	36.02	35.61	2.44	9.63	2840	22.9934	NA	NA
N 81	A27 CAST STEEL	26-Oct-82	20-Jul-83	5296	100	35.41	35.61	2.46	9.86	2800	22.2327	21.0285	91
N 67	A27 CAST STEEL	26-Oct-82	22-Nov-83	7576	100	35.64	36.40	2.44	9.68	2870	23.2754	21.0709	110
N 68	A27 CAST STEEL	26-Oct-82	22-Nov-83	7576	100	36.60	35.61	2.46	9.70	2890	23.5309	21.6939	94
N 107	A27 CAST STEEL	26-Oct-82	17-Sep-84	13245	100	35.66	35.43	6.35	9.65	3480	58.9214	55.1143	92
P 157	A27 NORM. CAST	25-Mar-83	NA	NA	100	35.64	35.36	1.52	9.27	2650	14.1034	NA	NA
P 149	A27 NORM. CAST	25-Mar-83	20-Jul-83	2352	100	35.53	35.20	1.52	9.25	2630	13.7566	11.9167	330
P 156	A27 NORM. CAST	25-Mar-83	20-Jul-83	2352	100	35.64	35.38	1.50	8.99	2650	13.9246	13.4967	77
P 152	A27 NORM. CAST	25-Mar-83	22-Nov-83	4632	100	35.56	35.33	1.50	8.99	2640	13.9311	12.4093	140
P 150	A27 NORM. CAST	25-Mar-83	22-Nov-83	4632	100	35.74	35.33	1.52	8.97	2660	14.1475	NA	NA
P 154	A27 NORM. CAST	25-Mar-83	22-Nov-83	4632	100	35.56	35.26	1.52	9.14	2640	13.8398	12.9780	79
P 151	A27 NORM. CAST	25-Mar-83	27-Feb-84	7080	100	35.56	35.33	1.50	9.14	2640	13.8938	11.9438	120
P 148	A27 NORM. CAST	25-Mar-83	09-Apr-84	7895	100	35.38	35.56	1.52	9.25	2640	14.1464	NA	NA
P 153	A27 NORM. CAST	25-Mar-83	17-Sep-84	11027	100	35.39	35.61	1.52	8.86	2660	14.1829	12.0673	81
P 155	A27 NORM. CAST	25-Mar-83	17-Sep-84	11027	100	35.56	35.31	1.52	9.27	2640	13.8457	11.8347	77
N 11	DUCTILE CAST IRON	01-Dec-82	NA	NA	100	35.74	35.53	2.51	10.03	2820	21.4442	NA	NA
N 9	DUCTILE CAST IRON	01-Dec-82	03-Mar-83	2160	100	35.53	35.51	2.51	10.03	2800	21.2246	20.5698	120
N 19	DUCTILE CAST IRON	01-Dec-82	03-Mar-83	2160	100	35.48	35.64	2.51	10.06	2810	21.1342	20.4070	130
N 18	DUCTILE CAST IRON	01-Dec-82	03-Mar-83	2160	100	35.48	35.31	2.49	10.06	2780	20.9734	20.4902	90
N 12	DUCTILE CAST IRON	01-Dec-82	20-Jul-83	4512	100	35.76	35.48	2.51	10.01	2820	21.3617	19.6662	150
N 14	DUCTILE CAST IRON	01-Dec-82	20-Jul-83	4512	100	35.76	35.51	2.51	10.11	2820	21.2602	NA	NA
N 10	DUCTILE CAST IRON	01-Dec-82	22-Nov-83	6792	100	35.46	35.59	2.49	10.06	2800	21.1626	NA	NA
N 13	DUCTILE CAST IRON	01-Dec-82	22-Nov-83	6792	100	35.48	35.43	2.51	10.03	2790	21.3153	19.9927	78
N 15	DUCTILE CAST IRON	01-Dec-82	22-Nov-83	6792	100	35.48	35.86	2.51	10.03	2830	21.3601	19.3174	120
N 8	DUCTILE CAST IRON	01-Dec-82	27-Feb-84	8514	100	35.43	35.51	2.46	9.98	2790	21.0341	19.0180	95
N 17	DUCTILE CAST IRON	01-Dec-82	17-Sep-84	12461	100	35.51	35.79	2.51	9.96	2820	21.3775	19.1147	72
N 16	DUCTILE CAST IRON	01-Dec-82	17-Sep-84	12461	100	35.48	35.71	2.51	9.58	2820	21.3861	18.5826	89
FE 12	PURE IRON	25-Mar-83	NA	NA	100	31.78	31.75	1.60	9.40	2130	11.6403	NA	NA
FE 6	PURE IRON	25-Mar-83	20-Jul-83	2352	100	31.78	31.70	1.57	9.50	2120	11.6323	11.2103	94
FE 10	PURE IRON	25-Mar-83	20-Jul-83	2352	100	31.67	31.65	1.63	9.42	2120	11.6375	10.7409	200
FE 11	PURE IRON	25-Mar-83	22-Nov-83	4632	100	31.72	31.67	1.55	9.47	2110	11.4532	NA	NA
FE 9	PURE IRON	25-Mar-83	22-Nov-83	4632	100	31.78	31.75	1.50	9.40	2110	11.5239	10.9212	69
FE 13	PURE IRON	25-Mar-83	22-Nov-83	4632	100	31.72	31.70	1.60	9.37	2120	11.4046	10.3023	130
FE 5	PURE IRON	25-Mar-83	27-Feb-84	7080	100	31.70	31.67	1.37	9.42	2080	10.1609	8.8721	97
FE 7	PURE IRON	25-Mar-83	17-Sep-84	11027	100	31.83	31.67	1.52	9.45	2120	11.3945	9.2420	100

IRRADIATION CORROSION

SAMPLE ******			TIME **********	IRRADIATION ***********		DIMENSIONS **********					WEIGHTS *******		CORROSION RATE *********
		START	END	TOTAL	RATE	LENGTH	WIDTH	HEIGHT	HOLE DI	AREA	INITIAL	FINAL	
NUMBER	MATERIAL	DATE	DATE	HR	KR/H	MM	MM	MM	MM	MM*MM	GM	GM	MICRON/YR
FE 8	PURE IRON	25-Mar-83	17-Sep-84	11027	100	31.70	31.75	1.50	9.32	2110	10.9087	8.7958	100
FE 14	PURE IRON	25-Mar-83	17-Sep-84	11027	100	31.78	31.67	1.42	9.37	2100	10.9622	9.6477	63

APPENDIX D

SLOW-STRAIN-RATE AND CORROSION FATIGUE TEST RESULTS

APPENDIX D.1

SUMMARY OF SLOW-STRAIN-RATE DATA

Specimen	Strain Rate, s^{-1}	T, °C	Solution	Sparge	Reduction of Area, %	Elongation, %	Yield Strength, MPa	Ultimate Strength, MPa	Yield Load, kg	Ultimate Load, kg	Initial Width, mm	Initial Thickness, mm	Initial Gage Length, mm	Final Width, mm	Final Thickness mm	Final Gage Length, mm	Energy To Max. Load, kg-m	Total Energy Absorbed, kg-m
Reference Cast Steel																		
Q249	1×10^{-6}	90	PBB2	Air exposed	18	15	-	-	-	-	5.10	4.98	25.4	4.65	4.50	29.2	-	-
Q250	1×10^{-4}	150	PBB2	Ar	20	16	251	446	630	1122	5.03	4.90	25.4	4.50	4.39	29.5	614	678
Q253	1×10^{-6}	Amb	PBB2	Air exposed	19	13	-	327	-	839	4.95	4.83	-	4.32	4.42	-	-	-
Q255	1×10^{-4}	150	PBB2	Ar	19	14	260	436	653	1095	5.08	4.85	25.4	4.70	4.26	28.9	455	491
Q258	2×10^{-7}	150	PBB2	Ar	16	11	237	460	594	1149	4.98	4.93	25.4	4.44	4.62	28.2	349	383
Q259	2×10^{-7}	90	PBB2	Air exposed	15	14	-	-	-	-	4.95	4.90	See Log	4.60	4.47	See Log	-	-
Q260	1×10^{-6}	150	PBB2	20% O_2 80% Ar	26	16	242	457	594	1124	5.00	4.83	25.4	4.24	4.22	-	518	614
Q261	1×10^{-4}	150	PBB2	20% O_2 80% Ar	17	14	237	442	567	1052	4.93	4.75	25.4	4.52	4.32	28.9	-	-
Q262	1×10^{-4}	150	Air	-	23	16	236	440	571	1067	4.98	4.77	25.4	4.42	4.14	-	502	564
Q264	1×10^{-5}	150	PBB2	20% O_2 80% Ar	25	18	270	449	648	1078	4.88	4.83	25.4	4.32	4.14	30.0	-	-
Q265	2×10^{-7}	150	Air		25	19	232	502	567	1228	5.00	4.80	25.4	4.42	4.11	30.2	-	-
Q266	1×10^{-6}	150	Air		33	17	282	474	708	1192	5.03	4.90	25.4	4.06	4.04	29.7	642	755
Q267	1×10^{-4}	150	PBB2	20% O_2 80% Ar	25	14	228	424	571	1061	5.00	4.90	25.4	4.32	4.27	28.9	421	521
Q268	1×10^{-7}	150	Air		15	17	257	496	653	1260	5.00	4.98	25.4	4.50	4.70	29.7	660	703

Specimen	Strain Rate, s^{-1}	T, °C	Solution	Sparge	Reduction of Area, %	Elongation, %	Yield Strength, MPa	Ultimate Strength, MPa	Yield Load, kg	Ultimate Load, kg	Initial Width, mm	Initial Thickness, mm	Initial Gage Length, mm	Final Width, mm	Final Thickness mm	Final Gage Length, mm	Energy To Max. Load, kg-m	Total Energy Absorbed, kg-m
Q269	1×10^{-5}	150	PBB2	20% O_2 80% Ar	14	13	241	440	612	1118	5.00	4.98	25.4	4.70	4.57	-	518	543
Q270	1×10^{-6}	150	PBB2	20% O_2 80% Ar	18	12	244	437	635	1139	5.80	4.90	25.4	4.72	4.44	-	397	431
Q271	1×10^{-4}	150	Air	-	23	17	247	448	616	1120	5.00	4.90	25.4	4.26	4.16	-	597	700
P558	2×10^{-7}	30	PBB2	Air exposed	13	14	-	-	-	-	5.03	5.03	-	4.67	4.72	-	-	-
P561	1×10^{-4}	90	PBB2	Air exposed	24	15	458	-	-	-	4.93	5.03	25.4	4.26	4.44	-	-	-
P562	1×10^{-4}	90	Air	-	40	22	-	482	-	-	4.90	5.03	25.4	-	-	-	-	-
P563	2×10^{-7}	90	PBB2	Air	15	-	-	355	-	-	4.98	5.03	-	4.65	4.57	-	-	-
P564	2×10^{-7}	90	PBB2	Air exposed	13	14	-	444	-	1116	4.93	5.00	-	4.65	4.62	-	-	-
P565	1×10^{-4}	30	Air	-	25	20	-	504	-	-	4.90	5.00	25.4	-	-	-	-	-
P566	0.005	90	Air	-	38	22	-	465	-	-	4.85	5.03	-	-	-	-	-	-
P567	2×10^{-7}	30	PBB2	Air exposed	13	14	-	426	-	-	4.98	5.03	-	-	-	-	-	-
P569	2×10^{-7}	150	Air	-	22	-	256	513	-	-	5.03	5.05	68.05	4.57	4.32	73.23	687	744
P570	2×10^{-7}	30	PBB2	Air exposed	16	16	245	465	630	1198	5.00	5.05	25.4	4.75	4.44	-	554	614
P572	2×10^{-7}	150	PBB2	20% O_2 80% Ar	-	12	301	502	776	1295	5.00	5.05	25.4	4.67	4.83	-	500	549

Specimen	Strain Rate, s^{-1}	T, °C	Solution	Sparge	Reduction of Area, %	Elon-gation, %	Yield Strength, MPa	Ultimate Strength, MPa	Yield Load, kg	Ultimate Load, kg	Initial Width, mm	Initial Thickness, mm	Initial Gage Length, mm	Final Width, mm	Final Thickness mm	Final Gage Length, mm	Energy To Max. Load, kg-m	Total Energy Absorbed, kg-m
P573	1×10^{-4}	150	Air	-	40	20	223	453	571	1179	5.00	5.03	25.4	3.93	3.81	-	601	810
P574	2×10^{-7}	150	PBB2	20% O_2 80% Ar	17	15	292	506	744	1292	4.95	5.05	25.4	4.54	4.54	-	511	646
P575	2×10^{-7}	150	Air	-	30	-	-	489	-	-	4.90	5.05	-	4.11	4.22	-	597	720
P576	2×10^{-7}	90	PBB2	20% O_2 80% Ar	23	16	223	445	562	-	4.90	5.05	25.4	4.19	4.52	-	539	577
1025 Cast Steel, Normalized																		
P289	1×10^{-4}	150	PBB2[(a)]	-	13	44	275	486	-	-	4.83	5.03	-	-	-	-	629	919
P291	1×10^{-4}	150	PBB2	-	48	27	-	-	-	-	5.00	5.05	68.28	-	-	75.18	710	1122
P292	2×10^{-7}	150	PBB2	Ar	12	15	130	519	-	-	4.93	5.03	-	-	-	-	441	508
P293	1×10^{-4}	150	Air	-	53	22	255	491	-	-	4.88	5.08	25.4	-	-	31.2	578	973
P294	2×10^{-7}	150	Air	-	40	21	293	553	-	-	4.93	5.08	25.4	-	-	30.7	772	1084
P295	1×10^{-4}	150	Air	-	24	19	263	489	-	-	4.95	5.08	25.4	-	-	30.2	642	797
P296	2×10^{-7}	150	Air	-	54	22	250	553	-	-	4.98	5.05	25.4	-	-	31.0	642	797
P297	2×10^{-7}	150	PBB2	O_2	-	-	-	-	-	-	4.62	5.03	-	-	-	-	-	- -
P298	2×10^{-7}	150	PBB2	Ar	18	15	249	528	-	-	4.80	5.08	-	-	-	-	435	501
P299	2×10^{-7}	150	PBB2	O_2	20	15	249	532	-	-	4.72	5.09	-	-	-	-	521	607
P300	2×10^{-7}	150	PBB2	-	14	12	239	506	-	-	4.93	4.98	-	-	-	-	493	573
P301	2×10^{-7}	150	PBB2	-	10	12	228	508	-	-	4.90	5.10	-	-	-	30.2	456	498
P302	1×10^{-4}	150	PBB2[(a)]	-	19	5	275	462	-	-	4.88	5.05	-	-	-	-	425	529
P304	1×10^{-4}	150	PBB2	-	50	22	275	499	-	-	4.98	5.05	-	-	-	31.0	724	1065

(a) Exposed to PBB2 for 12 weeks before straining.

Specimen	Strain Rate, s^{-1}	T, °C	Solution	Sparge	Reduction of Area, %	Elongation, %	Yield Strength, MPa	Ultimate Strength, MPa	Yield Load, kg	Ultimate Load, kg	Initial Width, mm	Initial Thickness, mm	Initial Gage Length, mm	Final Width, mm	Final Thickness mm	Final Gage Length, mm	Energy To Max. Load, kg-m	Total Energy Absorbed, kg-m
1025 Wrought Steel, Transverse Orientation																		
N356	2×10^{-7}	150	Air	-	63	28	-	-	-	-	4.93	6.32	25.4	-	-	32.3	-	-
N358	1×10^{-4}	150	PBB2	-	72	33	243	386	785	1247	4.98	6.35	25.4	2.72	3.33	33.3	-	-
N359	1×10^{-4}	150	Air	-	69	31	267	377	853	1202	4.93	6.35	25.4	2.77	3.48	33.0	-	-
N362	1×10^{-4}	150	Air	-	70	30	251	383	810	1234	4.98	6.35	25.4	2.77	3.45	33.0	-	-
N365	2×10^{-7}	150	PBB2	-	21	35	248	422	-	-	4.95	6.35	25.4	-	-	30.7	-	-
N369	1×10^{-4}	150	PBB2	-	71	32	263	408	844	1311	4.98	6.35	25.4	2.72	2.38	33.5	-	-
N370	2×10^{-7}	150	Air	-	60	30	-	-	-	-	4.95	6.35	25.4	-	-	32.8	-	-
N371	2×10^{-7}	150	PBB2	-	21	38	274	430	-	-	4.88	6.35	25.4	-	-	28.2	-	-
1025 Wrought Steel, Longitudinal Orientation																		
N372	2×10^{-7}	150	PBB2	-	29	18	304	499	-	-	4.90	6.30	25.4	-	-	29.7	-	-
N374	1×10^{-5}	150	Air	-	53	22	-	439	-	-	4.93	6.32	25.4	-	-	30.7	-	-
N377	1×10^{-4}	150	PBB2	-	53	23	295	424	-	-	4.85	6.35	25.4	-	-	31.0	-	-
N378	1×10^{-4}	150	PBB2	-	50	20	292	441	-	-	4.93	6.30	25.4	-	-	30.2	-	-
N381	2×10^{-7}	150	PBB2	-	28	17	301	487	-	-	4.95	6.27	25.4	-	-	29.5	-	-
N382	1×10^{-4}	150	PBB2	-	50	22	-	-	-	-	4.93	6.30	25.4	-	-	31.0	-	-
N384	1×10^{-4}	150	Air	-	56	22	298	430	955	1370	4.95	6.30	25.4	3.30	4.19	31.0	-	-
N389	2×10^{-7}	150	Air	-	52	24	291	480	-	-	4.95	6.32	25.4	-	-	31.2	-	-
N391	1×10^{-4}	150	Air	-	55	22	292	426	928	1354	4.93	6.32	25.4	3.30	4.22	31.0	-	-

Specimen	Strain Rate, s^{-1}	T, °C	Solution	Sparge	Reduction of Area, %	Elongation, %	Yield Strength, MPa	Ultimate Strength, MPa	Yield Load, kg	Ultimate Load, kg	Initial Width, mm	Initial Thickness, mm	Initial Gage Length, mm	Final Width, mm	Final Thickness mm	Final Gage Length, mm	Energy To Max. Load, kg-m	Total Energy Absorbed, kg-m
2 1/2% Cr, 1% Mo Steel																		
M877	1×10^{-4}	150	Air	-	63	21	-	-	-	-	4.98	5.08	25.4	-	-	30.7	-	-
M878	2×10^{-7}	150	PBB2	-	37	16	-	-	-	-	4.93	5.10	25.4	-	-	29.2	-	-
M879	1×10^{-4}	150	Air	-	64	18	-	-	-	-	4.98	5.13	25.4	-	-	30.0	-	-
M890	2×10^{-7}	150	PBB2	-	28	15	-	-	-	-	4.88	5.10	25.4	-	-	29.2	-	-
M891	2×10^{-7}	150	Air	-	60	19	-	-	-	-	4.93	5.10	25.4	-	-	30.0	-	-
M892	1×10^{-4}	150	PBB2	-	50	19	-	-	-	-	4.95	5.10	25.4	-	-	30.2	-	-
M893	1×10^{-4}	150	PBB2	-	53	20	-	-	-	-	4.88	5.08	25.4	-	-	30.5	-	-
Ductile Cast Iron																		
M894	1×10^{-4}	150	PBB2	-	3.8	5.0	-	-	-	-	4.93	5.08	25.4	-	-	26.7	-	-
M895	1×10^{-4}	150	PBB2	-	3.3	5.5	-	-	-	-	4.88	5.08	25.4	-	-	26.4	-	-
M896	2×10^{-7}	150	PBB2	-	3.0	4.4	-	-	-	-	4.93	5.08	25.4	-	-	26.4	-	-
M897	2×10^{-7}	150	PBB2	-	3.3	4.8	-	-	-	-	4.88	5.08	25.4	-	-	25.9	-	-
M898	1×10^{-4}	150	Air	-	4.5	7.5	-	-	-	-	4.95	5.08	25.4	-	-	26.7	-	-
M899	2×10^{-7}	150	PBB2	-	4.4	4.2	-	-	-	-	4.90	5.05	25.4	4.83	4.98	26.4	-	-
M900	2×10^{-7}	150	Air	-	3.0	6.0	-	-	-	-	4.83	5.08	25.4	-	-	29.5	-	-

APPENDIX D.2

CORROSION FATIGUE TEST RESULTS

TABLE D.2. Corrosion Fatigue Test Results

Specimen No. N426   Material 1025 steel   W 5.1 cm   B 1.3 cm
Load 635/63.5 kg   Frequency 10 Hz   Environment Air
Temperature 150°C

ΔK, MPa$\sqrt{m}$	da/dn, m/cycle
20.03	3.6×10^{-8} (a)
20.55	6.9×10^{-8}
21.34	8.1×10^{-8}
22.61	7.1×10^{-8}
23.93	7.6×10^{-8}
25.33	1.3×10^{-7}
27.87	9.7×10^{-8}
30.49	8.9×10^{-8}
32.72	1.2×10^{-7}
35.76	1.2×10^{-7}
39.64	1.3×10^{-7}
47.25	2.7×10^{-7}

(a) This observation was deleted from determination of the regression line.

Specimen No. N438   Material 1025 steel   W 5.1 cm   B 1.3 cm
Load 635/63.5 kg   Frequency 1 Hz   Environment PBB2
Temperature 150°C

ΔK, MPa$\sqrt{m}$	da/dn, m/cycle
27.6	2.8×10^{-8}
30.7	8.1×10^{-9}
32.5	1.2×10^{-8}
36.0	2.5×10^{-8}
40.0	1.0×10^{-8}
42.1	7.4×10^{-9}

Specimen No. N440 Material 1025 steel W 5.1 cm B 1.3 cm
Load 635/63.5 kg Frequency 1 Hz Environment DI water
Temperature 150°C

ΔK, MPa$\sqrt{m}$	da/dn, m/cycle
24.06	3.8×10^{-8}[(a)]
25.60	2.1×10^{-7}
26.39	2.4×10^{-7}
27.82	2.7×10^{-7}
30.18	1.2×10^{-6}
31.53	6.5×10^{-7}
33.48	1.4×10^{-6}
36.45	1.3×10^{-6}
39.55	1.1×10^{-6}
44.44	2.4×10^{-6}
49.62	2.0×10^{-6}
57.04	8.3×10^{-6}

(a) Observation deleted from determination of the regression line.

Specimen No. P623 Material A216 steel W 5.1 cm B 1.3 cm
Load 635/63.5 kg Frequency 5 Hz Environment Air
Temperature 150°C

ΔK, MPa$\sqrt{m}$	da/dn, m/cycle
27.6	3.1×1^{-7}
29.9	3.6×10^{-7}
32.2	4.2×10^{-7}
34.2	4.9×10^{-7}
37.0	6.2×10^{-7}
43.7	1.1×10^{-6}

Specimen No. P630 Material A216 steel W 5.1 cm B 1.3 cm
Load 635/63.5 kg Frequency 0.1 Hz Environment DI water
Temperature 150°C

ΔK, MPa$\sqrt{m}$	da/dn, m/cycle
34.6	3.0×10^{-6}
35.9	3.5×10^{-6}
37.0	3.9×10^{-6}
38.5	3.9×10^{-6}
40.0	8.2×10^{-6}
41.8	8.6×10^{-6}
43.5	1.3×10^{-5}
45.9	2.4×10^{-5}

Specimen No. P626 Material A216 steel W 5.1 cm B 1.3 cm
Load 635/63.5 kg Frequency 1 Hz Environment DI water
Temperature 150°C

ΔK, MPa$\sqrt{m}$	da/dn, m/cycle
31.5	6.4×10^{-7}
33.5	8.2×10^{-7}
34.5	1.6×10^{-6} (a)
36.0	1.2×10^{-7}
39.2	6.5×10^{-6}
41.8	4.0×10^{-6}
43.7	6.5×10^{-6}
46.8	4.9×10^{-6}
52.0	3.9×10^{-5}
57.3	3.1×10^{-5}

(a) Inadvertent overload. Deleted from the determination of the regression line.

Specimen No. P625   Material A216 steel   W 5.1 cm   B 1.3 cm

Load 635/63.5 kg   Frequency 0.1 Hz   Environment PBB2

Temperature 150°C

ΔK, MPa$\sqrt{m}$	da/dn, m/cycle
33.0	1.4×10^{-7}
33.4	2.8×10^{-8}
35.8	4.6×10^{-7} (a)
38.7	1.2×10^{-8} (a)
40.1	8.6×10^{-8}
41.8	2.0×10^{-7}
43.2	1.2×10^{-6}
45.2	7.1×10^{-6}
47.5	6.9×10^{-6}

(a) Inadvertent overload. Data not used in determination of the regression line.

APPENDIX E

COMPILATION OF STATISTICAL DATA

APPENDIX E

COMPILATION OF STATISTICAL DATA

Statistical Assumptions, Cautions, and Minor Conclusions:

- Most of the statistical analyses relied on the assumption of normally distributed error structures. This assumption was checked by performing the Shapiro-Wilk W test or the Kolomogorov D test for normality. Departures from normality were handled by data transformation; either taking the logarithm or ranking.
- Homogeneity of variance was also assumed for most analyses. This assumption implies that the underlying replicate variance is the same for each treatment combination. Data transformations applied to correct normality departures also corrected homogeneity problems.
- Some of the material differences in the experiments were somewhat confounded with specimen dimension differences and beginning date or ending date differences. Therefore, to conclude that differences among materials are due only to material differences, one must assume no significant dimension or date effect. In the case of the corrosion rate calculation, correction is made for the specimen dimension, which makes the assumption of no significant dimension effect very reasonable.
- All confidence limits are limits on the population mean, not on the individual values.
- Confidence intervals plotted in Figure 7 were derived from an analysis of A216 data only without assuming any log-linear trend over time. These confidence intervals and averages were obtained independently of the statistical analysis, including all materials for which a log-linear trend over time was assumed.

- In the statistical analysis of the moist salt tests, the true replicate error term that should be used to test material and water content differences is the container-to-container variability; not the within-container specimen variability. In order to obtain a statistical test for these differences one must assume no significant container-to-container variability. This assumption was examined by assuming a linear and quadratic trend only across water content and pooling the lack of fit into a container-to-container term. This term was not significant, which supports the assumption of no significant container effect.
- No statistical analysis was performed on the energy-absorbed data of the SSR tests.
- For completeness and possible future experimental design use, Table E.5 is included. The standard deviations and relative standard deviations are reported. The relative standard deviation is the standard deviation divided by the overall average represented as a percent.

TABLE E.1. Estimated Mean Rate (at time shown) and 95% Confidence Intervals About the Mean for A216 Steel in Intrusion Brine PBB2 at 150°C, Unirradiated

Experiment	Hours	Estimated Mean Rate, μm/yr	Standard Error	Upper 95% Conf. Limit	Lower 95% Conf. Limit
A216-Anoxic test	696	19.8	1.18	22.4	17.2
	2897	14.1	1.18	16.7	11.5
	5321	16.7	0.68	18.2	15.2
	5635	11.9	0.75	13.6	10.3
A216-Oxic test	736	27.2	2.19	32.2	22.2
	2908	27.6	2.10	32.3	22.8
	5384	24.9	1.03	27.3	22.6

TABLE E.2. Statistical Treatment of Data from PBB1/PBB3 Moist Salt Test--A216 Steel, 150°C

Test Duration, h	H_2O, %	Mg, %[a]	Estimated Mean Rate, mm/yr	Standard Error	Upper 95% Conf. Limit	Lower 95% Conf. Limit
767	20	1.7	0.615	0.031	0.696	0.535
767	30	2.7	0.665	0.050	0.794	0.537
1659	30	2.7	0.691	0.037	0.785	0.596
2178	5	0.42	0.469	0.011	0.497	0.440
2178	10	0.81	0.534	0.016	0.576	0.492
2178	20	1.7	0.669	0.007	0.687	0.626
2178	25	2.2	0.631	0.029	0.706	0.556
2178	30	2.7	0.663	0.037	0.758	0.567

(a) Calculated on a dry-weight basis.

TABLE E.3. Statistical Treatment of Corrosion Rate Data from Moist Salt Test of A216 Steel Having Various Heat Treatments

Environment	Material	Estimated Mean Rate, μm/yr	Standard Error	Upper 95% Conf. Limit	Lower 95% Conf. Limit
NaCl/NaCl	A216 (all treatments)[a]	4.59	0.32	5.29	3.89
PBB1/PBB1	A216 (all treatments)[a]	10.5	0.51	11.6	9.34
PBB1/PBB3	A216-C (as-cast)	577	73.2	743	412
PBB1/PBB3	A216-H (homogenized)	919	73.2	1080	753
PBB1/PBB3	A216-N (normalized)	766	73.2	932	600

(a) There was no significant difference among the rates of the three treatments of A216 in this environment; thus the data were combined to estimate an overall mean rate.

TABLE E.3. (contd)

	Environment					
	NaCl/NaCl		PBB1/PBB1		PBB1/PBB3	
Material	Rate, μm/yr	Comparison[a]	Rate, μm/yr	Comparison	Rate, μm/yr	Comparison
A216-C	4.68	A	10.94	A	577.2	B
A216-H	4.27	A	10.37	A	918.9	A
A216-N	4.82	A	10.06	A	766.0	AB
Standard Deviation:	1.18		1.90		146.4	

(a) Shared letters indicate no significant difference at 95% confidence level with respect to corrosion rates.

A statistical analysis of the data indicates that 1) the corrosion rates are significantly different depending on environment; 2) there are no significant differences among corrosion rates of the three types of A216 steel in the NaCl and PBB1/PBB1 environments; and 3) the A216-homogenized corrosion rate was significantly higher than the A216 as-cast corrosion rate in the PBB1/PBB3 environment.

TABLE E.4. Estimated Mean Rate (at time shown) and 95% Confidence Intervals About the Mean for A216 Steel in Intrusion Brine PBB2 at 150°C Irradiated at 2×10^3 rad/h and 1×10^5 rad/h

	Hours	Estimated Mean Rate, μm/yr	Standard Error	Upper 95% Conf. Limit	Lower 95% Conf. Limit
A216, 2×10^3 rad/h	768	21.1	1.55	24.6	17.6
	2180	13.9	1.56	17.4	10.4
	3974	11.1	0.98	13.3	8.9
	5099	13.7	0.98	15.9	11.4
A216, 1×10^5 rad/h	815	141	7.0	156	125
	2393	116	5.0	127	105
	3947	105	3.5	112	97

TABLE E.5. Variability Estimates for Each Experiment

Experiment	Random Standard Deviation	Relative Standard Deviation,%
General Corrosion--Anoxic	2.73	31.7
General Corrosion--Oxic	2.36	13.8
Irradiated at 2.3 kr/h	1.78	9.9
Irradiated at 50 kr/h	11.47	11.0
Moist Salt:		
A216 at 767 h	101.9	15.9
A216 at 1659 h	89.9	13.0
A216 at 2178 h	57.9	9.8
Ductile iron at 767 h	23.1	6.7
Ductile iron at 1659 h	3.69	1.1
Ductile iron at 2178 h	14.6	4.6
W1025 at 676 h	25.0	17.2
W1025 at 1659 h	7.32	9.7
W1025 at 2178 h	9.82	12.4
A216 in NaCl/NaCl	1.18	25.7
A216 in PBB1/PBB1	1.90	18.1
A216 in PBB1/PBB3	146.4	19.4
Slow Strain Rate:		
Reduction of area at 150°	4.42	11.2
Elongation at 150°	1.61	7.8
Reduction of area on A216--3 temps.	4.83	21.8
Elongation on A216--3 temps.	1.76	11.2

Summary of Statistical Data from Corrosion Fatigue Tests

The predicted values are points on the regression line. The lower 95% means and upper 95% means are the lower and upper confidence bands about the regression line. The values are Log(Rate) values.

Summary of Statistical Data from Corrosion Fatigue Tests, Specimen Number N426

Observation Number	Log of Lower Mean, m/cycle[a]	Log of Upper Mean, m/cycle[a]
1	-7.265	-7.0628
2	-7.2373	-7.049
3	-7.1955	-7.0272
4	-7.1557	-7.0046
5	-7.1174	-6.9804
6	-7.0582	-6.9345
7	-7.0099	-6.884
8	-6.9768	-6.8395
9	-6.9396	-6.7789
10	-6.9007	-6.7045
11	-6.8394	-6.5726

(a) Lower and upper confidence values about the regression line, 95% confidence.

Summary of Statistical Data from Corrosion Fatigue Tests, Specimen Number N440

Observation Number	Log of Lower Mean, m/cycle[a]	Log of Upper Mean, m/cycle[a]
1	-6.7691	-6.3324
2	-6.7054	-6.2938
3	-6.5962	-6.2254
4	-6.4324	-6.1152
5	-6.3477	-6.0527
6	-6.2366	-5.9619
7	-6.0913	-5.8211
8	-5.9656	-5.6722
9	-5.8038	-5.4417
10	-5.662	-5.2126
11	-5.4905	-4.9151

(a) Lower and upper confidence values about the regression line, 95% confidence.

Summary of Statistical Data from Corrosion Fatigue Tests, Specimen Number P623

Observation Number	Log of Lower Mean, m/cycle[a]	Log of Upper Mean, m/cycle[a]
1	-6.5974	-6.4857
2	-6.4881	-6.4025
3	-6.3911	-6.3214
4	-6.3172	-6.2503
5	-6.2284	-6.1499
6	-6.0561	-5.9222

(a) Lower and upper confidence values about the regression line, 95% confidence.

Summary of Statistical Data from Corrosion Fatigue Tests, Specimen Number P630

Observation Number	Log of Lower Mean, m/cycle[a]	Log of Upper Mean, m/cycle[a]
1	-5.7313	-5.4731
2	-5.5908	-5.3787
3	-5.4788	-5.2985
4	-5.3383	-5.1859
5	-5.2146	-5.0662
6	-5.0869	-4.9137
7	-4.9804	-4.7663
8	-4.8439	-4.5608

(a) Lower and upper confidence values about the regression line, 95% confidence.

Summary of Statistical Data from Corrosion Fatigue Tests, Specimen Number P626

Observation Number	Log of Lower Mean, m/cycle[a]	Log of Upper Mean, m/cycle[a]
1	-6.4344	-5.8437
2	-6.2135	-5.7079
3	-6.1096	-5.6413
4	-5.6816	-5.3294
5	-5.4885	-5.1504
6	-5.3657	-5.0156
7	-5.1916	-4.7926
8	-4.9478	-4.4259
9	-4.7364	-4.0749

(a) Lower and upper confidence values about the regression line, 95% confidence.

DISTRIBUTION

No. of
Copies

OFFSITE

30 DOE Technical Information Center

D. H. Alexander
Office of Geosciences
and Technology
Office of Civilian Radioactive
Waste Management
Washington, DC 20545

Allied Chemical Corporation
File Copy
505 2nd Street
Idaho Falls, ID 83401

Argonne National Laboratory
Reference Library
9800 South Cass Avenue
Argonne, IL 60439

R. G. Ballinger
Bldg. 24, Rm 215
Massachusetts Institute
of Technology
77 Massachusetts Avenue
Cambridge, MA 02139

A. Bauer
Office of Crystalline
Repository Development
P.O. Box 16595
Columbus, OH 43216-6595

Ernest Bondietti
Environmental Sciences
Division
Oak Ridge National Laboratory
Bldg. 1505
Oak Ridge, TN 37830

No. of
Copies

J. W. Braithwaite
Division 6312
Sandia National Laboratory
P.O. Box 5800
Albuquerque, NM 87185

A. Brandstetter
Office of Crystalline
Repository Development
9800 South Cass Avenue
Argonne, IL 60439

Brookhaven National Laboratory
Reference Section
Information Division
Upton, Long Island, NY 11973

R. B. Chitwood
DOE Division of Nuclear
Power Development
Washington, DC 20545

H. Clyde Claiborne
Oak Ridge National Laboratory
P.O. Box X
Oak Ridge, TN 37830

C. R. Cooley
Program Integration Division
Office of Policy, Integration,
and Outreach
Office of Civilian Radioactive
Waste Management
Washington, DC 20585

DOE, Office of Terminal Waste
Disposal and Remedial Action
Washington, DC 20545

P. Colombo
Brookhaven National Laboratory
Nuclear Waste Mgt. Group
Upton, Long Island, NY 11973

No. of
Copies

J. L. Crandall
E. I. du Pont de Nemours & Co.
Savannah River Laboratory
Aiken, SC 29801

J. Davis
U.S. Nuclear Regulatory Commission
Washington, DC 20555

Environmental Protection Agency
Office of Radiation Programs
Technical Assessment Division
AW559
Washington, DC 20460

A. Ogard
Los Alamos Scientific Laboratory
CNC-11, MS-514
Los Alamos, NM 87545

K. Flynn
Argonne National Laboratory
9700 South Cass Avenue
Argonne, IL 60439

R. G. Garvin
E. I. du Pont de Nemours & Co.
Savannah River Laboratory
Aiken, SC 29801

L. L. Hench
Dept. of Materials Science and Engineering
University of Florida
Gainesville, FL 32611

J. Holloway
Dept. of Chemistry
Arizona State University
Tempe, AZ 85281

D. Isherwood, L-205
Lawrence Livermore National Laboratories
P.O. Box 808, L-205
Livermore, CA 94550

No. of
Copies

L. H. Johnson
Fuel Waste Technology Branch
Atomic Energy of Canada, Ltd.
W.N.R.E. Pinawa, Manitoba
Canada ROE 1LO

D. A. Knecht
Exxon Nuclear
P.O. Box 2800
Idaho Falls, ID 83401

Lawrence Berkeley Laboratory
Reference Library
University of California
Berkeley, CA 94720

Lawrence Livermore National Laboratory
Reference Library
P.O. Box 808
Livermore, CA 94550

A. Lerman
Dept. of Geological Sciences
Northwestern University
Evanston, IL 60201

D. Langmuir
Department of Chemistry/Geochemistry
Colorado School of Mines
Golden, CO 80401

W. L. Lindsay
Centennial Professor
Colorado State University
Fort Collins, CO 80523

T. Longo
Siting Division
Office of Geologic Repositories
Office of Civilian Radioactive Waste Management
Washington, DC 20545

Los Alamos Scientific Laboratory
Reference Library
P.O. Box 1663
Los Alamos, NM 85744

No. of
Copies

R. Y. Lowrey
DOE Albuquerque Operations
Office
Albuquerque, NM 87115

R. W. Lynch
Manager, Department 4530
Sandia Laboratories
P.O. Box 5800
Albuquerque, NM 87185

S. A. Mann
DOE Chicago Operations and
Regional Office
Argonne, IL 60439

M. A. Molecke
Nuclear Waste Experimental
Programs
Division 4512
Sandia Laboratories
Albuquerque, NM 87185

J. P. Murray
Harvard University
Pierce Hall
Cambridge, MA 02138

K. Nuttall
Head, Fuel Waste Technology
Branch
Whiteshell Nuclear Research
Establishment
Pinawa, Manitoba, Canada
ROE 1LO

Oak Ridge National Laboratory
Central Research Library
Document Reference Section
Oak Ridge, TN 37830

D. LeClaire
Defense Waste and Byproducts
Management
Washington, DC 20545

J. D. Osnes
RE/SPEC
P.O. Box 725
One Concourse Drive
Rapid City, SD 57709

No. of
Copies

V. M. Oversby
Lawrence Livermore National
Laboratory
P.O. Box 808
Livermore, CA 94550

W. M. Pardue
Office of Crystalline
Repository Development
9800 South Cass Avenue
Argonne, IL 69439

F. L. Parker
Dept. of Environmental
Engineering
Vanderbilt University
Nashville, TN 37235

G. A. Parks
Stanford University
Department of Applied
Earth Sciences
Stanford, CA 94305

T. H. Pigford
University of California
Berkeley, CA 94720

G. F. Pinder
Dept. of Civil Engineering
Princeton University
Princeton, NJ 08540

M. S. Plodinec
E. I. du Pont de Nemours & Co.
Savannah River Laboratory
Aiken, SC 29801

J. Pomeroy
National Academy of Sciences
Committee of Radioactive
Waste Management
National Research Council
2101 Constitution Avenue
Washington, DC 20418

R. G. Post
College of Engineering
University of Arizona
Tucson, AZ 85721

No. of
Copies

L. D. Ramspott, L-204
Lawrence Livermore National Laboratory
P.O. Box 808
Livermore, CA 94550

D. W. Readey
Department of Ceramic Engineering
Ohio State University
2041 College Road
Columbus, OH 43210-1178

Savannah River Laboratory
Reference Library
Aiken, SC 29801

M. Seitz
Argonne National Laboratory
9700 South Cass Avenue
Argonne, IL 60439

R. Silva
Lawrence Livermore National Laboratory
P.O. Box 808
Livermore, CA 94550

M. J. Steindler
Chemical Engineering Division
Argonne National Laboratory
9700 South Cass Avenue
Argonne, IL 60439

T. T. Vandergraaf
Atomic Energy of Canada, LTD,
W.N.R.E., Pinawa, Manitoba
Canada ROE 1L0

R. D. Walton
Division of Waste Products
MSB-107
P.O. Box A
Aiken, SC 29801

Lars Werme
SKBF-Swedish Nuclear Fuel Supply Co.
Division KBS
Box 5864
S-102 48 Stockholm, Sweden

No. of
Copies

W. B. White
Materials Research Laboratory
Pennsylvania State University
University Park, PA 16802

J. B. Whitsett
DOE Operations Office
550 2nd Street
Idaho Falls, ID 83401

R. E. Wilems
INTERA, Environmental Consultants, Inc.
11999 Caty Freeway, Suite 610
Houston, TX 77079

R. F. Williams
Electric Power Research Institute
3412 Hillview Avenue
P.O. Box 104112
Palo Alto, CA 94303

Wilste Library
U.S. Nuclear Regulatory Commission
Washington, DC 20555

T. J. Wolery, L-202
Lawrence Livermore National Laboratory
P.O. Box 808
Livermore, CA 94550

20 Office of Nuclear Waste Isolation
505 King Street
Columbus, OH 43201
ATTN: S. J. Basham
G. K. Beall
W. A. Carbiener
J. A. Carr
D. E. Clark
J. C. Cunnane
P. L. Hofmann
J. F. Kircher
V. S. McCauley
D. P. Moak

No. of Copies

J. B. Moody
J. S. Perrin
G. E. Raines
B. A. Rawles (5)
R. A. Robinson
J. R. Schornhorst

2 Salt Repository Project Office
505 King Avenue
Columbus, OH 43201
ATTN: J. O. Neff
K. K. Wu

ONSITE

2 DOE Richland Operations Office

J. J. Sutey
P. A. Craig

3 Rockwell Hanford Operations

P. A. Salter
W. W. Schulz
M. J. Smith

Exxon Nuclear Company

S. J. Beard

Joint Center for Graduate Study

J. Cooper

UNC Nuclear Industries, Inc.

F. H. Bouse

3 Westinghouse Hanford Company

W. F. Brehm
L. A. James
J. M. Lutton

No. of Copies

62 Pacific Northwest Laboratory

L. L. Ames
M. J. Apted
W. F. Bonner
D. J. Bradley
H. C. Burkholder
T. D. Chikalla
D. G. Coles
F. H. Dove
J. S. Fruchter
J. H. Jarrett
E. A. Jenne
J. H. Haberman
C. O. Harvey
F. N. Hodges
M. R. Kreiter
K. M. Krupka
W. L. Kuhn
J. L. McElroy
G. L. McVay
J. E. Mendel
D. M. Merz
L. G. Morgan
L. R. Pederson
R. D. Peters
S. G. Pitman
B. A. Pulsipher
D. Rai
P. W. Reimus
W. A. Ross
J. T. A. Roberts
W. A. Ross
R. J. Serne
J. W. Shade
D. W. Shannon
L. A. Sigalla
R. P. Turcotte
R. E. Westerman (20)
J. H. Westsik, Jr.
P. L. Whiting
Technical Information (5)
Publishing Coordination (2)